ANAYSIS OF SATURATES, AROMATICS, RESINS, ASPHALTENES (SARA), WATER, AND CLAYS IN WATER-OIL EMULSIONS FOR STEAM-ASSISTED GRAVITY DRAINAGE (SAGD) & EXPANDING SOLVENT-SAGD (ES-SAGD)

A Thesis

by

TANIYA KAR

Submitted to the Office of Graduate and Professional Studies of
Texas A&M University
in partial fulfillment of the requirements for the degree of

MASTER OF SCIENCE

Chair of Committee,	Berna Hascakir
Committee Members,	David Burnett
	Yuefeng Sun
Head of Department,	A. Daniel Hill

August 2015

Major Subject: Petroleum Engineering

ABSTRACT

The presence of complex water-in-oil emulsions is a growing concern in heavy oil recovery due to the complexity and expenses involved in separating the water from the produced oil. Hence, it is of paramount importance to understand the components involved in stabilizing these emulsions.

It is well-known that clays and water play a very important role in stabilizing the water-in- oil emulsions by interacting with the heavy molecular-weight polar oil components like asphaltenes and resins. However, a quantitative estimation regarding the role of clays, crude oil components (saturates, aromatics, resins, and asphaltenes) and water in emulsion formation for SAGD has not been illustrated so far. Study of asphaltenes is complicated because of the varying structure, molecular weight, and composition of asphaltenes in different crude oils. Apart from asphaltenes, the common reservoir clays-kaolinite and illite have not been investigated as thoroughly as smectite. Their non-swelling nature causes one to think that their contribution towards reservoir damage would be ignorable. However, while these clays are non-swelling, they can cause formation damage due to their pore lining, pore bridging, and pore cementation features which may increase fluid trapping and consequently, reduce the oil recovery.

Thus, spent rock and residual oil analysis are imperative to understand the pore-scale displacement and wettability alterations occurring in the reservoir during steam injection processes. Wettability alteration studies have not been carried out as extensively for SAGD and ES-SAGD, as compared to other steam injection processes like steam

flooding and cyclic steam injection. Moreover, there are limited studies on the impact of clay type on wettability alteration.

This research focuses on the analyses of the types of emulsions formed during SAGD and ES-SAGD, and the effect of clay type and wettability alteration on emulsion formation. While illite travels in the oil phase, kaolinite is found in the water phase, hence, it has been concluded that illite contributes more towards the stable water-in-oil emulsion formation than kaolinite. The use of asphaltene non-solvents during ES-SAGD is recommended to reduce emulsion formation.

DEDICATION

I dedicate my thesis to my loving parents, Amar Kanti Kar and Tinku Kar, for their unconditional love and support throughout my life. None of this would be possible without them.

ACKNOWLEDGEMENTS

To begin with, I would like to thank my advisor, Dr. Berna Hascakir, for guiding and helping me in my research, every step of the way, and always encouraging me to persevere and work harder to achieve my goals.

I would like to thank my committee members, Mr. David Burnett and Dr. Yuefeng Sun, for their guidance and support throughout the course of this research.

I owe my heartfelt gratitude to all the members of the Heavy Oil, Oil shales, Oil sands, and Carbonate Analysis and Recovery Methods (HOCAM) research group for their help and support in my research. I would particularly like to thank Kristina Klock, Jun Jie Yeoh, and Matthew Williamson for helping me with measurements in the laboratory. Also, a special thanks to Albina Mukhametshina, as my research is a continuation of the SAGD and ES-SAGD experiments previously conducted by her. I would also like to thank Yasin Unal for helping me with the wettability and zeta potential measurements.

I sincerely thank my friends, colleagues, the department faculty, and staff of Petroleum Engineering for making my time at Texas A&M University a great experience.

Last, but not the least, I thank my family and friends for always supporting, loving, and inspiring me.

NOMENCLATURE

ASTM	American Society for Testing and Materials
EOR	Enhanced Oil Recovery
ES-SAGD	Expanding Solvent Steam Assisted Gravity Drainage
ES-SAGD1	ES-SAGD with co-injection of n-hexane with steam
ES-SAGD2	ES-SAGD with co-injection of n-hexane and toluene with steam
ES-SAGD3	ES-SAGD with cyclic-injection of n-hexane and toluene with steam
ES-SAGD4	ES-SAGD with co-injection of n-hexane and cyclohexane with steam
FTIR	Fourier Transform Infrared Spectroscopy
SAGD	Steam Assisted Gravity Drainage
SAGD1	SAGD using kaolinite
SAGD2	SAGD using a mixture of 90 wt% kaolinite and 10 wt% illite
SARA	Saturates, Aromatics, Resins, Asphaltenes
TGA/DSC	Thermogravimetric Analysis/ Differential Scanning Calorimetry
σ	Shear stress
γ	Shear rate
K	Flow consistency index
n	Flow behavior index

.

TABLE OF CONTENTS

Page

LIST OF FIGURES

Page

LIST OF TABLES

Page

CHAPTER I

INTRODUCTION

The decreasing conventional oil reserves and a drastic increase for oil demand with the growing world's population bring the necessity for a gradual shift in interest towards recovery from unconventional resources. Bitumen, heavy oil, and extra heavy oil account for unconventional resources, and are estimated to cover around 55% of the total oil reserves worldwide. Of these, the bitumen reserves are the most abundant, and exceed conventional oil deposits by approximately 2.6 times (Attanasi et al., 2010). Majority of the world's bitumen deposits are located in Alberta, Canada. Recovery of bitumen via conventional recovery techniques is challenging, owing to the high viscosity and consequent high flow resistance of bitumen in the reservoir. Application of thermal enhanced oil recovery (EOR) methods is particularly effective for bitumen extraction as it reduces the viscosity and mobilizes bitumen in the reservoirs via heat transfer, allowing it to flow into the producer wells (Kovscek, 2012).

Steam Assisted Gravity Drainage (SAGD) is a thermal enhanced oil recovery process, introduced by Dr. Roger Butler in the 1970s (Butler et al., 1979). It is particularly effective for bitumen recovery. It involves two horizontal wells which are drilled into the reservoir near the base. Steam is injected through the upper injector well, and travels into the reservoir, creating an expanding steam chamber. This steam chamber reduces the oil viscosity and increases oil mobility, which, combined with the gravity effect, enables the mobilized oil to flow out of the bottom producer well along with the condensed water

(Butler, 1980; Butler, 1998). The effectiveness of SAGD is essentially due to the large area of the reservoir covered by the expanding steam chamber, which improves the sweep efficiency of the process (Butler, 1991). Also, the oil flowing from the reservoir into the producer well remains hot due to the constant steam temperature maintained inside and on the boundary of the steam chamber (Mukhametshina and Hascakir, 2014).

Inspite of the effectiveness of SAGD for bitumen recovery, there are some significant drawbacks and environmental concerns associated with steam generation, such as greenhouse gas emissions, fresh water consumption, and energy requirements. One of the most pronounced alternative SAGD technologies to reduce the environmental drawbacks and increase oil production is Expanding Solvent-SAGD (ES-SAGD) (Nasr et al, 1991; Mukhametshina and Hascakir, 2014). It involves co-injection of a hydrocarbon solvent or a combination of solvents with steam to reduce the amount of steam required. The addition of solvent along with steam helps to further reduce the viscosity of oil because the hydrocarbon solvent can dissolve the oil and mobilize it further (McLean and Kilpatrick, 1997; Mokrys and Butler, 1993; Nasr et al., 2003). Selection of solvents for ES-SAGD is based on the solvent phase at steam temperature and pressure. Due to the need for simultaneous condensation of water and solvent at the steam chamber boundary, paraffinic solvents with low carbon numbers are generally preferred for ES-SAGD (McCain 1990; Nasr et al., 2003).

While it has been proved that the application of ES-SAGD has major advantages over SAGD, the produced oil quality and the effect of flow assurance related problems on the performance efficiency of SAGD and ES-SAGD are unknown. In the case of ES-

SAGD, on one hand, the hydrocarbon solvents may favor the deposition of heavy oil components on the reservoir rock, upgrading the produced oil, while, on the other hand, some solvents might dissolve asphaltenes and carry them along with the produced oil. The effect of solvent-asphaltene-clay-water interaction on the quality of produced oil and severity of water-in-oil emulsions have not been investigated widely. Since the major problems of steam injection processes are associated with water production (Acosta, 2010), oil-water emulsion formation in the reservoir, production lines, and downstream refineries is expected after SAGD and ES-SAGD (Minnie, 1933; Sztukowski et al., 2003). But, the mechanism of emulsion formation and its affecting factors are only known at a basic level (Nguyen et al., 2014). And there are limited studies explaining this mechanism from a full perspective (Sztukowski and Yarranton, 2005; Poteau et al., 2005). Most of these studies are conducted on synthetic emulsions, those which are prepared in the laboratory (Rajakovic and Skala, 2006; Xia et al., 2003).

It can be useful to provide a definition of emulsions at this stage. Emulsion can be defined as a suspension of colloids of dispersed phase in a solution of dispersion medium (Kilpatrick, 2012). In steam injection processes for heavy oil extraction, oil-in-water, water-in-oil, or complex emulsions are commonly observed (Kokal, 2005; Nenningsland et al., 2011). In complex emulsions, there are more than two layers of the dispersed phase, suspended in the dispersion medium. The stability of the oil-water emulsions is enhanced by the presence of a layer of emulsifiers between the dispersed and dispersion phases (Kokal, 2005). In a water-in-oil emulsion present in the produced oil from a steam injection process, the interfacial layer formed by the emulsifier is present around the water

droplets suspended in the oil medium, which sterically hinders the coalescence of the water droplets. This leads to an increase in emulsion severity, and makes it harder to separate the water from the produced oil (Nguyen et al., 2010; Nguyen and Balsamo, 2013; Nguyen et al., 2013; Nguyen et al., 2014).

Naturally existing emulsifiers in the reservoir include clay and sand fine particles, heavy molecular weight and polar components of oil in place, such as resins and asphaltenes (Binner et al., 2014; Evdokimov and Losev, 2014; da Silva et al., 2014; Martinez-Palou et al., 2013; Yarranton et al., 2007). Emulsifiers can also be introduced into the reservoir in the form of chemicals added for controlling scale and wax formation, or those present in drilling mud (Pietrangeli et al., 2014). Particularly for bitumen reservoirs, it has been reported that the concentration of asphaltenes and resins, along with their proportion with respect to the lighter oil components like saturates and aromatics, are crucial factors which affect emulsion severity (Sztukowski et al., 2003; Mohammadzadeh et al., 2010; Haghighat and Maini, 2010). Therefore, it is important to understand the contribution of individual fractions in the emulsion formation. Asphaltenes are defined as one of the heaviest molecular weight, polar components of crude oil. Their structures and compositions are complex (Mojelsky et al., 1992). The chemical composition and molecular weight of asphaltenes varies for different crude oils (Long, 1982). They essentially consist of a planar aromatic structure, with alkane groups and heteroatoms like sulfur, nitrogen, and oxygen attached to them (Groenzin and Mullins, 2000). They are soluble in the presence of aromatics solvents, but precipitate upon the addition of aliphatic solvents (Mullins, 2008; Speight, 1999). Also, the composition and properties of

asphaltenes change, depending on the solvent used for precipitation of asphaltenes from crude oil (Zhao et al., 2009). Although it has been determined that asphaltenes, aided by resins, stabilize these emulsions by coalescence of asphaltene aggregates at the oil-water interface, the stability has not been quantitatively measured. Qualitatively, it has been seen that the acidic parts of asphaltenes are predominant in more stable emulsions (Fingas, 2014).

Stability of asphaltenes during steam injection depends on reservoir pressure and temperature, solvents and precipitating agents used, and crude oil composition (Leontaritis et al., 1994; Theuerkorn et al., 2008). Based on these factors, the asphaltenes destabilize, and then, aggregate to form an interfacial layer between the water and oil phase in the emulsion, preventing the fusion of water drops in water-in-oil emulsions, or oil droplets in oil-in-water emulsions (Nguyen et al., 2014). In the literature, it has been proposed that with increase in asphaltene mass concentration at the interface, the emulsion stability decreases due to increase in asphaltene surface coverage area. However, experiments conducted on asphaltenes originated from Athabasca bitumen by Sztukowski et al. (2003) showed that the interfacial area doesn't change significantly with increasing mass concentration of asphaltenes. Nonetheless, it increases molar mass of asphaltenes and they self- associate to form larger aggregates. Increase in mass concentration leads to extension of the monolayer thickness rather than coverage area (Sztukowski et al., 2003).

Resins play an important role in asphaltene stability in the crude oil (Agrawala and Yarranton, 2001; Yarranton, 2005). Resins are polar, aromatic, and heavy oil components, with a lower polarity and molecular weight compared to asphaltenes (Goual and

Firoozabadi, 2002; Goual and Firoozabadi, 2004; Speight, 1999). Another significant difference between resins and asphaltenes is that resins dissolve in the presence of light and heavy n-alkanes (with the exception of liquid propane), but asphaltenes are insoluble in aliphatic solvents and soluble in aromatic solvents (Speight, 1999; Wiehe, 2012). Due to their similar chemical nature, resins are the oil components which have the strongest affinity towards asphaltenes (Wu et al., 2013). Asphaltenes, due to their strong intermolecular polar and hydrogen bonding, form a film on the water-oil interface, thereby stabilizing emulsions. Addition of resins solvates the insoluble precipitate portions of asphaltenes, reduces the aggregate size, and dissolves the aggregate particles. As a result, the film weakens and emulsion stability decreases (Spiecker et al., 2003). However, the characteristics of asphaltenes and the asphaltene-resin interactions differ, depending on the solvent or precipitating agent used (Shkalikov et al., 2010; Stachowiak et al., 2005; Gonzalez et al., 2006). Zhao et al. (2009) found that, for Athabasca bitumen, contrary to literature findings, n-pentane asphaltenes and resins have poor associations at 473 K (199.85 °C), where asphaltenes are mostly in liquid form. However, the same n-pentane asphaltene rich aggregates were found to consist of much larger proportions of heptane resins. It is also known from literature that higher the carbon number of the hydrocarbon solvent used for precipitating asphaltenes, lower is the amount of asphaltenes precipitated and more polar are the asphaltenes (Mullins et al., 2007; Shkalikov et al., 2010; Stachowiak et al., 2005). This implies that n-heptane asphaltenes will be more polar compared to n-pentane asphaltenes. Deo and Hanson (1993) conducted asphaltene analysis of original and residual oil by supercritical solvent extraction with propane. The

extraction was found to increase with reservoir pressure leading to an increase in asphaltene and resin concentration in the residual oil. The hydrogen to carbon ratio of the residual fraction was found more than the original oil, indicating the polarity of residual components to be higher than the extracted oil. Additionally, the asphaltene to resins ratio as well as the nitrogen and sulfur content of residual oil were measured to be higher than the original oil. Hence, to analyze the asphaltene content in the residual oil, an increase in polar fractions relative to non-polar fractions is more significant than the quantity of lighter components left behind.

The interaction of resins and asphaltenes with the reservoir rock has a significant impact on the emulsion stability. To better understand this interaction, wettability of the rock and quality of the residual oil should be further investigated. The interaction between the asphaltene particles and the clay minerals leads to the deposition of asphaltenes on the rock, thereby, changing the wettability of the reservoir to oil-wet (Anderson, 1986; Unal et al., 2015). The type of clays present in the oilfields are mainly illite, kaolinite, and smectite (Czarnecka and Gillott, 1980). Smectite is known to cause problems in the reservoir due to its water-sensitive and swelling nature, as compared to the non-swelling clays- illite and kaolinite (Bennion et al., 1992). But, apart from water sensitivity, other physical and chemical properties of clays can affect the wettability, and also the stability of emulsions. Clay particles and fines are dispersed by the asphaltene flocs and get combined with the crude oil due to their oil-wet nature (Leontaritis et al., 1994). These fines, along with the asphaltenes and resins, can further increase the stability of oil-water interface in the produced oil, thus, strengthening the water-in-oil emulsions (Alvarado et

al., 2011; Sztukowski and Yarranton, 2005). Illite, which is more hydrophilic compared to kaolinite (Bantignies et al., 1997), is more prone to migration, owing to high sensitivity of quartz-illite system towards temperature variations (Schembre and Kovsek, 2004). At high temperature conditions, kaolinite can alter into water swelling smectite, causing permeability reduction (Bennion et al., 1992). Non-swelling clays like illite and kaolinite can still affect the reservoir permeability and oil-water emulsion stability (Unal et al., 2015). In addition to clay migration and alteration, reservoir clays are notorious for permeability reduction through pore filling - kaolinite, pore lining –chlorite and pore bridging - illite (Wilson and Pittman, 1977). Minor quantities of diagenic clays like illite can decrease the permeability of the formation by a great extent (Nadeau, 1998). The quantity of deposited asphaltenes is affected by the clay type, which, in turn, defines reservoir wettability (Baker, 1988). Generally, it has been found that there is a shift towards water-wetness in the reservoir, with the progression of steam injection, due to decrease in oil saturation (Poston et al., 1970). However, there have been many reported cases of increase in oil-wetness during steam propagation (Bennion et al., 1992; Escrochi et al., 2008), which is believed to be due to the precipitation of the heavy molecular weight oil components (asphaltenes, resins) and their interactions with clays (Pang et al., 2010).

The investigation of residual oil in the spent rock after steam injection processes through qualitative and quantitative analysis can give a very good idea about the severity of interaction of clays with the oil, and also about the role of clays in oil-water emulsion severity in the produced oil.

CHAPTER II

EXPERIMENTAL PROCEDURE

2.1. Summary of Previous Experiments

Previously, two SAGD and four ES-SAGD experiments were conducted (Morrow et al., 2014; Mukhametshina 2013; Mukhametshina et al., 2014; Mukhametshina et al., 2015). The experiments were performed on a Peace River bitumen sample and the process conditions for the experiments were designed to simulate the Peace River reservoir in Canada by mixing 85 wt% Ottawa sand with 15 wt% clay (Bayliss and Levinson, 1976). The corresponding 32 volume% of pore space was filled with 84 wt%; 54,000 cP; and 8.8 API gravity bitumen and 16 wt% distilled water (Hamm and Ong, 1995). Two types of clay were used to prepare the reservoir rock (Unal et al., 2015). While for SAGD1, 100 wt% kaolinite (Clay1) was used, for SAGD2 and all the ES-SAGD experiments, a mixture of 90 wt% kaolinite and 10 wt% illite (Clay2) was used. It should be noted that Clay2 better represents the original reservoir rock (Bayliss and Levinson, 1976). The four ES-SAGD experiments varied in terms of solvent type and injection strategy. ES-SAGD1 had co-injection of n-hexane with steam, ES-SAGD2 had co-injection of mixture of n-hexane and toluene in equal amounts with steam, ES-SAGD3 used a cyclic injection of n-hexane and toluene with steam, and ES-SAGD4 used a co-injection of n-hexane and cyclohexane with steam. In all experiments, steam injection rate was kept constant at 18 ml/min and in the ES-SAGD experiments, a constant solvent:steam ratio of 2:18 ml/min was used. Table

1 summarizes the experimental and initial conditions, along with the cumulative oil recoveries for all experiments (Mukhametshina and Hascakir, 2014).

Table 1: Experimental details of the six SAGD and ES-SAGD experiments (Mukhametshina, 2013)

Experiment	Clay Type	Solvent Type	IS	q, ml/min	t, hours	Cumulative Oil Recovery (wt%)*
SAGD1	K	-	-	-	12	47
SAGD2	K+ I	-	-	-	12	32
ES-SAGD1	K+ I	C6	Cont.	2	9	36
ES-SAGD2	K+ I	C6+T	Cont.	1+1	9	45
ES-SAGD3	K+ I	C6/T	Cyclic	2/2	9	45
ES-SAGD4	K+ I	C6+C	Cont.	1+1	3.5	-

IS: Injection Strategy for Solvents, q: Solvent Injection Rate, ml/min, t: Total Experiment Time, hours, K : Kaolinite, K+I : 90 wt% kaolinite + 10% wt% illite, C6 : n-hexane, C6+T: continuous injection of n-hexane + toluene with steam, C6/T : cyclic injection of n-hexane and toluene with steam, C6+C: continuous injection of n-hexane + cyclohexane with steam, *includes both water and clay

It should be noted that for ES-SAGD3, n-hexane and toluene were alternately co-injected with steam, beginning with n-hexane in the first hour. ES-SAGD4 lasted for only 2.8 hours, and had to be stopped due to delayed asphaltene precipitation which occurred in the production lines and caused plugging in the lines (Mukhametshina et al., 2015).

2.2. Materials & Methods

2.2.1. Produced Oil Analysis

The produced oil obtained from five experiments (SAGD1, SAGD2, ES-SAGD1, ES-SAGD2, and ES-SAGD3) have been analyzed extensively and compared to original bitumen.

The emulsion type in the produced oil has been first visualized with Meiji Techno Japan- Microscope and ProgRes CT5- Camera. A 100X magnification has been used for all images. Viscosity and rheology of the produced oil samples have been measured using a Brookfield RVDV-III Rheometer.

The rheological behavior of the produced oil has been studied by measuring their apparent viscosities as a function of shear stress to shear rate with increasing temperature; 35 °C, 45 °C, and 55 °C. The results have been compared to those of original bitumen.

Water content of samples have been determined by evaporating water. A NETZSCH Thermogravimetric Analysis/ Differential Scanning Calorimetry (TGA/DSC) is used for this purpose. Produced oil samples are subjected to heating under air injection till reaching 200 °C at a constant heating rate (10 °C/min). A sharp weight loss is observed at different temperature values ranging between 52 °C to 144 °C for each experimental sample. At the same temperature values in where the sudden weight loss is observed in TGA graphs, DSC curves indicate an endothermic peak which is due to vaporization of water present in the samples (Chen et al., 2012; Jones et al., 2013). This has been verified by conducting a similar analysis for distilled water sample, under the same heating rate. Hence, this sudden weight loss in TGA graphs is used to calculate the water content of the samples.

After determination of water content in each of the produced samples, the bulk produced oil and original bitumen were separated into their saturates, aromatics, resins, and asphaltenes (SARA) fractions, by following the ASTM standard D2007-11 method (ASTM, 2011) to observe the role of each fraction in forming and stabilizing oil-water emulsions. The ASTM method is based on solubility of petroleum fractions in different organic solvents (Speight, 1999). Asphaltenes are initially separated from the bulk oil samples using n-pentane, hence, the asphaltenes discussed throughout the thesis are n-pentane insoluble asphaltenes. The deasphalted oil (maltenes) are then introduced into the SARA separating columns, along with n-pentane. The upper column has Attapulgus clay which adsorbs the resins, which are later desorbed from this column using a mixture of toluene and acetone. The remaining portion of the oil (saturates and aromatics) flow down to the second, interconnected column which consists of a layer of Attapulgus clay at the top and activated silica gel at the bottom. The aromatics are adsorbed by the silica gel, and the saturates, which remain unadsorbed, flow down into the collecting conical flask. The columns are washed with n-pentane to aid the separation and flow. After separation, the solvents (n-pentane, toluene, and acetone mixture) are evaporated from the oil components and their weights are determined. The weight of aromatics are determined by weight difference, since aromatics can't be recovered from the silica gel column (ASTM, 2011).

The bulk oil samples and their individual SARA fractions are then analyzed with Agilent Fourier Transform Infrared Spectroscopy (FTIR). The FTIR spectra obtained of the produced samples are compared with the FTIR spectra of the reference samples used in the experiments (original bitumen, distilled water, clay, sand, toluene, n-hexane,

cyclohexane, n-pentane, acetone, Attapulgus clay, and silica gel). In the FTIR spectra of the bulk oil samples and asphaltene fractions, significant clay signatures are observed (Kar et al., 2014). A filtration technique is used to separate clays from the bulk samples and asphaltenes. Both the clay-oil and clay-asphaltene interactions are discussed. During filtration, first, the bulk oil samples are mixed with toluene and filtered through a filter paper with pore size of less than 2 microns, which is less than the average particle size of clay used to prepare the reservoir rock (Unal et al., 2015). The same procedure is implemented to the asphaltenes.

The asphaltenes obtained from produced oil are subjected to zeta potential measurements by using Zeta PALS Brookhaven instrument. Zeta potential value has been used to interpret the stability of colloids suspended in a solution (Nguyen et al., 2014). 50 mg of asphaltene is mixed with 15 ml of ethanol. This mixture is then homogenized in an ultrasound tub for 20 minutes. 1.5 ml of this homogenized mixture is added to 100 ml of 1 mM Potassium Chloride (KCl) solution. This prepared solution is then used to measure the zeta potential of the asphaltene particles in produced oil (Parra-Barraza et al., 2003). It should be noted that higher the absolute value of zeta potential, more stable is the colloid in the solution (Quan et al., 2012).

2.2.2. Residual Oil Analysis

For both SAGD and ES-SAGD, the pore-scale displacement is different inside the steam chamber compared to outside steam chamber, since steam is effective in the steam chamber region. This leads to variations in the residual oil saturations in the spent rock. The pore-scale displacement in SAGD is affected by various factors, like steam phase and gravity, along with the phase of solvents, in case of ES-SAGD. While steam, n-hexane, and cyclohexane are effective inside the steam chamber due to their vapor phase, toluene is effective at the bottom of the cell, since it is in liquid phase at experimental conditions of 165 °C and 75 psig (Mukhametshina et al., 2015). The effect of gravity keeps the toluene in the lower portion of the cell/reservoir. Understanding how these concepts affect the overall process performance of SAGD and ES-SAGD will enhance our knowledge towards the emulsion formation mechanism. Therefore, in this study, residual oil originated both from inside and outside steam chamber regions are investigated. Because of the growth of steam chamber, water-wet behavior is anticipated inside steam chamber. While, for outside steam chamber, more oil-wet nature is expected. Hence, first, the wettability of spent rocks has been determined on the samples taken from both inside and outside steam chamber zones, before residual oil removal.

Krüss DSA30S Drop Shape Analyzer is used to determine the wettability by measuring the contact angle values of the oil sand samples. A drop of distilled water is released on the flattened surface of the postmortem sample, and the resulting shape made by the water drop on the surface is video recorded (Krüss, 2004-2011). The water-air contact angle values are recorded and used to determine wettability. Even though, the

water-oil contact angle measurements are used to determine wettability in literature (Anderson, 1986; Alotaibi et al., 2010), the water-air contact angle measurements still provide important information on the wettability characteristics of solid surfaces. Since water is in vapor phase during the SAGD and ES-SAGD experiments, similar to air in gas phase, the wettability will represent more the situation at the steam chamber edge (Unal et al., 2015).

Then, the residual oil is extracted through toluene extraction and several analyses are conducted on the residual oil extracted from the spent rock samples (Amyx et al., 1960; Mullins, 2008).

The components of residual oil samples are determined by using the similar procedures explained in "Produced Oil Analysis" section; water content is determined by TGA/DSC analysis, filtration is implemented to separate clays, and the ASTM standard method is applied to quantify the SARA fractions of the oil component in residual oil.

CHAPTER III

EXPERIMENTAL RESULTS AND DISCUSSION

3.1. Effect of Clay Type

In this section, the role of clay type on emulsion formation mechanism is investigated. Two SAGD experiments conducted with two different clays are analyzed. It might be of worth to remind that the only variable in these experiments is the clay type used; SAGD1 was conducted with Clay1 (100 wt% kaolinite) and SAGD2 was conducted with Clay2 (90 wt% kaolinite and 10 wt% illite) (Table 1). This change in clay type resulted in 15.4 wt% reduction in oil production; the cumulative oil production for SAGD is reported to be 47.4 wt% and that for SAGD2 to be 32 wt% (Unal et al., 2015). The measured viscosity and API gravity of the produced oil from SAGD1 and SAGD2 are 53,151 cP, 8.8 °API for SAGD1; and 50,165 cP, 8.9 °API for SAGD2 (Mukhametshina, 2013).

There is no significant difference in the produced oil quality in terms of viscosity and API gravity. To find the reason behind the difference in oil recovery from the two experiments, the produced oil samples are first analyzed with microscopic images (100X magnification) to visualize the emulsion types in produced oil. Complex, triple emulsion (oil-in-water-in-oil) is observed for SAGD2, although no apparent emulsions are visible for original bitumen and traces of water-in-oil emulsions are observed in SAGD1 (Fig. 1).

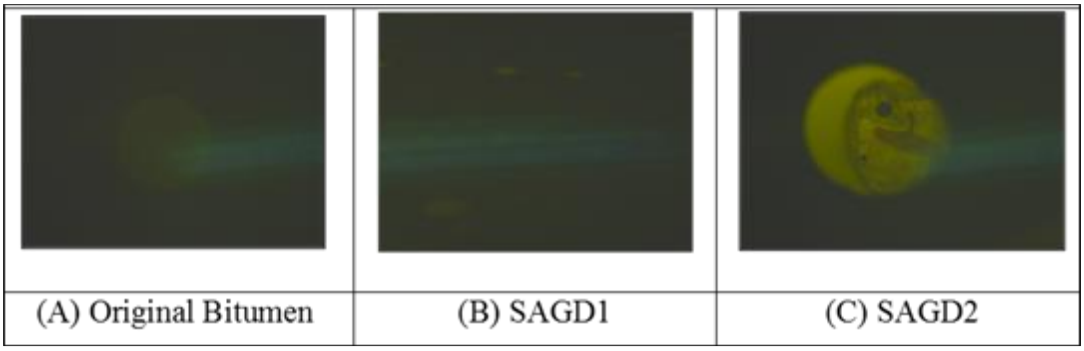

Figure 1: Microscopic images of emulsions in produced oil compared with original bitumen (100X magnification)

The water content in the produced oil and bitumen is determined through TGA/DSC analysis. The TGA/DSC curves (Fig. 48, Fig. 53, Fig. 54) are interpreted to determine the water content. The endotherms (increase in DSC curves) provide information on evaporation of water (Chen et al., 2012; Jones et al., 2013). Hence, the amount of water present in the samples is determined by noting the weight loss in the TGA curve, for the corresponding endothermic peak in the DSC curve. For reference, a TGA/DSC analysis is performed on a distilled water sample, and the complete evaporation of distilled water is noted at 143.8 °C (Fig. 47). For some samples, more than one endothermic peaks are observed, which can be interpreted as the evaporation of water in stages- at first, the free water gets evaporated, and at higher temperatures, the water which is more firmly bound to the different layers in the produced oil/asphaltene sample gets evaporated. The evaporation at higher temperatures can also be of light hydrocarbons that have boiling points lower than water. To verify this, TGA/DSC analysis is performed on saturates, aromatics, and resins fractions of the produced oil from SAGD1 (Fig. 49, Fig.

50, Fig. 51). It is seen that the weight loss of these fractions up to the temperature of distilled water evaporation is negligible. Table 2 provides an analysis of the sequential evaporation of water in the bulk produced oil.

Table 2: Water content in 100 grams of bulk produced oil and original bitumen (Interpreted from Fig. 48, Fig. 53, Fig. 54)

Sample	**Temp- Weight loss (°C- grams)**	**Endotherm observed in DSC curves**				**Total water (grams)**
		1st	**2nd**	**3rd**	**4th**	
Bitumen	**Temperature, °C**	119.36	-	-	-	-
	Weight loss, grams	10.6	-	-	-	10.6
SAGD1	**Temperature, °C**	86.66	-	126.66	139.16	-
	Weight loss, grams	12.08	-	19.36	11.56	43.0
SAGD2	**Temperature, °C**	86.5	96.5	119.01	131.51	-
	Weight loss, grams	2.15	1.35	8.54	41.96	54.0

From Table 2, it is observed that for the produced oil from SAGD2, there are 4 endotherm peaks (Fig. 54), which might be an indication that water gets evaporated from the produced oil in four stages. This indicates towards the complexity of emulsions in SAGD2 (Fig. 1C). Due to the asphaltene-clay-water layers present in the triple emulsions, the water gets evaporated in parts, depending on the severity of attachment of water to the

asphaltenes and clays. Interestingly, for SAGD1, three endotherm peaks for water evaporation are observed, even though no significant emulsions are observed in the produced oil (Fig. 1B).

Saturates, aromatics, resins, and asphaltenes fractions are separated through ASTM method (Fig. 2) for 100 grams each of original bitumen and produced oil samples, and the clay content is measured by filtration (as explained in the Materials and Methods).

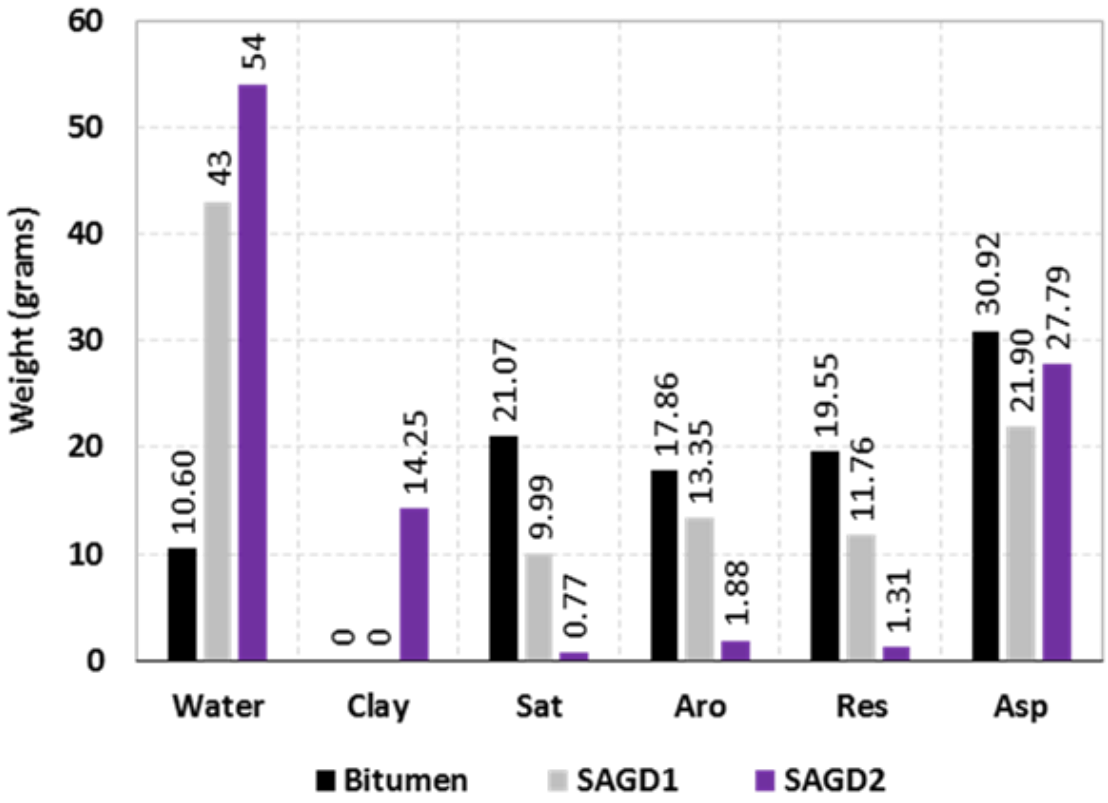

Figure 2: Normalized weight of water, clay and SARA fractions on the basis of 100 grams of original bitumen and bulk produced oil
Sat: saturates, Aro: aromatics, Res: resins, Asp: asphaltenes; in bulk oil

The water content is 10.6 grams in original bitumen, and it is higher for SAGD2 (54 grams) compared to SAGD1 (43 grams), for 100 grams of original bitumen or produced oil samples (Fig. 2).

No clays are found in the produced oil for SAGD1. On the other hand, the bulk produced oil obtained from SAGD2 contains a high amount (14.25 grams) of clays. The presence of clays in the produced oil for SAGD2 and the absence of clays in SAGD1 are confirmed by the FTIR spectra, which show clay peaks in the produced oil for SAGD2 but no clay peaks in SAGD1 (Fig. 15 compared with Fig. 12). This proves that for SAGD2, clays from the reservoir have migrated and preferred the oil phase for migration (Unal et al., 2015). It supports the theory of migration of clay particles into the crude oil owing to their oil-wet behavior (Leontaritis et al., 1994). The migration of Clay2, which is a mixture of 90 wt% kaolinite and 10 wt% illite, into the oil phase, also proves the migration tendency of illite compared to kaolinite, as quartz-illite system is more sensitive towards the variations in temperatures (Schembre and Kovsek, 2004), occurring in steam injection processes.

On comparing the amount of SARA fractions in original bitumen and bulk produced oil from SAGD1 and SAGD2, it is observed that the proportion of resins to asphaltenes as well as the proportion of deasphalted oil to asphaltenes is decreasing with the decrease in viscosity from original bitumen to SAGD1 and then SAGD2 (Fig. 2). This indicates that the proportion of the heavy fractions of oil have a direct relation to the viscosity of produced oil. It should be noted that the amount of lighter oil components (saturates and aromatics) are also higher for SAGD1. The presence of higher proportion

of lighter oil components is an important factor in the higher cumulative oil recovery and absence of complex emulsions in the produced oil obtained from SAGD1 (Fig. 1B). The produced oil from SAGD1 contains a high amount of resins along with asphaltenes (Fig. 2). Even in the absence of clays, water forms layers by interaction with resins and with asphaltenes, due to the similar polar nature of all these components (Mullins et al., 2007; Spiecker et al., 2003; Kar and Hascakir, 2015). This can explain the 3 endotherm peaks observed in the DSC curve for SAGD1 in Table 2.

After produced oil analysis, the spent rock samples from SAGD1 and SAGD2 are divided into two zones each- inside steam chamber and outside steam chamber. By visual inspection, the color of spent rock is significantly darker for SAGD2 compared to SAGD1 (Fig. 3) (Mukhametshina, 2013). This indicates that the residual oil content is considerably higher for SAGD2, due to poor sweep efficiency and probably more severe clay-asphaltene interactions, when compared to SAGD1, which caused more oil-retention for SAGD2. For SAGD1, color of inside steam chamber zone is found to be much lighter than outside steam chamber (Mukhametshina, 2013).

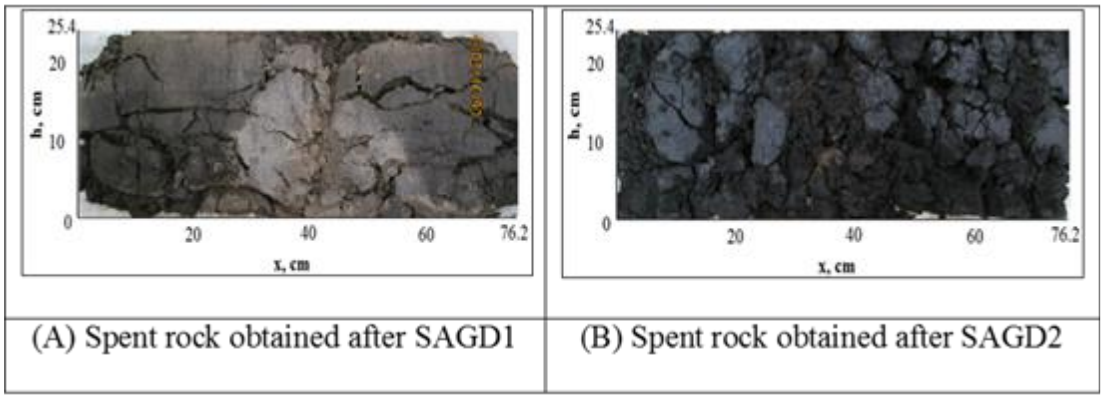

Figure 3: Visualization of the spent rock obtained after oil extraction for SAGD1 and SAGD2 **(**Mukhametshina, 2013)

The wettability of the spent rock is determined by contact angle measurements and presented in Table 3.

Table 3: Water-air contact angle values for oil-sand packing and spent rock, inside and outside steam chamber (* Unal et al., 2015)

Sample	**Contact Angle Values (Degrees)**		
	Initial Oil sand packing	**Inside steam chamber**	**Outside steam chamber**
SAGD1	109.57*	49.71*	118.19*
SAGD2	95.27	121.44	113.11

The spent rock zones, with the exception of inside steam chamber zone for SAGD1, are all oil-wet in nature, with slight variations in the degree of wettability (Table 3). Higher the contact angle value, more oil-wet is the surface (Alotaibi et al., 2010). The

inside steam chamber zone for SAGD1 is water-wet. This supports the improved sweep efficiency and higher cumulative oil recovery for SAGD1 compared to SAGD2.

The residual oil from the inside and outside steam chamber zones is extracted and subjected to detailed analysis to obtain a complete material balance, similar to produced oil analysis. Initially, residual oil is extracted from the spent rock using toluene with a filter paper of pore size 25 microns, which is greater than clay particle size (as described in the Materials and Methods section). It is observed that both for SAGD1 and SAGD2, residual oil content is lower for inside steam chamber compared to outside (Table 4). This implies that sweep efficiency of SAGD process in general is better inside steam chamber, due to the formation of isothermal steam chamber (Butler, 1991). However, SAGD1 and SAGD2 show variations in terms of degree of sweep efficiency, due to clay content. It is determined that SAGD1 sweeps the reservoir more efficiently than SAGD2.

FTIR spectra of the residual oils (extracted using filter paper with pore size of 25 microns) indicate presence of clays in them (Fig. 27, Fig. 37). Therefore, the filtration technique (as explained in Materials and Methods) is implemented to quantify the clays present in the residual oil. Table 4 presents the amount of residual oil and clays in residual oil for 100 grams of spent rock, compared to the amount of oil in 100 grams of initial oil-sand mixture before the experiment. It is found that in case of SAGD1, clay-oil interaction is higher for inside steam chamber zone than outside. However, for SAGD2, this association is significant for outside steam chamber. The strong interaction of clays with oil outside steam chamber for SAGD2 traps more oil in the reservoir, thereby decreasing the cumulative oil recovery.

Table 4: Determination of residual oil and clay content in residual oil in terms of 100 grams of spent rock

Sample	**Inside steam chamber**		**Outside steam chamber**		**Oil in 100 grams of initial rock (grams)**
	Residual Oil (grams)	**Clay (grams)**	**Residual Oil (grams)**	**Clay (grams)**	
SAGD1	5.86	1.02	8.73	0.39	14.27
SAGD2	9.42	0.41	12.24	1.32	14.21

Apart from the clay content determination via filtration, saturates, aromatics, resins, and asphaltenes fractions of residual oil samples are separated through ASTM method for 100 grams of bulk oil, both for inside steam chamber (Fig. 4) and for outside steam chamber regions (Fig. 5).

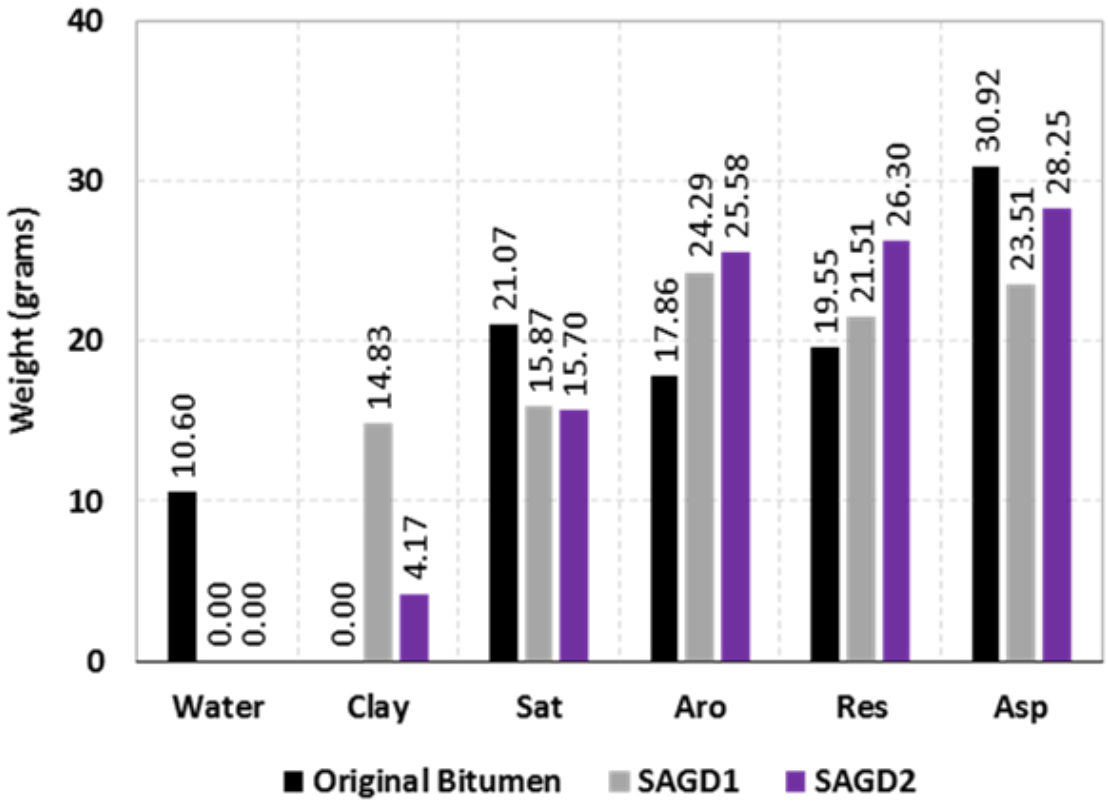

Figure 4: Normalized weight of water, clay, and SARA fractions based on 100 grams of original bitumen and residual oil inside steam chamber
Sat: saturates, Aro: aromatics, Res: resins, Asp: asphaltenes; in bulk oil

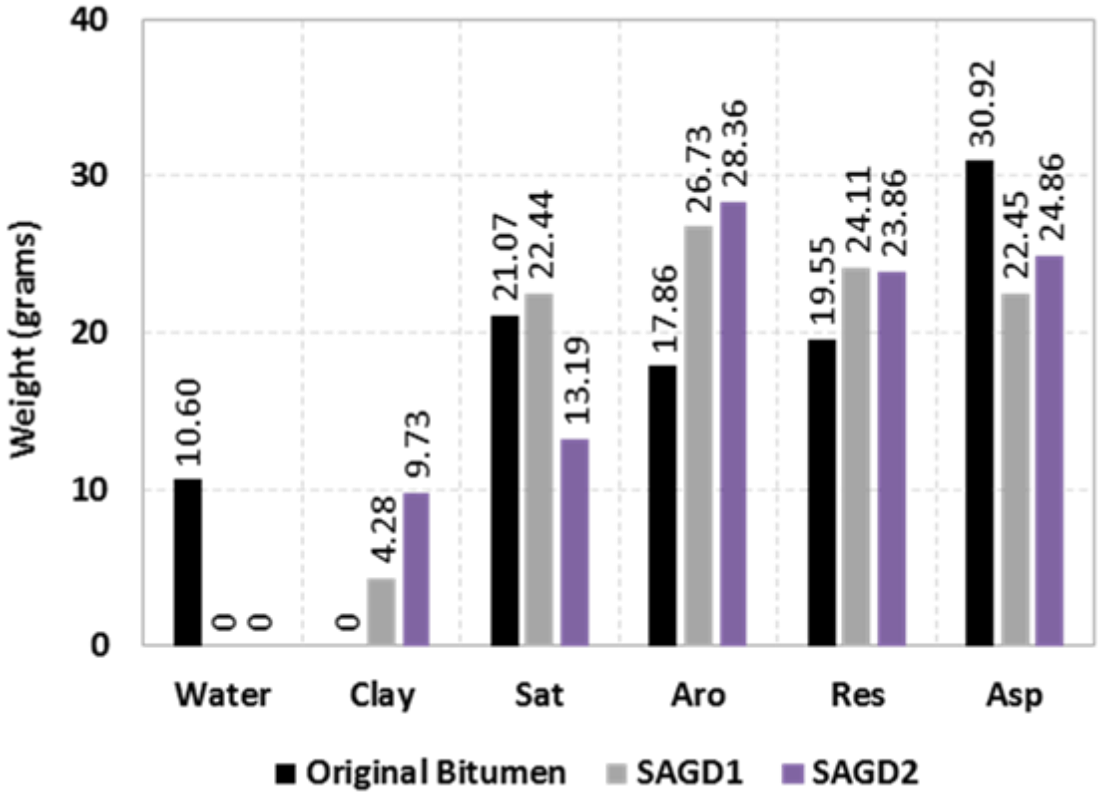

Figure 5: Normalized weight of water, clay, and SARA fractions based on 100 grams of original bitumen and residual oil outside steam chamber
Sat: saturates, Aro: aromatics, Res: resins, Asp: asphaltenes; in bulk oil

All the spent rock samples were kept under the hood overnight to remove any free water present on the surface. Therefore, it is observed that water content is nil for residual oil samples for both experiments, for both inside and outside steam chamber (Fig. 4 and Fig. 5). Also, consequent FTIR spectra support that negligible water remain in the spent rock samples (Fig. 25, Fig. 26) and the residual oil samples (Fig. 27, Fig. 37). In the case of SAGD1, clay-oil interaction is higher for inside steam chamber zone than outside. However, for SAGD2, this association is more pronounced for the outside steam chamber

region. Kaolinite (Clay1) - oil interactions are interpreted to be favorable at the steam temperature and pressure inside steam chamber. X-Ray Diffraction (XRD) analyses of spent rock have shown that a portion of Clay1 is altered from kaolinite to a mixture of illite and smectite (Unal et al., 2015). The water swelling smectite clay (Bennion et al., 1992) further enhances the clay-residual oil interactions inside steam chamber. However, when the oil is swept from the inner to outer zones and out of the steam chamber boundary, these interactions are considerably reduced (compare Fig. 4 and Fig. 5). But in the presence of illite (Clay2), clay-oil association is persistent in the outside steam chamber zone, which traps the residual oil, and reduces its flow to the producer well. This lowers the overall sweep efficiency of SAGD2 compared to SAGD1. From these results (Table 4, Fig. 4, and Fig. 5), it is seen that the amount of clays attached to the residual oil is affected by the water phase (vapor phase inside steam chamber and liquid phase outside steam chamber), the temperature and pressure, the type of clay (kaolinite or a mixture of kaolinite and illite), and the amount of residual oil in the spent rock zone. All these factors are related to each other and interdependent, because of which no linear relationship can be found between the degree of clay-oil association and just one of the above mentioned factors.

The asphaltene-rock association has been investigated in terms of the amount of asphaltenes retained on the rock due to clay-asphaltene interactions (precipitated asphaltenes) and the remaining amount of free asphaltenes which are moved or swept into the outside steam chamber zone (in case of inside steam chamber) and/or into the produced

oil (in case of outside steam chamber) (Table 5). Calculations for Table 5 are explained in Appendix IV (Table 16).

Table 5: Percentage distribution of precipitated and moved asphaltenes for inside and outside steam chamber zones based on 100 grams of asphaltenes in initial bitumen sample

Sample	**Inside steam chamber**		**Outside steam chamber**	
	Precipitated Asphaltenes (%)	**Moved Asphaltenes (%)**	**Precipitated Asphaltenes (%)**	**Moved Asphaltenes (%)**
SAGD1	79.80	20.20	67.80	32.20
SAGD2	85.22	14.77	79.62	20.38

The precipitated asphaltenes for SAGD1 are higher for inside steam chamber compared to outside steam chamber zone (Table 5). For SAGD2, the retention/precipitation of asphaltenes is higher in the outside steam chamber zone, compared to SAGD1. This indicates towards the greater asphaltene-clay affinity outside steam chamber for SAGD2, which retains the oil and reduces the cumulative oil recovery. It is also observed from Table 5 that the percentage of asphaltenes swept into the produced oil from outside steam chamber zone is higher for SAGD1 (32.20 %) compared to SAGD2 (20.38 %).

FTIR spectra of asphaltenes extracted from produced oil indicate presence of clays and water (Fig. 23), while those extracted from residual oil show presence of clays (Fig.

35, Fig. 45). Hence, to quantitatively analyze the asphaltene-water-clay interactions, the clay and water content in the asphaltenes from produced and residual oil have been determined with TGA/DSC and filtration and are presented in Table 6.

Table 6: Water and clay content in asphaltenes for 100 grams of bulk produced/residual oil

Sample	**Produced Oil**			**Residual Oil**			
				Inside SC*		**Outside SC***	
	Asp	**Water**	**Clay**	**Asp**	**Clay**	**Asp**	**Clay**
Bitumen	30.92	3.38	0	-	-	-	-
SAGD1	21.90	18.57	0	23.51	6.54	22.45	2.78
SAGD2	27.79	1.87	14.25	28.25	4.17	24.86	1.03

*SC: Steam chamber; All values provided in the above table are in grams, and are based on 100 grams of produced oil/residual oil

All the clays in the produced oil for SAGD2 are attached to the asphaltenes (compare Fig. 2 and Table 6). Even though, the water content in produced oil of SAGD2 is higher than for SAGD1 (Fig. 2), the amount of water attached to asphaltenes is higher for SAGD1 compared to SAGD2 (Table 6). The rest of the water is thought to interact with the deasphalted oil or lie in between the asphaltenes and resins. It is believed that this water is separated from deasphalted oil (maltenes) during separation of saturates, aromatics, and resins using ASTM D2007-11 standard method. The complex, triple emulsions in SAGD2 (Fig. 1C) are mainly governed by the type and/or particle size of

clay. Although the amount of water attached to asphaltenes in produced oil is higher for SAGD1 than SAGD2 (Table 6), there are no clays to strengthen the emulsion formation. This makes it easier for the water drops to coalesce, due to absence of clay layer (Alvarado et al., 2011; Kokal, 2005; Sztukowski and Yarranton, 2005) (Fig. 1B). It is concluded that it is not the actual weight of asphaltenes, but the intensity of asphaltene-clay-water interactions in the produced oil which defines the emulsions.

Although it is known that illite is more water-wet in nature compared to kaolinite (Bantignies et al., 1997), our results and analyses show that Clay2 (90 wt% kaolinite + 10 wt% illite) is interacting with the oil-phase (mostly with asphaltenes) in the produced oil, while this interaction is negligible in the produced oil for SAGD1 which had Clay1 (100 wt% kaolinite). This might be due to the fragmental structure of illite (Green and Willhite, 1998; Luffel et al., 1993; Nadia et al., 1984), which may favor the affinity of illite towards oil, compared to kaolinite-oil association. Also, studies on produced water obtained from these same experiments, SAGD1 and SAGD2, by Unal et al. (2015) show that clay migration into the produced water occurred for SAGD1 (Clay1), while no evident clay migration was observed in the produced water sample obtained from SAGD2 (Clay2). Owing to more water-wet nature of illite compared to kaolinite, illite is believed to interact with the injected steam and forms lumps with sand in the reservoir due to cementation (as observed by Unal et al., 2015). The cementation caused by the clay in the spent rock of SAGD2 leads to blocking of pore spaces, which can trap more residual oil in the cementation. This leads to a reduction in permeability and consequently, a poorer sweep

efficiency for SAGD2 compared to SAGD1 (Unal, 2014). Clay behavior varies with the nature and wetting conditions of the reservoir and the composition of the oil-in-place.

In this chapter, the effect of clay type on SAGD performance has been discussed to explain the factors which affect the quality of the produced oil. It has been established that the presence of illite in the reservoir leads to clay-asphaltene-water interactions in the produced oil due to clay migration, causing emulsions. The illite-oil association in the reservoir also retains the oil, reducing the overall sweep efficiency of the SAGD process. Most reservoirs of heavy oil have illite present in good proportions (Czarnecka and Gillott, 1980). Hence, there is a need to modify the SAGD technique to reduce the negative impact of clay type on the thermal EOR process.

3.2. Effect of Solvent Type and Injection Strategy

In this chapter, first, the produced oil obtained from 4 experiments- SAGD2, ES-SAGD1, ES-SAGD2 and ES-SAGD3 (Table 1) have been investigated to understand the factors affecting the quality of the produced oil and the oil displacement mechanism in pore scale for both SAGD and ES-SAGD processes. It should be noted that during ES-SAGD3, n-hexane and toluene were cyclically injected and the produced oil sample has been collected from toluene injection cycle. For ES-SAGD4, the experiment had to be terminated midway due to plugging in the production lines (Mukhametsina et al., 2015). Therefore, enough produced oil was not available for analysis for ES-SAGD4. For all 5 experiments, although the clay type is constant- Clay2 (90 wt% of kaolinite and 10 wt% of illite), the solvent type and injection strategy are varying (Table 1).

On addition of hydrocarbon solvents with steam in ES-SAGD, the cumulative oil recovery improved to 33.71 wt% for ES-SAGD1 (co-injection of n-hexane with steam), 45.15 wt% for ES-SAGD2 (co-injection of n-hexane and toluene with steam), and 44.91 wt% for ES-SAGD3 (cyclic-injection of n-hexane and toluene with steam) (Mukhametshina, 2013). The quality of the produced oil obtained from SAGD2, ES-SAGD1, ES-SAGD2, and ES-SAGD3 and the residual oil quality extracted from the spent rock (for inside and outside steam chamber zones) for SAGD2, ES-SAGD1, ES-SAGD2, ES-SAGD3, and ES-SAGD4 are analyzed in this chapter.

Microscopic images of emulsions in produced oil are compared with original bitumen. All images are with 100X magnification and are presented in Fig. 6. The produced oil samples show stable emulsions consisting of different sizes and types. In the case of SAGD1 (Fig. 6B), complex, triple emulsions (oil-in-water-in oil) are observed, which has been discussed earlier (Fig. 1C). For ES-SAGD produced oil samples, the emulsions are less complex compared to SAGD2. These are water-in-oil emulsions, as opposed to oil-in-water-in-oil emulsions observed in SAGD2. Also, the size of the water drops become smaller as we move from ES-SAGD1 to ES-SAGD3. Although the ES-SAGD emulsions seem to be more stable compared to SAGD2 (due to the smaller size of the water droplets suspended in the oil in ES-SAGD emulsions (Alvarado et al., 2011)), however, they are not so complex and might be easier to treat.

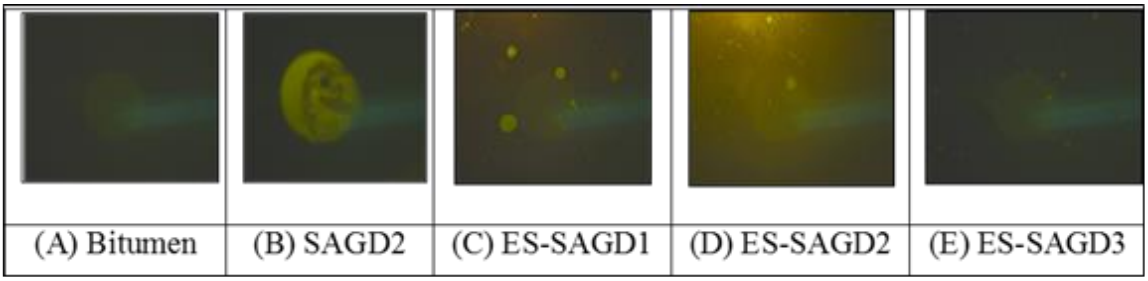

Figure 6: Microscopic images of emulsions in produced oil compared with original bitumen (100X magnification)

It is a known fact that emulsion complexity in oil increases with the viscosity of oil (Ezeuko et al., 2012). Hence, the viscosity and rheological properties of the produced oil samples are further investigated to see if they can provide information on the type of emulsions observed. The measured viscosity and API gravity at room temperature for the produced oil samples are 50,165 cP and 8.9 °API for SAGD2, 35,768 cP and 9.5° API for ES-SAGD1, 3,587 cP and 10.5 ° API for ES-SAGD2, and 3,667 cP and 10.1 ° API for ES-SAGD3 (Mukhametshina, 2013). The apparent viscosities of the samples as a function of shear stress to shear rate with increasing temperature are measured (Kar et al., 2014). The shear stress and corresponding shear rates have been measured at three different temperatures; 35 °C, 45 °C, and 55 °C. The results obtained have been compared with those of original bitumen sample (Table 7).

Power-law model, represented by the equation: $\sigma = K\gamma^n$ (Equation 1) in Table 7, is used to describe the rheology of the fluid, in where, σ = shear stress (dyne/cm^2) and γ = shear rate (1/sec). The ratio σ/γ gives apparent viscosity at a given temperature. K is the flow consistency index and n refers to flow behavior index (Green and Willhite, 1998).

Table 7: Rheological behavior of produced oil compared to original bitumen **(**Kar et al., 2014)

Samples	**Rheology at varying temperatures**				
	Temp (°C)	**Power Law Equation**	**K**	**n**	**R^2**
Bitumen	35	$\sigma = 133.35\gamma^{0.6888}$	133.35	0.6888	0.8576
	45	$\sigma = 31.254\gamma^{0.9762}$	31.254	0.9762	1
	55	$\sigma = 11.789\gamma^{0.9907}$	11.789	0.9907	0.9909
SAGD2	35	$\sigma = 504.44\gamma^{0.9117}$	504.44	0.9117	1
	45	$\sigma = 176.36\gamma^{0.9445}$	176.36	0.9445	1
	55	$\sigma = 75.49\gamma^{0.9623}$	75.49	0.9623	0.9999
ES-SAGD1	35	$\sigma = 126.06\gamma^{0.9578}$	126.06	0.9578	1
	45	$\sigma = 45.935\gamma^{0.9688}$	45.935	0.9688	1
	55	$\sigma = 18.68\gamma^{0.9900}$	18.68	0.9900	1
ES-SAGD2	35	$\sigma = 36.881\gamma^{0.9843}$	36.881	0.9843	1
	45	$\sigma = 16.394\gamma^{0.9995}$	16.394	0.9995	1
	55	$\sigma = 7.2404\gamma^{1.0419}$	7.2404	1.0419	0.9992
ES-SAGD3	35	$\sigma = 142.17\gamma^{1.0208}$	142.17	1.0208	0.9989
	45	$\sigma = 73.312\gamma^{0.9579}$	73.312	0.9579	0.9853
	55	$\sigma = 33.579\gamma^{1.0241}$	33.579	1.0241	0.9940

R represents the correlation coefficient which indicates the degree of linear relationship between the two variables. A value of R^2 near or equal to 1 indicates that the rheology fits into the power law model.

With the increase in temperature and shear stress, the apparent viscosity decreases for all cases (Table 7). The value of "n" is less than 1 in most cases, which indicates pseudoplastic (shear-thinning) behavior of produced oil (decrease in viscosity with increasing shear stress) (Bird et al., 2006). In all the cases, the Power Law model has been constructed with three readings each of viscosity change with change in shear rate. With greater number of readings, slight differences in the model are expected.

The water content in the produced oil and bitumen is determined through TGA/DSC analysis (Fig. 48, Fig. 54, Fig. 55, Fig. 56, Fig. 57), the clay content is measured by filtration (as explained in the Materials and Methods), and saturates, aromatics, resins, and asphaltenes fractions are separated through ASTM method for 100 grams each of original bitumen and produced oil samples (Fig. 7).

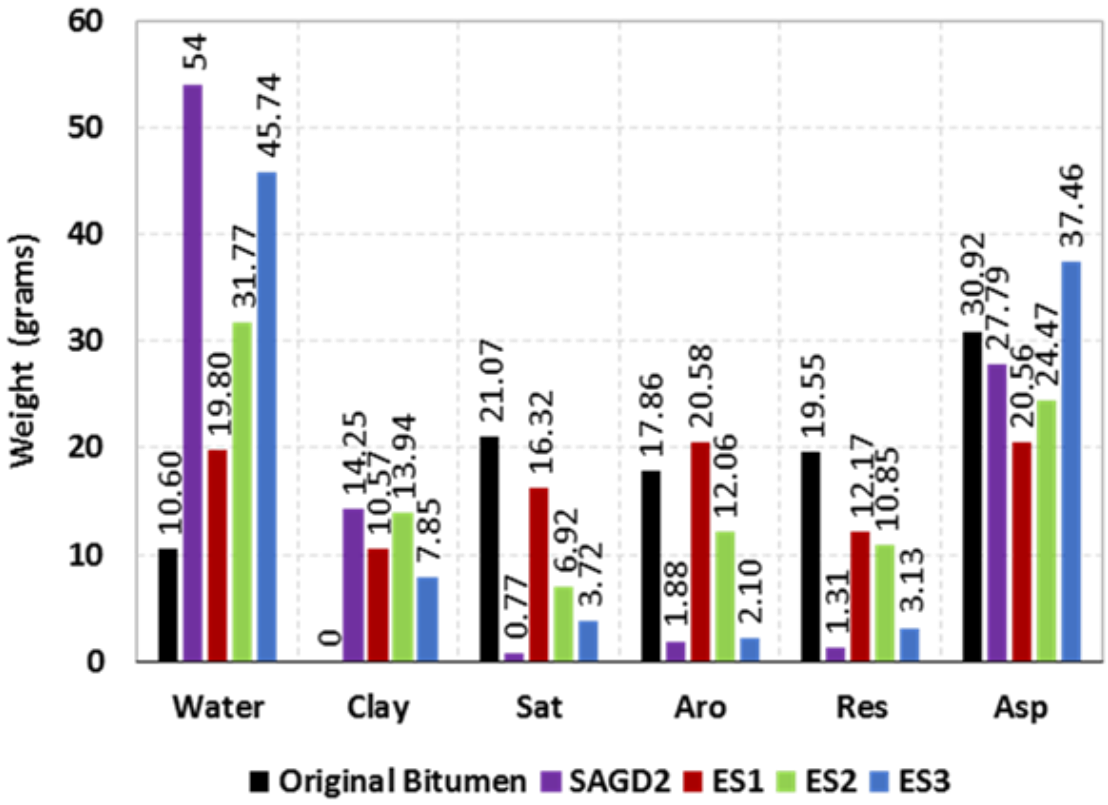

Figure 7: Normalized weight of water, clay, and SARA fractions on the basis of 100 grams of original bitumen and bulk produced oil
Sat: saturates, Aro: aromatics, Res: resins, Asp: asphaltenes; in bulk oil

The water content in produced oil is observed to be the highest for SAGD2 and considerably high even for ES-SAGD2 and ES-SAGD3 (Fig. 7). The lowest water content is found in the produced oil sample from ES-SAGD1 (19.80 grams). Clay content in produced oil is found to be highest for SAGD2 and reduced values for ES-SAGD1, ES-SAGD2, and ES-SAGD3 samples. This strong presence of both water and clays in the produced oil for SAGD2 can be linked to the triple emulsions observed (Fig. 6B). Considering the amount of water and clays in the produced oil samples for SAGD2 and

the ES-SAGD experiments, it is to be noted that the highest actual cumulative oil recovery is obtained from ES-SAGD1 (co-injection of n-hexane with steam) (Table 1).

The weight of asphaltenes including water and clays, in 100 grams of bulk oil, are found to be 43.91 gm for SAGD2, 24.09 gm for ES-SAGD1, 31.09 gm for ES-SAGD2, and 39.1 gm for ES-SAGD3. The weight of water and the asphaltenes (with attached water and clays) in the bulk oil are plotted in Fig.8.

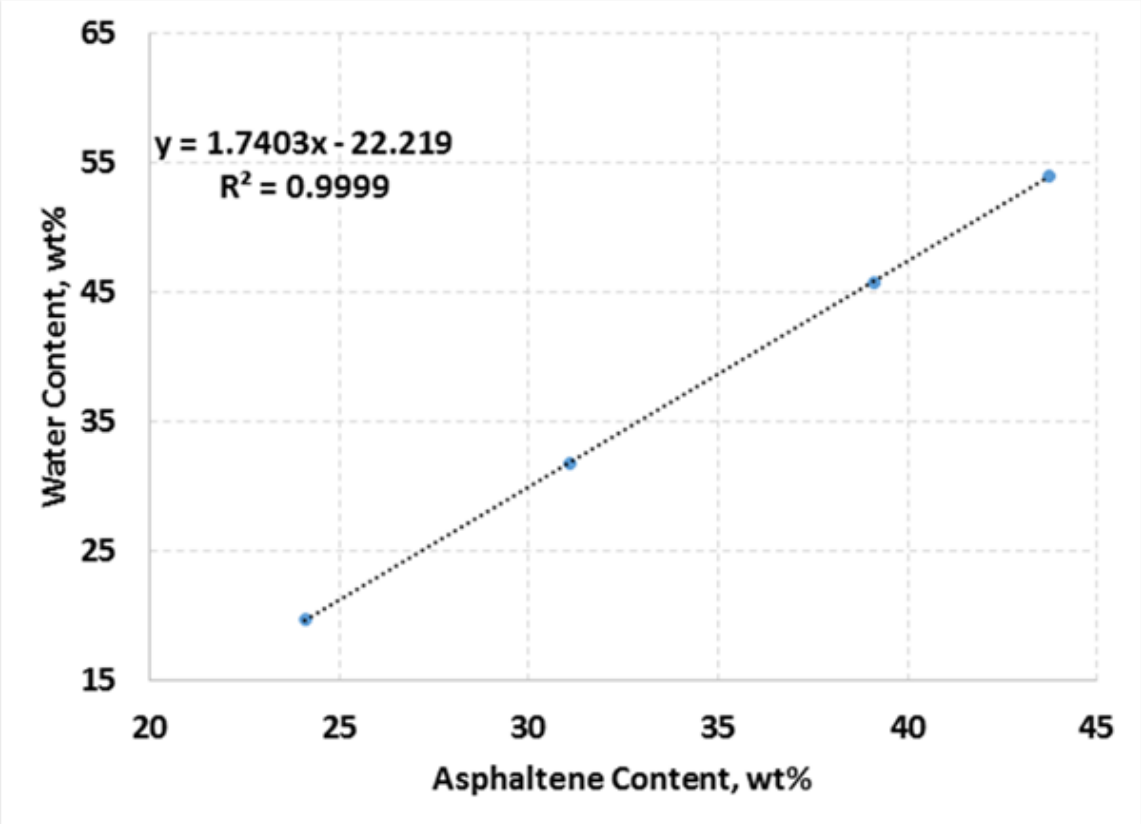

Figure 8: Relationship plotted between asphaltene content in the produced oil (x-axis) and water content in the produced oil (y-axis)

It is proved that the amount of water and asphaltenes (containing clays and water) present in bulk oil are linearly related (Fig. 8).

The determination of SARA fractions in Fig. 7 is based on 100 grams of bulk produced oil for all experiments. However, it is known that the oil production was not the same for every experiment (Table 1). Thus, additional material balance calculations have been performed, based on the weight of initial oil sand mixture and the amount of oil produced in the individual experiments. Based on these calculations, the overall precipitated and produced asphaltenes are represented in Table 8. Calculations for Table 8 are explained in Appendix IV (Table 18).

Table 8: Normalized wt% of precipitated and produced asphaltenes

Sample	**Precipitated Asphaltenes (wt%)**	**Produced Asphaltenes (wt%)**
SAGD1	32.92	38.42
SAGD2	27.77	87.53
ES-SAGD1	36.39	29.53
ES-SAGD2	30.63	45.06
ES-SAGD3	20.56	80.72
ES-SAGD4	34.59	-

The wt% of produced asphaltenes for ES-SAGD4 are missing as the experiment had to be terminated due to plugging in production lines (Mukhametshina et al., 2015). A

comparison of Fig. 7 and Table 8 show that there are wide variations in the values when moving from laboratory scale to field scale considerations. Fig. 7 values are based on ideal scenario, assuming that all experiments will have the same recovery. On the other hand, Table 8 calculations are based on the respective cumulative oil recoveries from each experiment, and represents the field scale better. In Table 8, on comparing the wt% of precipitated asphaltenes, the highest value is found for ES-SAGD1. This is because n-hexane is insoluble in asphaltenes, hence, it leaves behind the maximum amount of asphaltenes on the reservoir rock (Mullins, 2008). The amount of precipitated asphaltenes among the ES-SAGD experiments are the lowest for ES-SAGD2 and ES-SAGD3. The toluene present in these two ES-SAGD experiments dissolves the asphaltenes and carries it into the produced oil (Speight, 1999, Wiehe, 2012). Coming to the produced asphaltene wt% for ES-SAGD experiments, the highest and lowest values are obtained for ES-SAGD3 and ES-SAGD1, respectively. This supports the solubility and insolubility of asphaltenes in toluene and n-hexane, respectively. On comparing SAGD1 and SAGD2, it is observed that the wt% of precipitated asphaltenes are comparable, with SAGD1 slightly higher than SAGD2. However, in the produced oil, the wt% of asphaltenes are significantly higher for SAGD2 (87.53 wt%) than SAGD1 (38.42 wt%). It should be noted that this huge difference in the production of asphaltenes is caused only due to the presence of illite with kaolinite in the case of SAGD2, as compared to the presence of just kaolinite in SAGD1. This again reaffirms the fact that the clay type is one of the primary factors affecting SAGD performance.

Similar to Chapter 3.1, the type of emulsions observed in produced oil have been compared for SAGD2 and the ES-SAGD experiments, based on the number of endothermic peaks observed, and subsequent water evaporation in the TGA/DSC curves (Fig. 48, Fig. 54, Fig. 55, Fig. 56, Fig. 57). The results are summarized in Table 9.

Table 9: Water content in 100 grams of bulk produced oil and original bitumen (Fig. 48, Fig. 54, Fig. 55, Fig. 56, Fig. 57)

Sample	**Temp-Weight loss (°C-g)**	**Endotherm observed in DSC curves**						**Total water (g)**
		1st	**2nd**	**3rd**	**4th**	**5th**	**6th**	
Bitumen	**Temp.**	-	-	-	119.36	-	-	-
	Wt. loss	-	-	-	10.6	-	-	10.6
SAGD2	**Temp.**	86.5	96.5	-	119.01	-	131.51	-
	Wt. loss	2.15	1.35	-	8.54	-	41.96	54.0
ES-SAGD1	**Temp.**	-	92.73	-	-	125.23	130.23	-
	Wt. loss	-	2.52	-	-	8.95	8.33	19.8
ES-SAGD2	**Temp.**	-	93.95	-	-	126.45	131.45	-
	Wt. loss	-	2.81	-	-	18.15	10.81	31.77
ES-SAGD3	**Temp.**	83.56	106.06	111.06	113.56	121.06	128.56	-
	Wt. loss	5.19	3.67	3.25	2.2	6.56	24.87	45.74

For ES-SAGD1 and ES-SAGD2, the lowest number of endothermic peaks are observed which indicates that it will be easier to break the emulsions originated due to ES-SAGD1 and ES-SAGD2 by only thermal means with a lower amount of energy, than that required for SAGD2 and ES-SAGD3. Between ES-SAGD1 and ES-SAGD2, the water content is considerably low for the produced oil in ES-SAGD1. So, the produced oil obtained in this experiment has the lowest amount of water, which can be separated from the oil more easily compared to the other samples. This supports the use of n-hexane solvent as the best choice for ES-SAGD process, compared to cyclohexane and toluene, because asphaltenes are insoluble in n-hexane. From Table 9, it is observed that the highest number of endothermic peaks are observed for ES-SAGD3, even though the produced oil sample from this experiment has the lowest amount of clays and considerably low amount of resins (Fig. 7). However, this sample contains the highest amount of asphaltenes. In ES-SAGD3, the injection strategy is complex (Table 1). N-hexane and toluene are alternately co-injected with steam every hour. It is known that asphaltenes are soluble in toluene, but precipitate in the presence of n-hexane (Mullins, 2008; Speight, 1999; Wiehe, 2012). Due to this, the asphaltenes in the bulk oil will have different characteristics, some will be in dissolved phase and some will be in the form of aggregates. Since this particular sample is collected from toluene injection cycle, higher proportion of asphaltenes are expected to be in dissolved phase in the produced oil. Owing to this heterogeneity in the asphaltenes, the interaction between water and the asphaltenes becomes complex.

The residual oil extracted from inside and outside steam chamber zones have been investigated to enhance our understanding towards emulsion analysis.

Based on visual inspection of spent rock, unlike the comparison between SAGD1 and SAGD2 (in Chapter 3.1), in which there was a clear difference in color; there is no significant color difference in the spent rock for SAGD2 and the four ES-SAGD experiments (Fig. 9) (Mukhametshina, 2013). All the spent rock samples are considerably dark in color, indicating the presence of a good amount of residual oil in them (Table 11). However, the consolidation of the spent rock is different for different experiments. Due to the insolubility of asphaltenes in n-hexane, the spent rock from ES-SAGD1 is more consolidated (Fig. 9B).

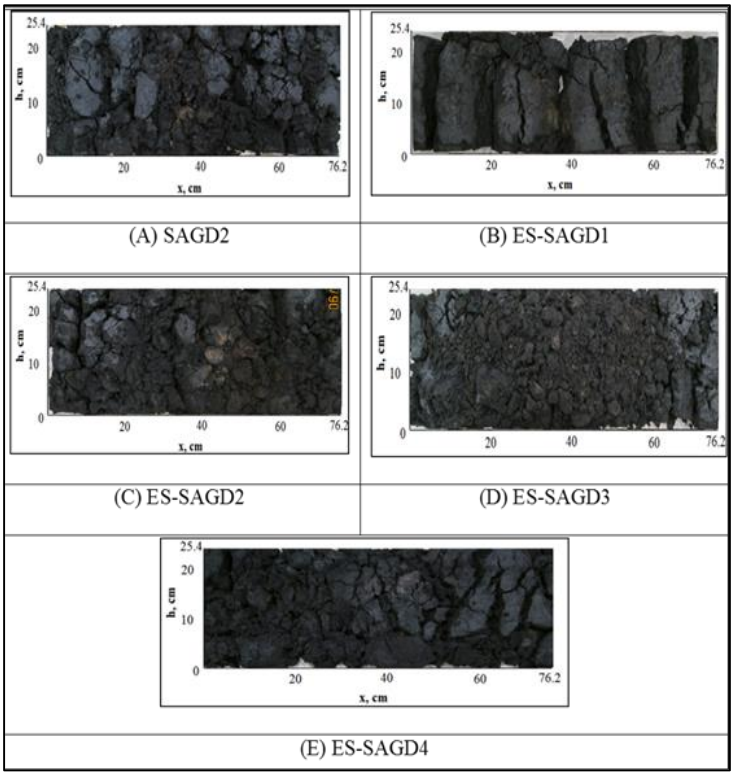

Figure 9: Visualization of the spent rock samples obtained after oil extraction for SAGD2, ES-SAGD1, ES-SAGD2, ES-SAGD3, and ES-SAGD4 (Mukhametshina, 2013)

To better understand the wettability of the samples, contact angle measurements are conducted, and are presented in Table 10.

Table 10: Water-air contact angle values for oil-sand packing and spent rock, inside and outside steam chamber **(**Kar et al., 2015)

Sample	**Water-Air Contact Angle Values (Degrees)**		
	Initial oil sand packing	**Inside steam chamber**	**Outside steam chamber**
SAGD2	95.27	121.44	113.11
ES-SAGD1	95.50	118.11	107.78
ES-SAGD2	102.24	117.22	97.58
ES-SAGD3	99.92	111.66	104.05
ES-SAGD4	101.40	93.89	112.83

Wettability analysis of the spent rock samples via contact angle measurements (between water and air) reveal that all the spent rock samples (including inside and outside steam chamber zones) are oil-wet in nature (Alotaibi et al., 2010). However, there are slight differences in the consolidation of the spent rock, which is further investigated by extraction of the residual oil.

The extraction of residual oil from spent rock is carried out first, using a 25 micron pore size filter paper. FTIR spectra of residual oil indicate presence of clays in them

(compare Fig. 12D with Fig. 28, Fig. 38). Then, using a filter paper with pore size of less than 2 microns, clays are separated from residual oil. The results (residual oil and clay content in spent rock) are summarized in Table 11, along with the amount of oil in 100 grams of initial oil-sand mixture before the experiment.

Table 11: Determination of residual oil and clay content in residual oil in terms of 100 grams of spent rock

Sample	**Inside steam chamber**		**Outside steam chamber**		**Oil in 100 grams of initial rock (grams)**
	Residual Oil (grams)	**Clay (grams)**	**Residual Oil (grams)**	**Clay (grams)**	
SAGD2	9.42	0.41	12.24	1.32	14.21
ES-SAGD1	10.91	0.03	11.78	1.06	14.19
ES-SAGD2	10.06	0.77	11.23	0.85	14.17
ES-SAGD3	10.57	1.26	11.80	1.43	14.17
ES-SAGD4	11.50	1.45	12.37	1.13	14.17

It is observed that for all the spent rock samples, amount of residual oil is lower for the inside steam chamber compared to the outside steam chamber regions. This shows the effectiveness of steam chamber and solvent expansion in improving the sweep efficiency of SAGD and ES-SAGD, inside steam chamber (Nasr et al., 2003). However, the amount of residual oil is higher for the ES-SAGD experiments compared to SAGD2, for the inside steam chamber zone. The ES-SAGD experiments become complicated due

to the presence of solvents. At the experimental conditions of 165 °C and 75 psig, n-hexane and cyclohexane are in vapor phase and toluene is in liquid phase (Fig. 63). This implies that n-hexane and cyclohexane will expand inside steam chamber, while toluene will remain in liquid form, at the bottom layer of the reservoir due to gravity, both in the inside and the outside steam chamber zones. Also, n-hexane is insoluble in asphaltenes, cyclohexane is partially soluble in asphaltenes, while toluene dissolves asphaltenes completely (Gray, 1994). Hence, the co-injection and cyclic-injection of these solvents with steam leads to complex mechanisms between the injected steam, solvents and the oil-in-place. For inside steam chamber, the highest sweep efficiency is observed for SAGD2 (which has the lowest residual oil). However, on moving from inside to outside steam chamber zone, the sweep efficiency for SAGD2 decreases considerably. This can be due to the poor development of temperature profile of steam chamber in the case of SAGD2 (Mukhametshina and Hascakir, 2014). This reduces the overall sweep efficiency, and thus, the cumulative oil recovery for SAGD2. For the outside steam chamber region, the highest sweep efficiency (or the lowest residual oil) is observed for ES-SAGD2 (which involves co-injection of n-hexane and toluene with steam). This is believed to be due to asphaltene-soluble nature of toluene, which is more effective in the bottom part of the reservoir outside steam chamber (due to the liquid phase of toluene). Toluene helps to dissolve the asphaltenes in the oil and reduces the residual oil content outside steam chamber for ES-SAGD2.

Another point to be noted is that the heterogeneity in the spent rock samples has to be taken into account. N-hexane and cyclohexane are more effective in the middle and

top portions of the reservoir, while toluene remains in the bottom layer due to the effect of gravity. Thus, the position from where the sample is picked for analysis from the inside and outside steam chamber zones is very important. Also, the results may vary for spent rock samples picked from different locations, even if they are from the same zone, inside or outside steam chamber, for the ES-SAGD experiments.

The spent rock samples were kept under the hood overnight, to remove free water present on the samples. FTIR spectra of residual oil (Fig. 28, Fig. 38) indicate that negligible water is left in the samples.

The clay content in the residual oil (Table 11), and the weight of SARA fractions (separated by ASTM method) in 100 grams of bulk residual oil, are presented in Fig. 10 and Fig. 11, for inside and outside steam chamber zones, respectively.

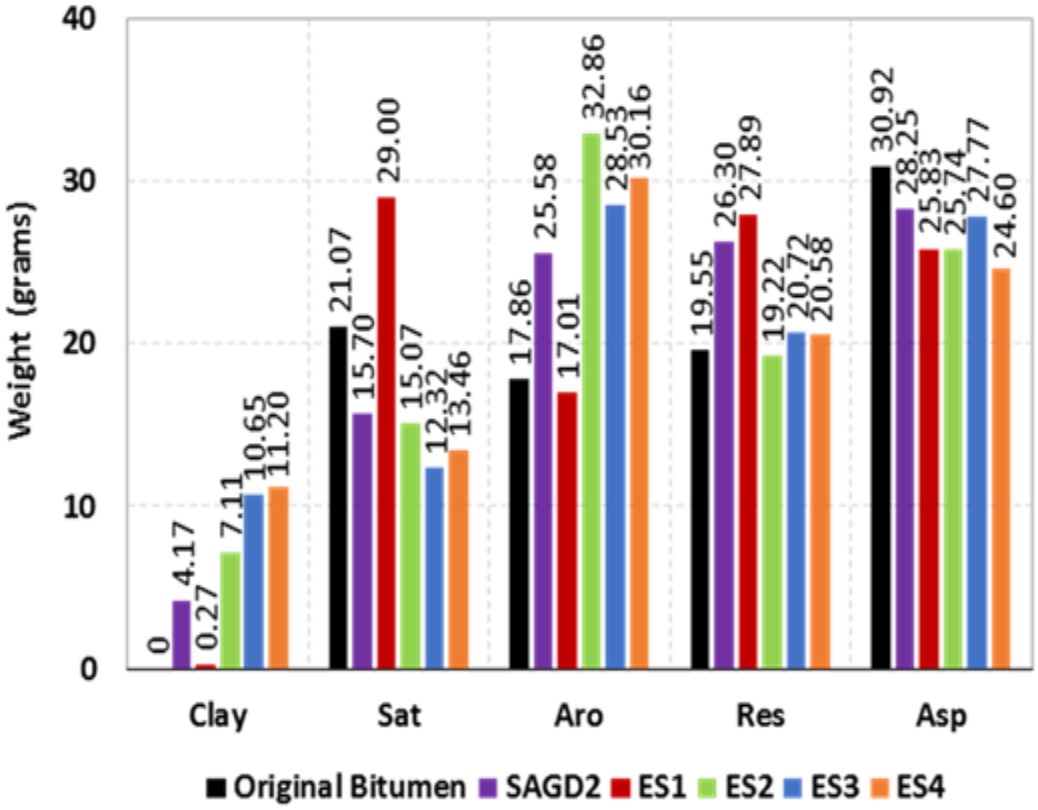

Figure 10: Normalized weight of clay and SARA fractions on the basis of 100 grams of original bitumen and residual oil inside steam chamber
Sat: saturates, Aro: aromatics, Res: resins, Asp: asphaltenes; in bulk oil

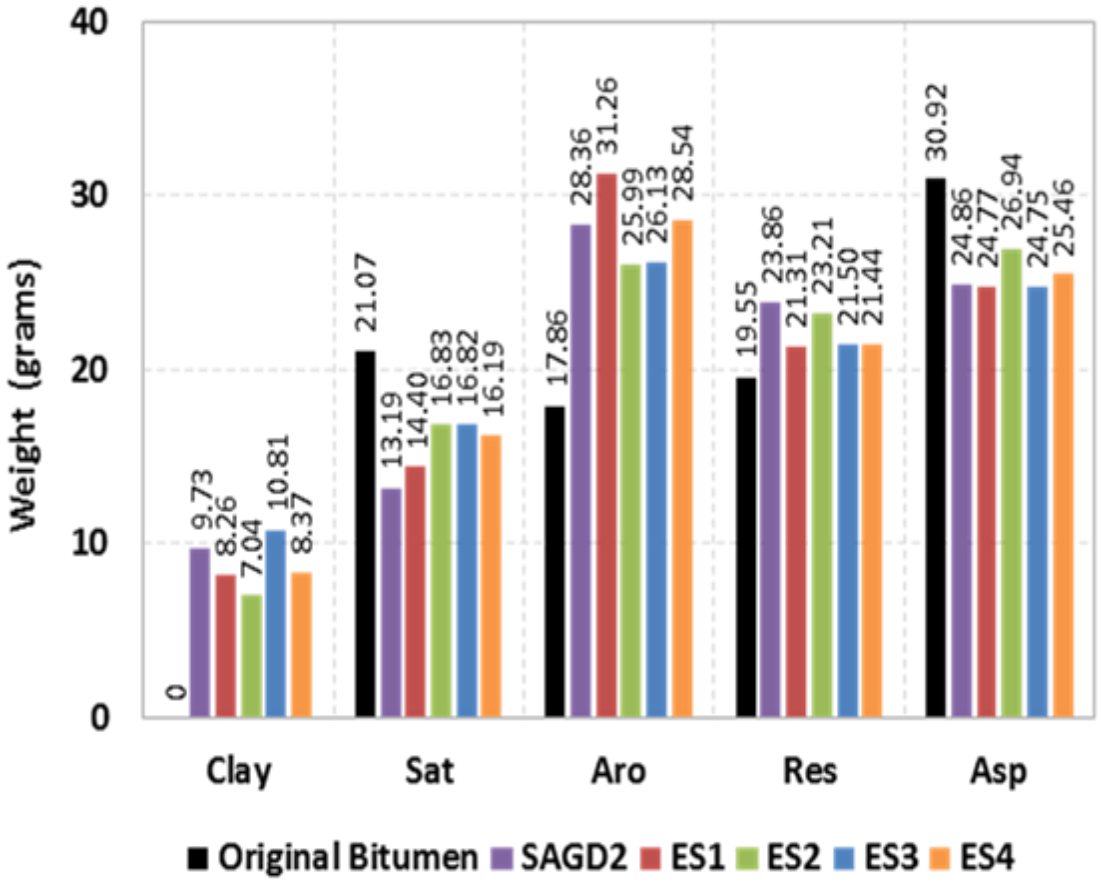

Figure 11: Normalized weight of clay and SARA fractions on the basis of 100 grams of original bitumen and residual oil outside steam chamber
Sat: saturates, Aro: aromatics, Res: resins, Asp: asphaltenes; in bulk oil

On comparing the SARA fractions in the residual oil for inside (Fig. 10) and outside steam chamber (Fig. 11), it is observed that the asphaltene content in the residual oil for all samples is less than that for original bitumen. Note that the values presented in Fig. 10 and Fig. 11 are based on 100 grams of bulk residual oil for all experiments. The results obtained on the basis of actual cumulative oil recoveries from the experiments have been discussed in Table 8. The FTIR spectra of saturates, aromatics, and resins fractions

for all the samples are comparable (Fig. 30, Fig. 32, Fig. 34, Fig. 40, Fig. 42, Fig. 44), and don't show any significant differences. Inside steam chamber, the clay content is lowest for residual oil of ES-SAGD1, and its saturates content is the highest (Fig. 10). This shows similar trend with the results obtained from produced oil analysis (Fig. 7), in which the clay content is low and the amount of saturates the highest, for produced oil of ES-SAGD1. For outside steam chamber (Fig. 11), the amounts of clay and SARA fractions in the residual oil are comparable for all the experiments. Therefore, no conclusive interpretation can be made from Fig. 11.

Similar to Table 5 in Chapter 3.1, the percentage of precipitated and moved asphaltenes have been determined for SAGD2 and the ES-SAGD experiments, for both the inside and the outside steam chamber regions, in Table 12. Calculations for Table 12 are explained in Appendix IV (Table 16). For the inside steam chamber zone, the percentage of precipitated asphaltenes is the highest for ES-SAGD3. It should be noted that ES-SAGD3 involved cyclic-injection of n-hexane and toluene with steam, and the experiment ended with n-hexane cycle (Table 1), asphaltenes being insoluble in n-hexane (Mullins, 2008; Speight, 1999). However, on comparing the values of precipitated and moved asphaltenes in the outside steam chamber zone, the values are close to each other and there is no significant difference between the experiments to make a strong argument. Also, these experiments involve complex injection strategies of solvents with different degrees of asphaltene solubility.

Table 12: Percentage distribution of precipitated and moved asphaltenes for inside and outside steam chamber zones based on 100 grams of asphaltenes in initial bitumen sample

Sample	**Inside steam chamber**		**Outside steam chamber**	
	Precipitated Asphaltenes (%)	**Moved Asphaltenes (%)**	**Precipitated Asphaltenes (%)**	**Moved Asphaltenes (%)**
SAGD2	85.22	14.77	79.62	20.38
ES-SAGD1	74.88	25.12	78.05	21.95
ES-SAGD2	80.11	19.89	83.78	16.22
ES-SAGD3	89.85	10.15	80.22	19.78
ES-SAGD4	80.09	19.91	80.33	19.67

The FTIR spectra of asphaltene samples separated from produced oil and residual oil indicate presence of clays and water in them (Fig. 24, Fig. 36, Fig. 46). Therefore, the clay content of asphaltenes in produced oil and residual oil is determined by filtration (as explained in Materials and Methods), and the amount of water in asphaltenes from produced oil is calculated by TGA/DSC (Fig. 52, Fig. 59, Fig. 60, Fig. 61, Fig. 62). The results are shown in Table 13.

Table 13: Water & clay content in asphaltenes for 100 grams of bulk produced/residual oil

Sample	Produced Oil			Residual Oil			
				Inside SC*		Outside SC*	
	Asp	Water	Clay	Asp	Clay	Asp	Clay
Bitumen	30.92	3.38	0	-	-	-	-
SAGD2	27.79	1.87	14.25	28.25	4.17	24.86	1.03
ES-SAGD1	20.56	0.74	2.79	25.83	0.27	24.77	1.88
ES-SAGD2	24.47	0.74	5.88	25.74	3.10	26.94	1.88
ES-SAGD3	37.46	1.64	0	27.77	3.08	24.75	6.42
ES-SAGD4	-	-	-	24.60	2.41	25.46	5.54

*SC: Steam chamber; All values provided in the above table are in grams, and are based on 100 grams of produced oil/residual oil

From Table 13, the water content in the asphaltenes from produced oil are comparable for all samples, although it is the highest for SAGD2. The clay content is significantly high for SAGD2, very low for ES-SAGD1 and ES-SAGD2, and negligible for ES-SAGD3. The FTIR spectra of asphaltenes (Fig. 24) support these results. For ES-SAGD3, significant presence of water in asphaltenes does not increase the emulsion complexity due to absence of clay particles to act as an emulsifier. This finding is similar to the comparison of emulsions in the produced oil between SAGD1 and SAGD2 (Table 4). The low amount of water interacting with the asphaltenes and clays (Table 13) shows that Clay2 (90 wt% kaolinite and 10 wt% illite), which has been used in all experiments

in this chapter, has little affinity towards water. This supports the discussion made in Chapter 3.1. Also, the reduced amount of clays attached to the asphaltenes in the produced oil and inside the steam chamber for the ES-SAGD experiments (Table 13) is indicative of the presence of an additional solvent layer which alleviates the clay-asphaltene interaction.

The oil recovery is calculated for all 5 experiments after removing the contribution of water and clays present in the produced oil. These values are compared with the cumulative oil recovery (with clays and water) obtained after the experiments, and are presented in Table 14. Calculations for Table 14 are explained in Appendix IV (Table 17).

Table 14: Actual oil recovery vs cumulative oil recovery **(*** Mukhametshina, 2013**)**

Experiment	**Actual Oil Recovery (wt%)**	**Cumulative Oil Recovery (wt%)***
SAGD1	27.03	47.41
SAGD2	10.20	32.12
ES-SAGD1	23.47	33.71
ES-SAGD2	24.52	45.15
ES-SAGD3	20.84	44.91

After removing the weight of water and clays from the oil, the oil recovery is considerably reduced for all experiments (Table 14). The highest actual oil recovery is observed for SAGD1 (27.03 wt%), which had kaolinite, while the lowest oil recovered is from SAGD2 (10.20 wt%), which had a mixture of 90 wt% kaolinite and 10 wt% illite

(Table 1). It is clear that the clay type (presence of illite) is the most affecting factor with respect to the oil recovery. However, the oil recovery is considerably increased for Clay2 type by applying ES-SAGD. The actual oil recovery from ES-SAGD1 (23.47 wt%) and ES-SAGD2 (24.52 wt%) is close to that obtained from SAGD1. Hence, for Peace River bitumen, co-injection of n-hexane, and co-injection of n-hexane and toluene are favorable injection strategies for ES-SAGD.

To interpret the stability of the asphaltenes and their affinity towards water in the emulsions of the produced oil samples, zeta potential of the asphaltenes is calculated by following the procedure explained in Chapter 2. The zeta potential values have been measured for asphaltenes, both before and after removal of clays from them, to analyze the effect of clay on asphaltene stability in the produced oil. The results are presented in Table 15.

Table 15: Zeta Potential Measurements of asphaltenes in produced oil compared to asphaltenes in original bitumen

Experiment	**Zeta Potential of Asphaltenes in Produced Oil (mV)**	
	With Clays	**Without Clays**
Bitumen	-32.18	-32.18
SAGD1	-37.84	-37.84
SAGD2	-22.55	-26.02
ES-SAGD1	-22.09	-22.01
ES-SAGD2	-20.82	-20.61
ES-SAGD3	-19.13	-19.13

Lower the zeta potential value, lower is the stability of the colloids in the suspension and lower is the water-wetness of the particles in the suspension (Quan et al., 2012). The same values are provided for zeta potential of asphaltenes with and without clays for original bitumen, SAGD1, and ES-SAGD3, since these samples do not contain clays (Table 6, Table 13). The zeta potential values of the asphaltenes are the highest for SAGD1 and original bitumen, compared to the rest of the samples (Table 15). This means that the asphaltenes in the bulk oil for SAGD1 and original bitumen are more stable than the other asphaltene samples. Since the asphaltenes in the produced oil for SAGD1 have a lesser tendency to precipitate, the complexity of emulsions observed in the produced oil is much less (Fig. 1B). This is because, due to the stability of asphaltenes in the oil, there will be lesser tendency for asphaltenes to precipitate, aggregate and strengthen the

interfacial film between oil and water in the emulsions. In case of SAGD2, higher absolute value of zeta potential after clay removal implies that once the clay layer is separated, the affinity of asphaltenes towards water increases. This is interpreted as a presence of clay layer between the asphaltenes and water layer in the produced oil of SAGD2, which leads to the triple emulsions observed (Fig. 6B). The zeta potential values are not significantly different for ES-SAGD1 and ES-SAGD2 before and after clay removal. This means that the clay layer is not actually interfering with the asphaltenes and water layer in the produced oil for ES-SAGD1 and ES-SAGD2. Hence, these emulsions are not complex in nature (Fig 6C and Fig. 6D). The zeta potential values of asphaltenes for the ES-SAGD experiments are not significantly different and no conclusive statement can be made based on these values (Table 15). The interpretation of zeta potential values becomes complicated due to the presence of multiple polar components in the produced oil samples; resins, and water, which can interact with the asphaltenes and also among themselves. Nguyen et al. (2014) conducted zeta potential measurements on water-oil emulsions to interpret the emulsion stability. They could not get conclusive results due the presence of complex asphaltene-resin-water network in the emulsions.

CHAPTER IV

CONCLUSIONS

In this thesis, the produced oil and spent rock samples obtained from two SAGD and four ES-SAGD experiments were analyzed to investigate the contribution of clay type, amount of clays, water, and SARA fractions in the emulsions observed in the produced oil. The spent rock samples were also examined to determine wettability alterations and pore-scale displacement.

Changing the clay type from a mixture of kaolinite and illite (in SAGD2) to kaolinite (in SAGD1) resulted in more than 100% increase in oil production. The complex, oil-in-water-in-oil emulsions observed in the produced oil for SAGD2, containing illite, was interpreted to be due to the presence of both water and clays in considerable amounts in the produced oil. The clay migrated into the oil phase and strengthened the interfacial film of asphaltenes around the water droplets in the produced oil. In the spent rock, for the inside steam chamber zone, kaolinite-residual oil interactions were significant in SAGD1. However, outside the steam chamber zone, higher amount of oil was retained due to increased association of illite with residual oil in SAGD2, which lowered the sweep efficiency and oil recovery in SAGD2.

The presence of polar oil components and the process conditions (temperature and pressure) of SAGD influence the wettability by altering the clays, either chemically or physically. The fragmental structure of illite favored trapping of the oil phase due to pore cementing behavior of illite.

Keeping the clay type constant, ES-SAGD resulted in higher oil recovery compared to SAGD. The highest oil recovery was calculated for ES-SAGD with n-hexane, and ES-SAGD with co-injection of n-hexane and toluene. However, when the water content of produced oil is considered, since n-hexane results in lesser water, it might be preferred more as a solvent for ES-SAGD, compared to toluene.

It is seen that the clay type and size are the major factors affecting emulsion formation. In ES-SAGD, the addition of solvent layer at the interfacial film between water and asphaltenes reduces the interaction of clays with these polar components in the produced oil. We recommend the use of asphaltene non-solvents during ES-SAGD to reduce the formation of emulsions. Finally, clay type of the reservoir should be determined prior to either SAGD or ES-SAGD and accordingly, solvent selection should be made.

REFERENCES

Acosta, E. 2010. "Achieving Sustainable, Optimal SAGD Operations." Journal of Petroleum Technology, Vol. 62(11), 24-28.

Agrawala, M., Yarranton, H. W. 2001. "An Asphaltene Association Model Analogous to Linear Polymerization." Industrial and Engineering Chemistry Research, Vol. 40(21), 4664-4672.

Alotaibi, M. B., Azmy, R. M., Nasr-El-Din, H. A. 2010. "Wettability Studies Using Low-Salinity Water in Sandstone Reservoirs." Offshore Technology Conference, Houston, Texas, USA.

Alvarado, V., Wang, X., Moradi, M. 2011. "Stability Proxies for Water-in-Oil Emulsions and Implications in Aqueous-based Enhanced Oil Recovery." Energies, Vol. 4(7), 1058-1086.

Amyx, J. W., Bass, D. M., Whiting, R. L., 1960. "Petroleum Reservoir Engineering" McGraw Hill, ISBN 07-001600-3: 103-104.

Anderson, W. G. 1986. "Wettability Literature Survey- Part 1: Rock/Oil/Brine Interactions, and the Effects of Core Handling on Wettability." Journal of Petroleum Technology, Vol. 38(10), 1125-1149.

ASTM. 2011. "D2007-11: Standard Test Method for Characteristic Groups in Rubber Extender and Processing Oils and Other Petroleum-Derived Oils by the Clay-Gel Absorption Chromatographic Method."

Attanasi, E. D., Meyer, R. F. 2010. "Natural Bitumen and Extra-Heavy Oil." World Energy Council. London, UK. http://www.worldenergy.org/documents/ser_2010_report_1.pdf, Accessed on 10/15/2013.

Baker, L. E. 1988. "Three-Phase Relative Permeability Correlations." SPE Enhanced Oil Recovery Symposium, 16-21 April, Tulsa, Oklahoma, USA. SPE-17369-MS.

Bantignies, J. –L., Moulin, C. C. D., Dexpert, H. 1997. "Wettability Contrasts in Kaolinite and Illite Clays: Characterization by Infrared and X-Ray Absorption Spectroscopies." Clays and Clay Minerals, Vol. 45(2), 184-193.

Bayliss, P., Levinson, A. A. 1976. "Mineralogical Review of the Alberta Oil Sand Deposits (Lower Cretaceous, Mannville Group)." Bulletin of Canadian Petroleum Geology, Vol. 24(2), 211-224.

Bennion, D. B., Thomas, F. B., Sheppard, D. A. 1992. "Formation Damage Due to Mineral Alteration and Wettability Changes During Hot Water and Steam Injection in Clay-Bearing Sandstone Reservoirs." SPE Formation Damage Control Symposium, 26-27 February, Lafayette, Louisiana, USA. SPE-23783-MS.

Binner, E. R., Robinson, J. P., Silvester, S. A., Kingman, S. W., Lester, E. H. 2014. "Investigation into the Mechanisms by which Microwave Heating Enhances Separation of Water-in-Oil Emulsions." Fuel, Vol. 116, 516-521.

Bird, R. B., Stewart, W. E., Lightfoot, E. N. 2006. "Transport Phenomena, Revised 2nd Edition."

Butler, R. M. 1980. "A Method for Continuously Producing Viscous Hydrocarbons by Gravity Drainage While Injecting Heated Fluids." UK Pat. Appl GB 2,053,328.

Butler, R. M., 1991. "Thermal Recovery of Oil and Bitumen". Prentice Hall Inc., New Jersey.

Butler, R. M. 1998. "SAGD Comes of Age!" Journal of Canadian Petroleum Technology, Vol. 37(7), 9-12.

Butler, R. M., McNab, G. S., Lo, H. Y. 1979. "Theoretical Studies on the Gravity Drainage of Heavy Oil During In-Situ Steam Heating." 29th Canadian Chemical Engineering Conference, Sarnia, Ontario, Canada.

Chen, K., Liu, H., Guo, A., Ge, D., Wang, Z. 2012. "Study of the Thermal Performance and Interaction of Petroleum Residue Fractions during the Coking Process." Energy & Fuels, 26(10), 6343-6351.

Czarnecka, E., Gillott, J. E. 1980. "Formation and Characterization of Clay Complexes with Bitumen from Athabasca Oil Sand." Clay and Clay Minerals, Vol. 28(3), 197-203.

da Silva, E. B., Santos, D., de Brito, M. P., Guimaraes, R. C. L., Ferreira, B. M. S., Freitas, L. S., de Campos, M. C. V., Franceschi, E., Dariva, C., Santos, A. F., Fortuny, M. 2014. "Microwave Demulsification of Heavy Crude Oil Emulsions: Analysis of Acid Species Recovered in the Aqueous Phase." Fuel, Vol. 128, 141-147.

Dean, J. A. 1998. "Lange's Handbook of Chemistry, 15th Edition", McGraw-Hill, Inc. p. 1476, ISBN 0-07016384-7.

Deo, M. and Hanson, F. 1993. “Asphaltene Precipitation: A Need for a Broader View.” SPE International Symposium on Oilfield Chemistry, 2-5 March, New Orleans, Louisiana, USA. SPE-25193-MS.

Escrochi, M., Nabipour, M., Ayatollahi, S. S., Mehranbod, N. 2008. “Wettability Alteration at Elevated Temperatures: The Consequences of Asphaltene Precipitation.” SPE International Symposium and Exhibition on Formation Damage Control, 13-15 February, Lafayette, Louisiana, USA. SPE-112428-MS.

Evdokimov, I. N., Losev, A. P. 2014. “Microwave Treatment of Crude Oil Emulsions: Effects of Water Content.” Journal of Petroleum Science and Engineering, Vol. 115, 24-30.

Ezeuko, C. C., Wang, J., Gates, I. D. 2012. “Investigation of Emulsion Flow in SAGD and ES-SAGD.” SPE Heavy Oil Conference, 12-14 June, Calgary, Alberta, Canada. SPE-157830-MS.

Fingas, M. 2014. “Water-in-Oil Emulsions: Formation and Prediction” Journal of Petroleum Science Research, Vol. 3(1).

Gonzalez, G., Sousa, M. A., Lucas, E. F. 2006. “Asphaltenes Precipitation from Crude Oil and Hydrocarbon Media.” Energy & Fuels, Vol. 20(6), 2544-2551.

Goual, L., Firoozabadi, A. 2002. “Measuring Asphaltenes and Resins, and Dipole Moment in Petroleum Fluids.” American Institute of Chemical Engineers Journal, Vol. 48(11), 2646-2663.

Goual, L., Firoozabadi, A. 2004. “Effect of Resins and DBSA on Asphaltene Precipitation from Petroleum Fluids.” American Institute of Chemical Engineers Journal, Vol. 50(2), 470-479.

Gray, M. R. 1994. “Upgrading Petroleum Residues and Heavy Oils.” New York, Marcel Dekker, Inc. CRC press.

Green, D. W. and Willhite, G. P. 1998. “Enhanced oil recovery.” Richardson, Tex.: Henry L. Doherty Memorial Fund of AIME, Society of Petroleum Engineers.

Groenzin, H., Mullins, O. C. 2000. “Molecular Size and Structure of Asphaltenes from Various Sources.” Energy & Fuels, Vol. 14(3), 677-684.

Haghighat, P. and Maini, B. B. 2010. “Role of Asphaltene Precipitation in VAPEX Process.” Journal of Canadian Petroleum Technology, Vol. 49(3), 14-21.

Hamm, R. A., Ong, T. S. 1995. “Enhanced Steam-Assisted Gravity Drainage: A New Horizontal Well Recovery Process for Peace River, Canada.” Journal of Canadian Petroleum Technology, Vol. 34(4), 33-40.

Hodgman, C. D. 1962. “CRC Handbook of Chemistry and Physics, 44th Edition.”

Jones, F., Tran, H., Lindberg, D., Zhao, L., Hupa, M. 2013. “Thermal Stability of Zinc Compounds.” Energy & Fuels, Vol. 27(10), 5663-5669.

Kar, T., Williamson, M., Hascakir, B. 2014. “The Role of Asphaltenes in Emulsion Formation for Steam Assisted Gravity Drainage (SAGD) and Expanding Solvent SAGD (ES-SAGD).” SPE Heavy and Extra Heavy Oil Conference- Latin America, 24-26 September, Medellin, Colombia. SPE-171076-MS.

Kar, T., Hascakir, B. 2015. “The Role of Resins, Asphaltenes, and Water in Water-Oil Emulsion Breaking with Microwave Heating.” Energy & Fuels, Vol. 29(6), 3684-3690.

Kar, T., Yeoh, J., Ovalles, C., Rogel, E., Benson, I. P., Hascakir, B. 2015. “The Impact of Asphaltene Precipitation and Clay Migration on Wettability Alteration for Steam Assisted Gravity Drainage (SAGD) and Expanding Solvent-SAGD (ES-SAGD).” SPE Heavy Oil Conference, 9-11 June, Calgary, Alberta, Canada. SPE-174439-MS.

Kilpatrick, P. K. 2012. “Water-in-Crude Oil Emulsion Stabilization: Review and Unanswered Questions.” Energy & Fuels, Vol. 26(7), 4017-4026.

Kokal, S. L. 2005. "Crude Oil Emulsions: A State-of-the-Art Review." SPE Production & Facilities 20(01), 5-13. SPE-77497-PA.

Kovscek, A. 2012. "Emerging Challenges and Potential Futures for Thermally Enhanced Oil Recovery." Journal of Petroleum Science and Engineering, Vol. 98-99, 130-143.

Krüss DSA3 Software for Drop Shape Analysis, 2004-2011. “User Manual Part 1: Installation, Introduction, Working in Standard Mode.” Vol. 1.8(2), Krüss GmbH, Hamburg.

Leontaritis, K., Amaefule, J., Charles, R. E. 1994. "A Systematic Approach for the Prevention and Treatment of Formation Damage Caused by Asphaltene Deposition." SPE Production & Facilities 9(03), 157-164. SPE-23810-PA.

Long, R. B. 1982. “The Concept of Asphaltenes.” Chemistry of Asphaltenes, Chapter 2, 17-27.

Luffel, D. L., Herrington, K. L., Walls, J. D. 1993. “Effect of Drying on Travis Peak Cores Containing Fibrous Illite.” SPE Advanced Technology Series, Vol. 1(01), 188-194. SPE-20725-PA.

Martinez-Palou, R., Ceron-Camacho, R., Chavez, B., Vallejo, A. A., Villanueva-Negrete, D., Castellanos, J., Karamath, J., Reyes, J., Aburto, J. 2013. “Demulsification of Heavy Crude Oil-in-Water Emulsions: A Comparative Study between Microwave and Thermal Heating.” Fuel, Vol. 113, 407-414.

McCain, W. D. 1990. “The Properties of Petroleum Fluids. Second Edition.” 17, PennWell Books.

McLean, J. D.; Kilpatrick, P. K. 1997. “Effects of Asphaltene Aggregation in Model-Toluene Mixtures on Stability of Water-in-Oil Emulsions.” Journal of Colloid and Interface Science, Vol. 196(1), 23-34.

Minnie, J. 1933. “Treatment of Crude Oil Emulsions”. World Petroleum Congress, 18-24 July, London, UK. WPC-1117.

Mohammadzadeh, O., Rezaei, N., Chatzis, I. 2010. "Pore-Level Investigation of Heavy Oil and Bitumen Recovery Using Solvent− Aided Steam Assisted Gravity Drainage (SA-SAGD) Process." Energy & Fuels 24(12), 6327-6345.

Mojelsky, T. W., Ignasiak, T. M., Frakman, Z., McIntyre, D. D., Lown, E. M., Montgomery, D. S., Strausz, O. P. 1992. “Structural Features of Alberta Oil Sand Bitumen and Heavy Oil Asphaltenes.” Energy & Fuels, Vol. 6(1), 83-96.

Mokrys, I. J., Butler, R. M. 1993. “In-Situ Upgrading of Heavy Oil and Bitumen by Propane Deasphalting: The VAPEX Process.” SPE Production Operations Symposium, 21-23 March, Oklahoma City, Oklahoma, USA. SPE-25452-MS.

Morrow, A., Mukhametshina, A., Aleksandrov, D., Hascakir, B. 2014. “Environmental Impact of Bitumen Extraction with Thermal Recovery.” SPE Heavy Oil Conference, 10-12 June, Calgary, Alberta, Canada. SPE-170066-MS.

Mukhametshina, A. 2013. “Reducing the Environmental Impact of Bitumen Extraction with ES-SAGD.” MSc Thesis, Texas A&M University.

Mukhametshina, A., Hascakir, B. 2014 “Bitumen Extraction by Expanding Solvent-Steam Assisted Gravity Drainage (ES-SAGD) with Asphaltene Solvents and Non-Solvents” SPE Heavy Oil Conference, 10-12 June, Calgary, Alberta, Canada. SPE-170013-MS.

Mukhametshina, A., Kar, T., Hascakir, B. 2015. "Asphaltene Precipitation during Bitumen Extraction with Expanding Solvent Steam Assisted Gravity Drainage (ES-SAGD): Effects on Pore-Scale Displacement." SPE Journal, In Press.

Mukhametshina, A., Morrow, A., Aleksandrov, D., Hascakir, B. 2014. "Evaluation of Four Thermal Recovery Methods for Bitumen Extraction." SPE Western North America and Rocky Mountain Joint Regional Meeting, 16-18 April, Denver, Colorado, USA. SPE-169543-MS.

Mullins, O. C., Sheu, E. Y., Hammami, A., Marshall, A. G. 2007. "Asphaltenes, Heavy Oils, and Petroleomics." Springer Science+Business Media, LLC.

Mullins, O. C. 2008. "Review of the Molecular Structure and Aggregation of Asphaltenes and Petroleomics." SPE Journal, Vol. 13(1), 48-57. SPE-95801-PA.

Nadeau, P. H. 1998. "An Experimental Study of the Effects of Diagenetic Clay Minerals on Reservoir Sands." Clays and Clay Minerals, Vol. 46(1), 18-26.

Nadia P., Wilson, J., McHardy, B. 1984. "The Relationship between Permeability and the Morphology of Diagenetic Illite in Reservoir Rocks." Journal of Petroleum Technology, Vol. 36(12), 2225-2227.

Nasr, T. N., Beaulieu, G., Golbeck, H., 2003. "Novel Expanding Solvent-SAGD Process "ES-SAGD"." Journal of Canadian Petroleum Technology, Vol. 42(1), 13-16.

Nasr, T. N., Kimber, K. D., Vendrinsky, D. A., Jha, K. N. 1991. "Process Enhancement in Horizontal Wells through the use of Vertical Drainage Channels and Hydrocarbon Additives." SPE Western Regional Meeting, 20-22 March, Long Beach, California, USA. SPE-21794-MS.

Nenningsland, A. L., Gao, B., Simon, S., Sjoblom, J. 2011. "Comparative Study of Stabilizing Agents for Water-in-Oil Emulsions." Energy & Fuels, Vol. 25(12), 5746-5754.

Nguyen, D., Phan, T., Hera, J. 2010. "Oil-Water Separation of Fluids Resulting from Chemical EOR Applications." Rio Oil and Gas Expo and Conference, 13-16 September, Rio de Janeiro, Brazil. IBP2114-10.

Nguyen, D., Balsamo, V. 2013. "Emulsification of Heavy Oil in Aqueous Solutions of Poly(Vinyl Alcohol): A Method for Reducing Apparent Viscosity of Production Fluids." Energy & Fuels, Vol. 27(4), 1736-1747.

Nguyen, D., Balsamo, V., Phan, J. 2013. “Effect of Diluents on Interfacial Properties and SAGD Emulsion Stability: I. Interfacial Rheology.” SPE Heavy Oil Conference, 11-13 June, Calgary, Alberta, Canada. SPE-165405-MS.

Nguyen, D., Balsamo, V., Phan, J. 2014. “Effect of Diluents and Asphaltenes on Interfacial Properties and Steam-Assisted Gravity Drainage Emulsion Stability: Interfacial Rheology and Wettability.” Energy & Fuels, Vol. 28(3), p 1641-1651.

Pang, Z. X., Liu, H. Q., Liu, X. L. 2010. "Characteristics of Formation Damage and Variations of Reservoir Properties during Steam Injection in Heavy Oil Reservoir." Petroleum Science and Technology, Vol. 28(5), 477-493.

Parra-Barraza, H., Hernandez-Montiel, D., Lizardi, J., Hernandez, J., Urbina, R. H., Valdez, M. A. 2003. “The Zeta Potential and Surface Properties of Asphaltenes Obtained with Different Crude oil/n-heptane Proportions.” Fuel, Vol. 82(8), 869-874.

Pietrangeli, G., Quintero, L., Jones, T., Darugar, Q. 2014. “Treatment of Water in Heavy Crude Oil Emulsions with Innovative Microemulsion Fluids.” SPE Heavy and Extra Heavy Oil Conference: Latin America, 24-26 September, Medellin, Colombia. SPE-171140-MS.

Poston, S. W., Ysrael, S., Hossain, A. K. M. S., Montgomery III, E. F. 1970. “The Effect of Temperature on Irreducible Water Saturation and Relative Permeability of Unconsolidated Sands.” SPE Journal, Vol. 10(2). SPE-1897-PA.

Poteau, S., Argillier, J. F., Langevin, D., Pincet, F., Perez, E. 2005. “Influence of pH on Stability and Dynamic Properties of Asphaltenes and Other Amphiphilic Molecules at the Oil-Water Interface.” Energy & Fuels, Vol. 19(4), 1337-1341.

Quan, X., Jiazhong, W., Jishun, Q., Qingjie, L., Desheng, M., Li, L., Manli, L. 2012. “Investigation of Electrical Surface Charges and Wettability Alteration by Ions Matching Waterflooding.” International Symposium of the Society of Core Analysts, 27-30 August, Aberdeen, Scotland, UK.

Rajakovic, V., Skala, D. 2006. “Separation of Water-in-Oil Emulsions by Freeze/Thaw Method and Microwave Radiation.” Separation and Purification Technology, Vol. 49(2), 192-196.

Schembre, J. M., Kovsek, A. R. 2004. “Thermally Induced Fines Mobilization: Its Relationship to Wettability and Formation Damage.” SPE International Thermal Operations and Heavy Oil Symposium and Western Regional Meeting, 16-18 March, Bakersfield, California, USA. SPE-86937-MS.

Shkalikov, N. V, Vasil'ev, S. G., Skirda, V. K. 2010. "Peculiarities of Asphaltene Precipitation in n-Alkane–Oil Systems." Colloid Journal, Vol. 72(1), 133–140.

Speight, J. G. 1999. "The Chemistry and Technology of Petroleum", 3rd ed.; Marcel Dekker: New York, and references therein.

Spiecker, P. M., Gawrys, K. L., Trail, C. B., Kilpatrick, P. K. 2003. "Effects of Petroleum Resins on Asphaltene Aggregation and Water-in-Oil Emulsion Formation." Colloids and Surfaces A: Physicochemical and Engineering Aspects 220(1), 9-27.

Stachowiak, C., Viguie, J. R., Grolier, J. P. E., Rogalski, M. 2005. "Effect of n-Alkanes on Asphaltene Structuring in Petroleum Oils." Langmuir, Vol. 21(11), 4824-4829.

Sztukowski, D. M. and Yarranton, H. W. 2005. "Oilfield Solids and water-in-Oil Emulsion Stability." Journal of Colloid and Interface Science, Vol. 285(2), 821-833.

Sztukowski, D., Jafari, M., Alboudwarej, H., Yarranton, H. W. 2003. "Asphaltene Self-Association and Water-in-Hydrocarbon Emulsions." Journal of Colloid and Interface Science, Vol. 265(1), 179-186.

Theuerkorn, K., Horsfield, B., Wilkes, H., di Primio, R., Lehne, E. 2008. "A Reproducible and Linear Method for Separating Asphaltenes from Crude Oil." Organic Geochemistry, Vol. 39(8), 929-934.

Unal, Y. 2014. "Thermally Induced Wettability Change During SAGD for Oil Sand Extraction." MSc Thesis, Texas A&M University.

Unal, Y., Kar, T., Mukhametshina, A., Hascakir, B. 2015. "The Impact of Clay Type on the Asphaltene Deposition during Bitumen Extraction with Steam Assisted Gravity Drainage." SPE International Symposium on Oilfield Chemistry 2015, 13-15 April 2015, The Woodlands, Texas, USA, SPE-173795-MS.

Wiehe, I. A. 2012. "Asphaltene Solubility and Fluid Compatibility." Energy & Fuels, Vol. 26(7), 4004-4016.

Wilson, M. D., Pittman, E. D. 1977. "Authigenic Clays in Sandstones: Recognition and Influence on Reservoir Properties and Paleoenvironmental Analysis." Journal of Sedimentary Petrology, Vol. 47(1), 3-31.

Wu, G., He, L., Chen, D. 2013. "Sorption and Distribution of Asphaltene, Resin, Aromatic and Saturate Fractions of Heavy Crude Oil on Quartz Surface: Molecular Dynamic Simulation." Chemosphere, Vol. 92(11), 1465-1471.

Xia, L., Lu, S., Cao, G. 2003. “Stability and Demulsification of Emulsions Stabilized by Asphaltenes or Resins.” Journal of Colloid and Interface Science, Vol. 271(2), 504-506.

Yarranton, H. W. 2005. “Asphaltene Self-Association.” Journal of Dispersion Science and Technology, Vol. 26(1), 5-8.

Yarranton, H. W., Sztukowski, D. M., Urrutia, P. 2007. “Effect of Interfacial Rheology on Model Emulsion Coalescence: I. Interfacial Rheology.” Journal of Colloid and Interface Science, Vol. 310(1), 253-259.

Zhao, B., Becerra, M., Shaw, J. M. et al. 2009. "On Asphaltene and Resin Association in Athabasca Bitumen and Maya Crude Oil." Energy & Fuels, Vol. 23(9), 4431-4437.

APPENDIX I

FOURIER TRANSFORM INFRARED (FTIR) SPECTRA RESULTS

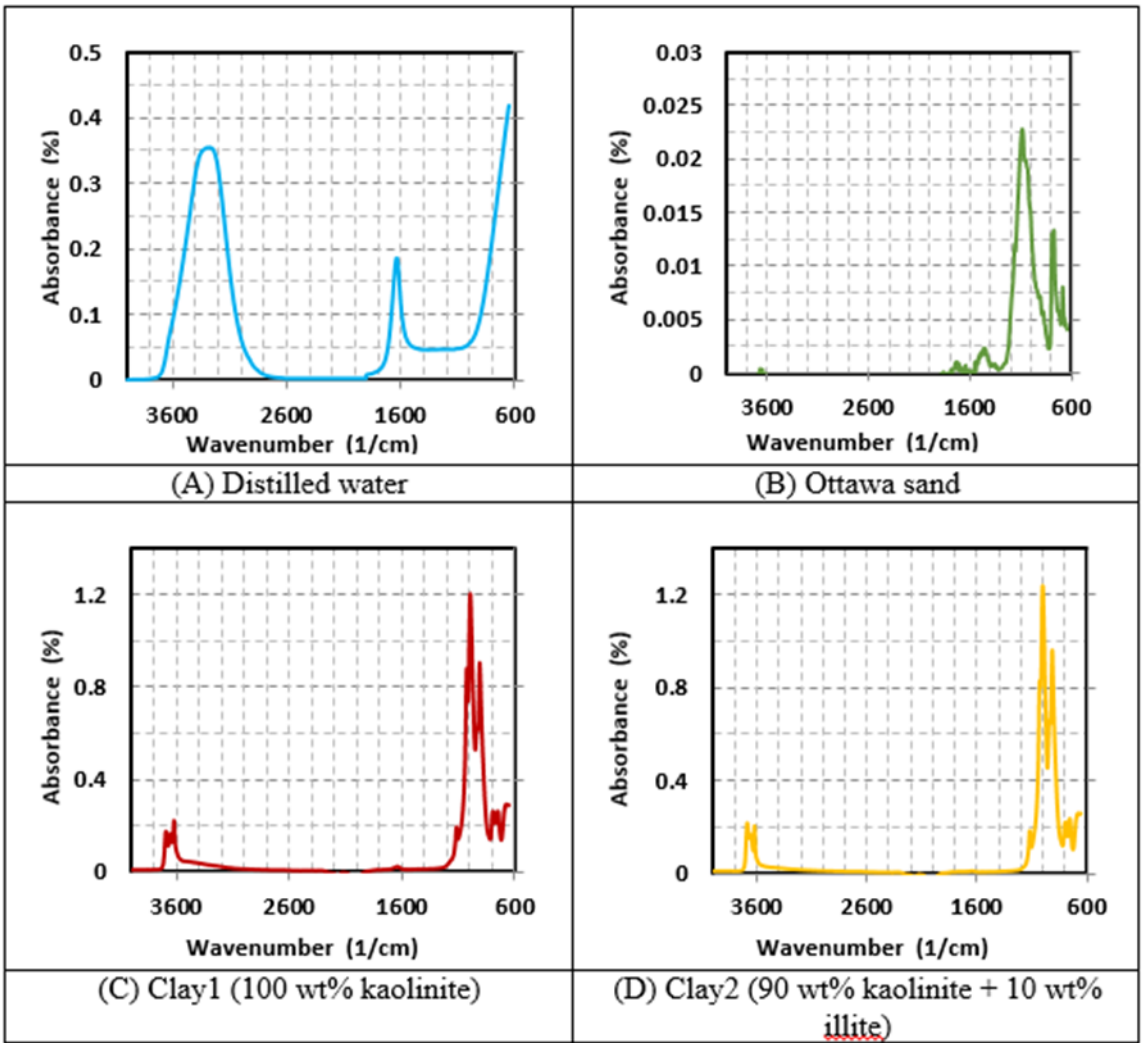

Figure 12: FTIR spectra of reference samples (A) Distilled water, (B) Ottawa sand, (C) Clay1, and (D) Clay2

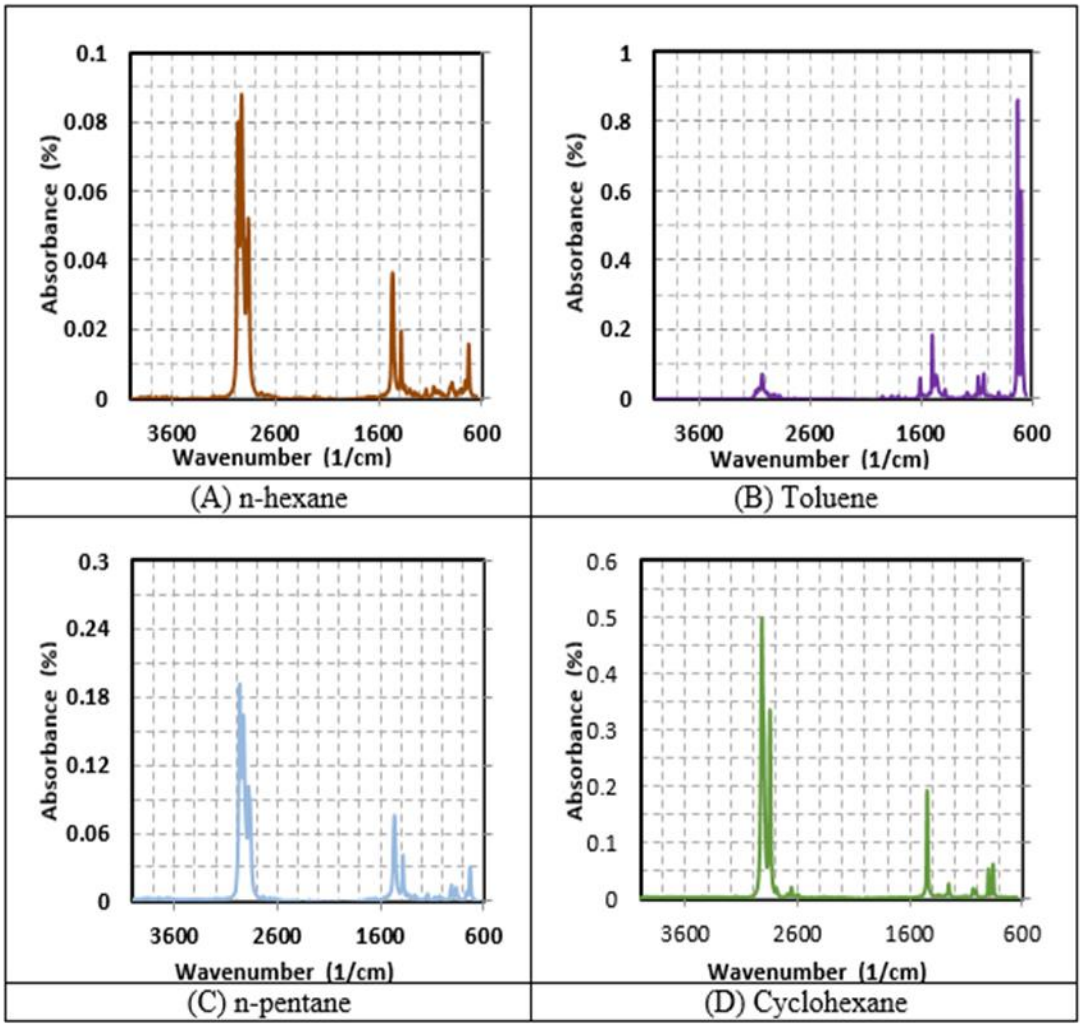

Figure 13: FTIR spectra of reference samples (A) n-hexane, (B) Toluene, (C) n-pentane, and (D) Cyclohexane

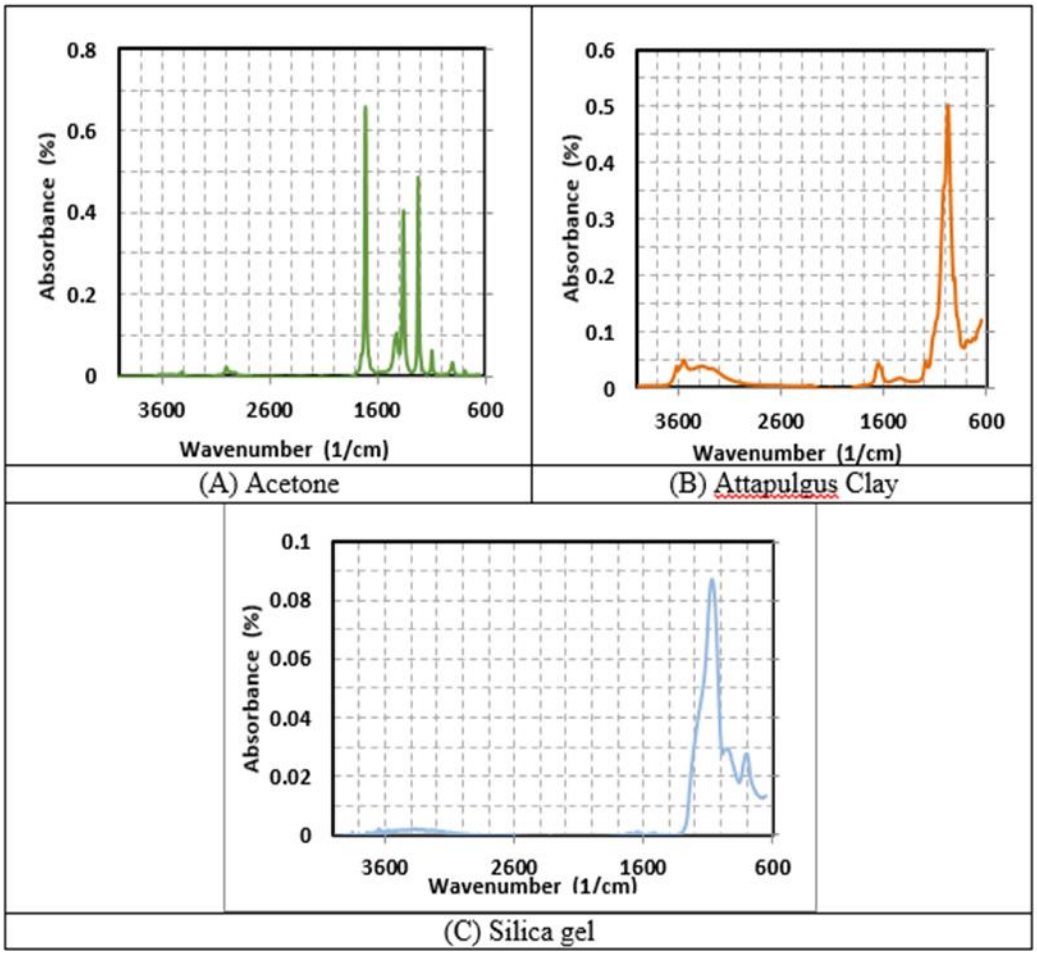

Figure 14: FTIR spectra of reference samples (A) Acetone, (B) Attapulgus Clay, and (C) Silica gel

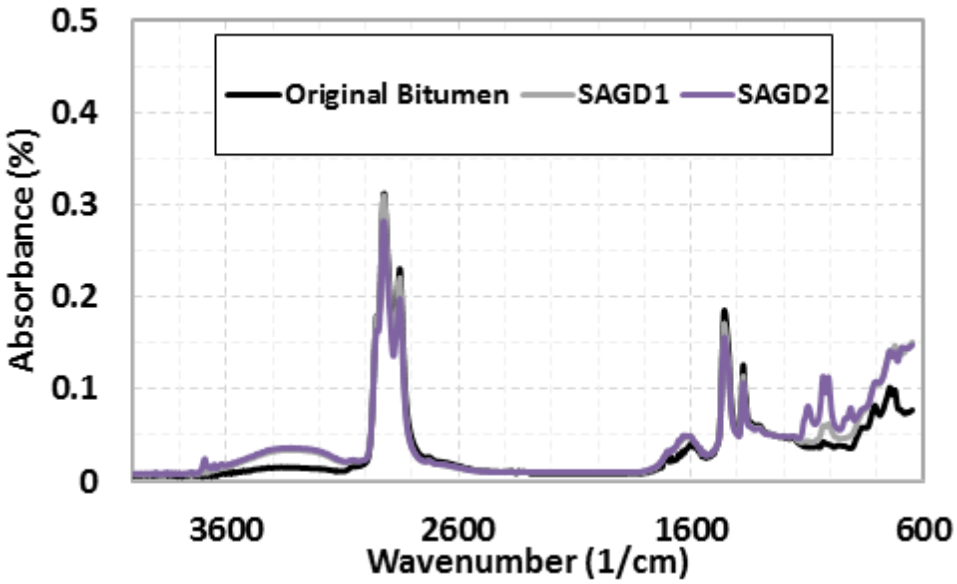

Figure 15: FTIR spectra of original bitumen and produced oil samples from SAGD1 and SAGD2

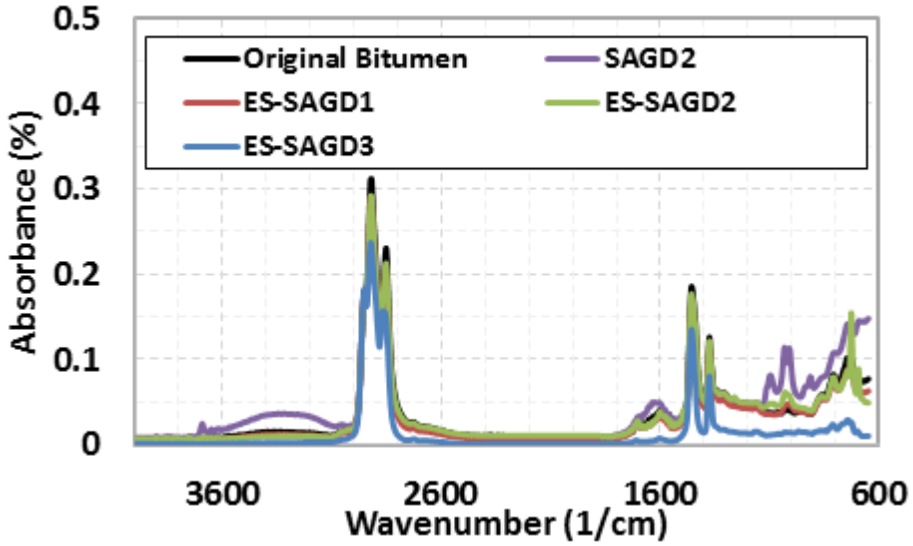

Figure 16: FTIR spectra of original bitumen and produced oil samples from SAGD2, ES-SAGD1, ES-SAGD2, and ES-SAGD3

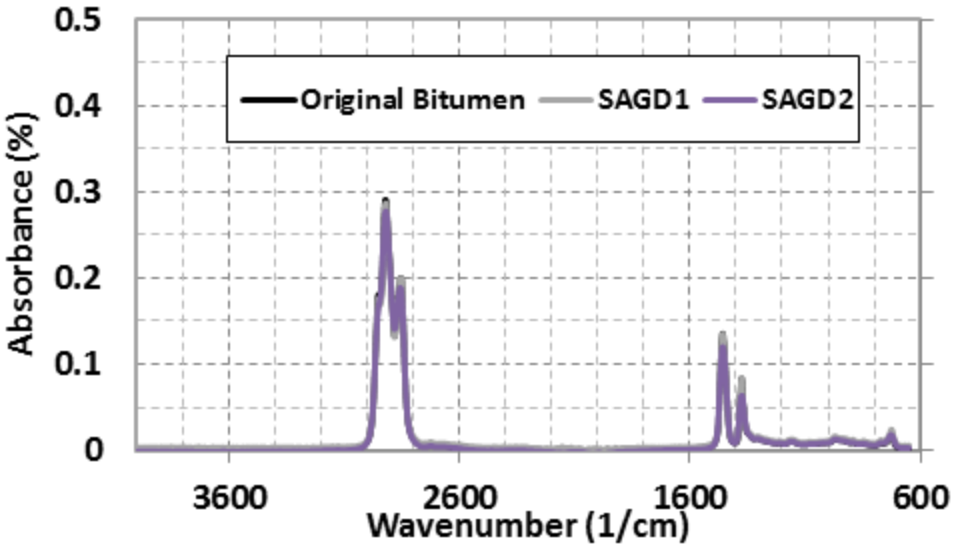

Figure 17: FTIR spectra of saturates in original bitumen and produced oil samples from SAGD1 and SAGD2

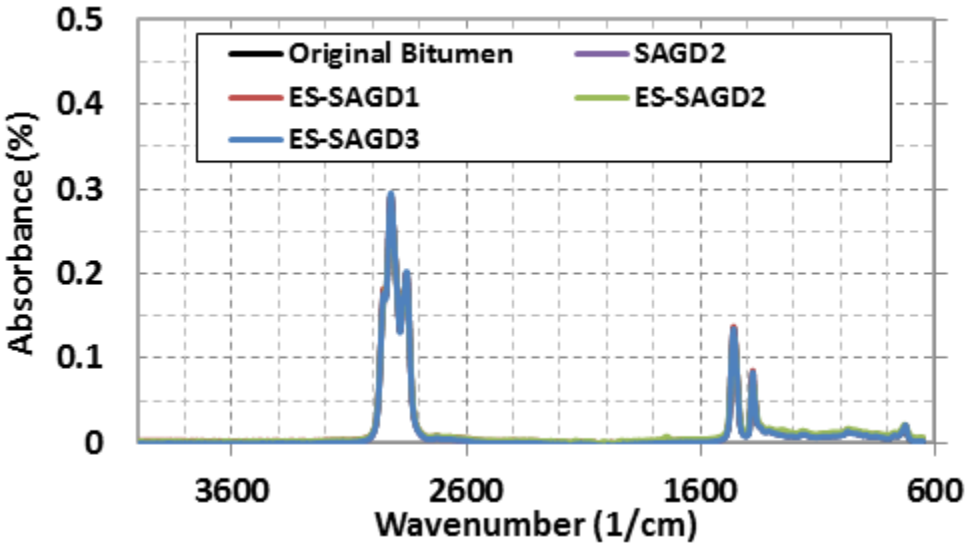

Figure 18: FTIR spectra of saturates in original bitumen and produced oil samples from SAGD2, ES-SAGD1, ES-SAGD2, and ES-SAGD3

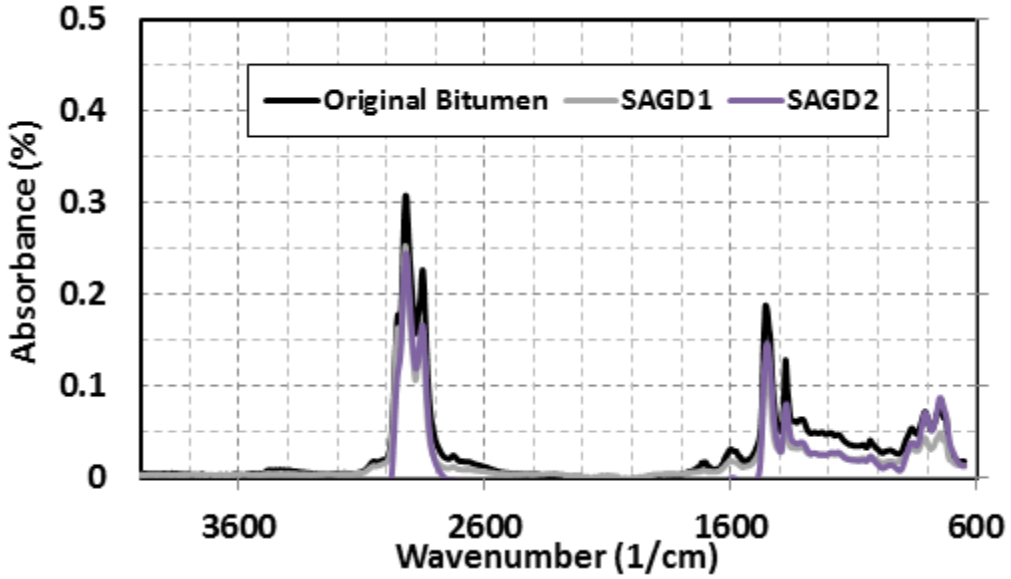

Figure 19: FTIR spectra of aromatics in original bitumen and produced oil samples from SAGD1 and SAGD2

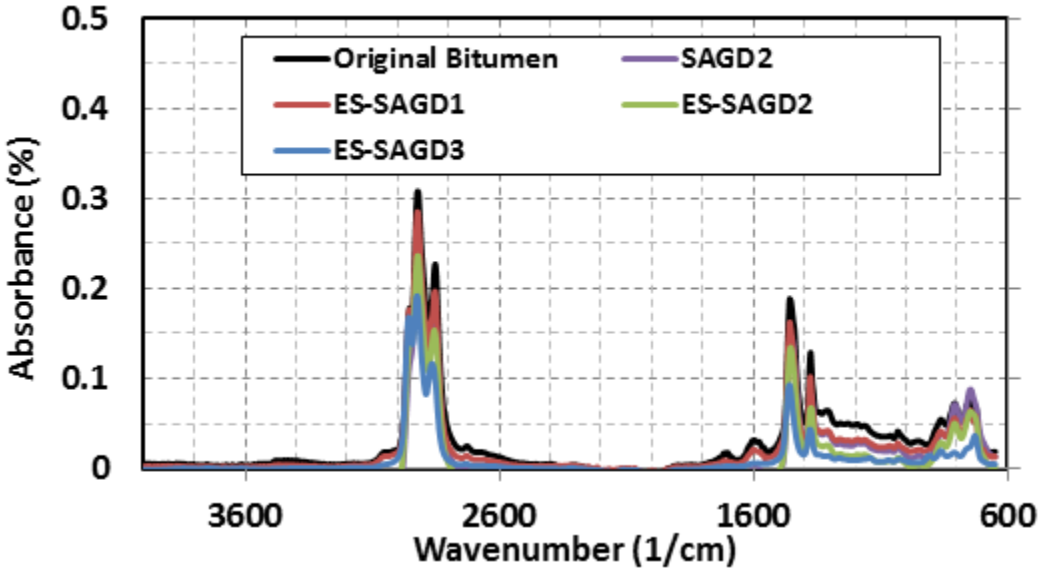

Figure 20: FTIR spectra of aromatics in original bitumen and produced oil samples from SAGD2, ES-SAGD1, ES-SAGD2, and ES-SAGD3

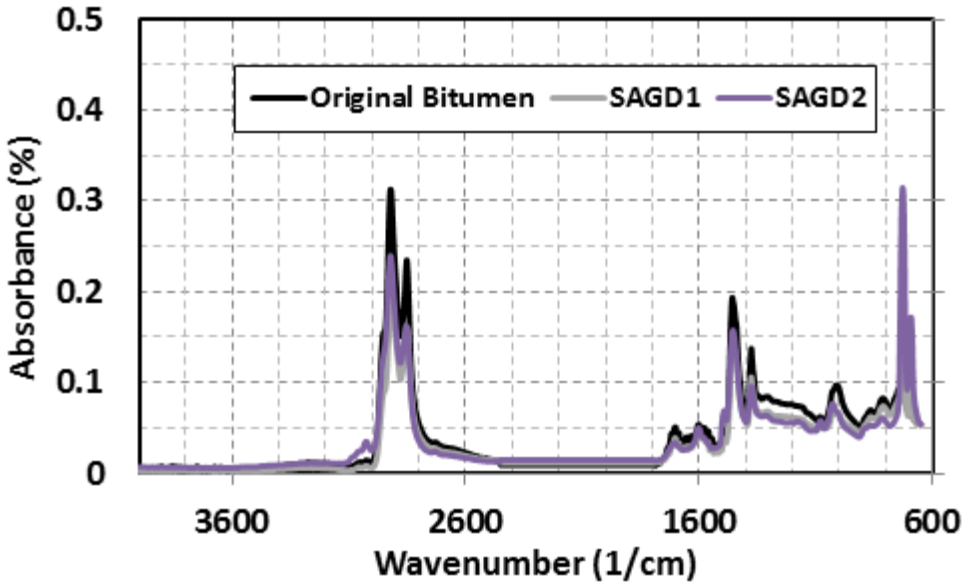

Figure 21: FTIR spectra of resins in original bitumen and produced oil samples from SAGD1 and SAGD2

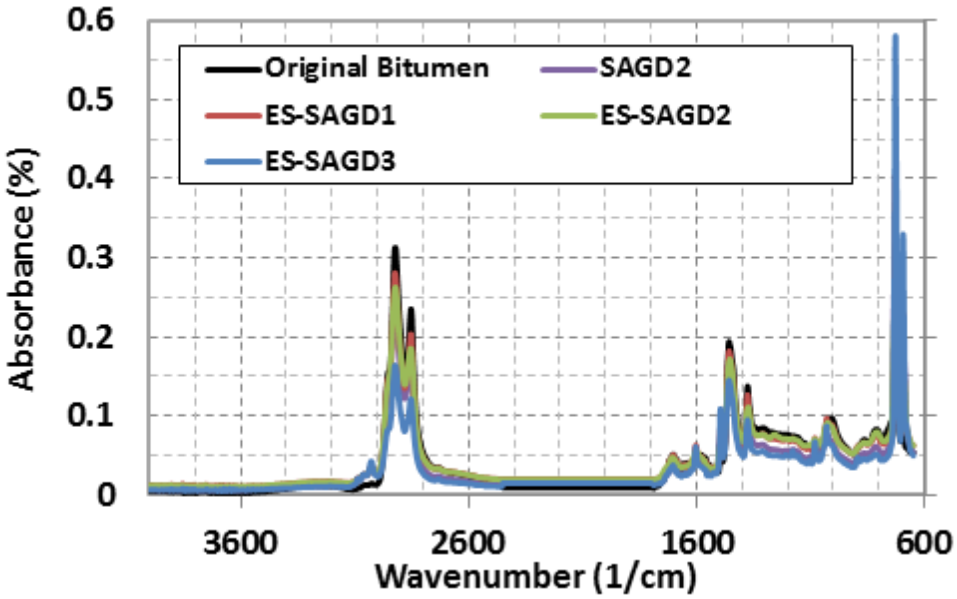

Figure 22: FTIR spectra of resins in original bitumen and produced oil samples from SAGD2, ES-SAGD1, ES-SAGD2, and ES-SAGD3

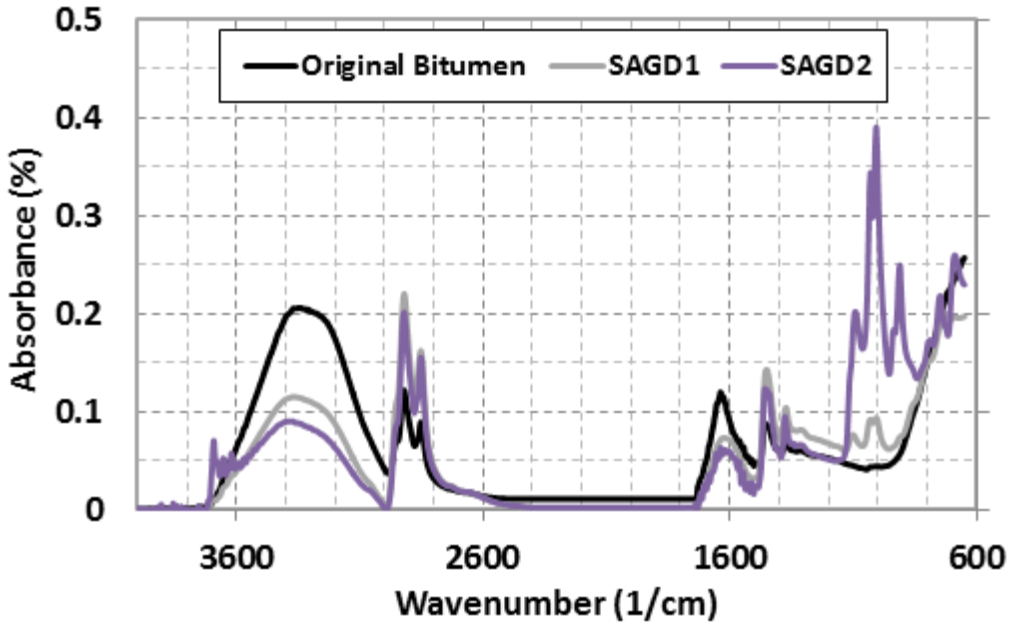

Figure 23: FTIR spectra of asphaltenes in original bitumen and produced oil samples from SAGD1 and SAGD2

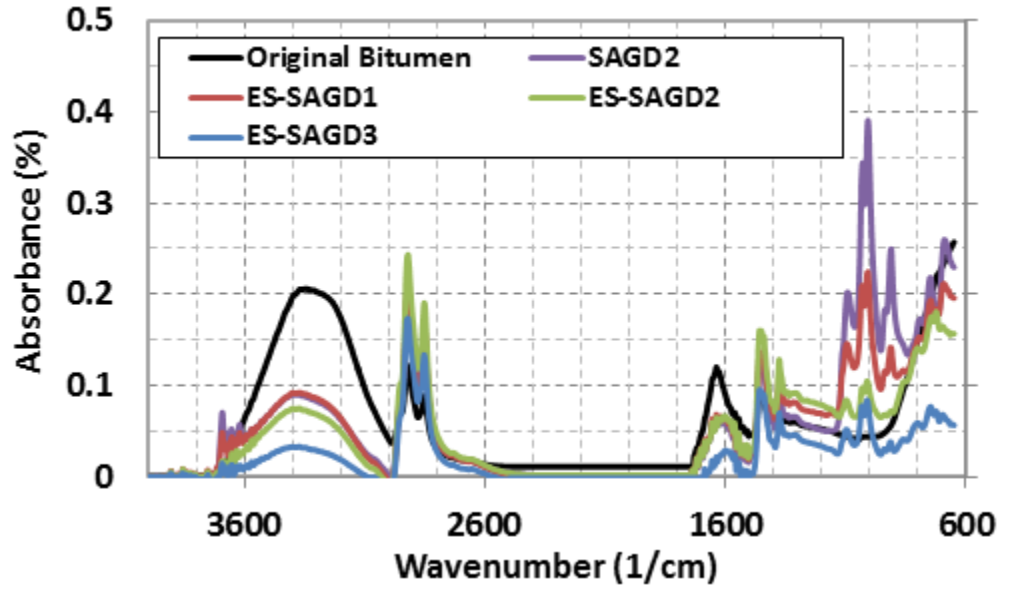

Figure 24: FTIR spectra of asphaltenes in original bitumen and produced oil samples from SAGD2, ES-SAGD1, ES-SAGD2, and ES-SAGD3

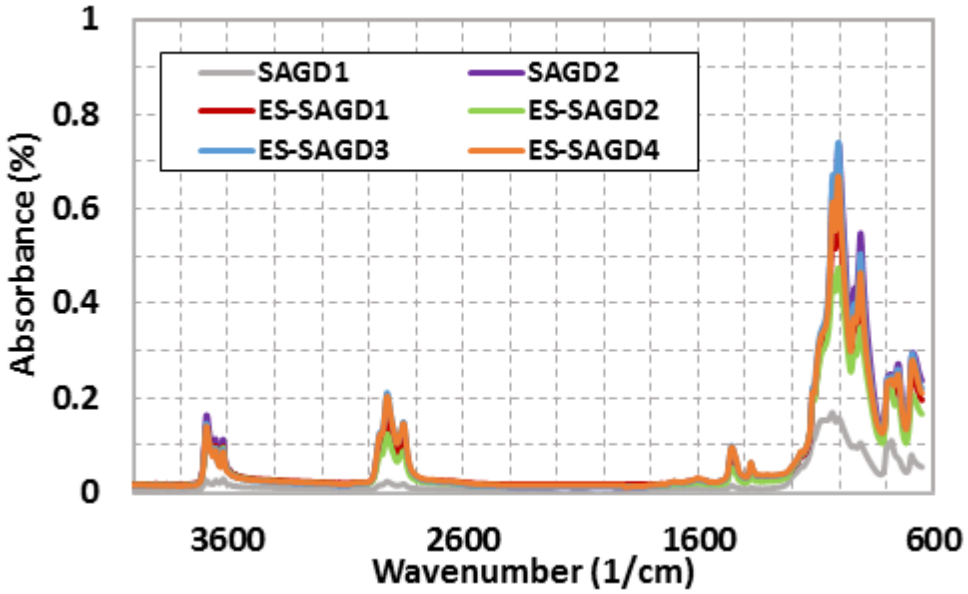

Figure 25: FTIR spectra of spent rock samples inside steam chamber from SAGD1, SAGD2, ES-SAGD1, ES-SAGD2, ES-SAGD3, and ES-SAGD4

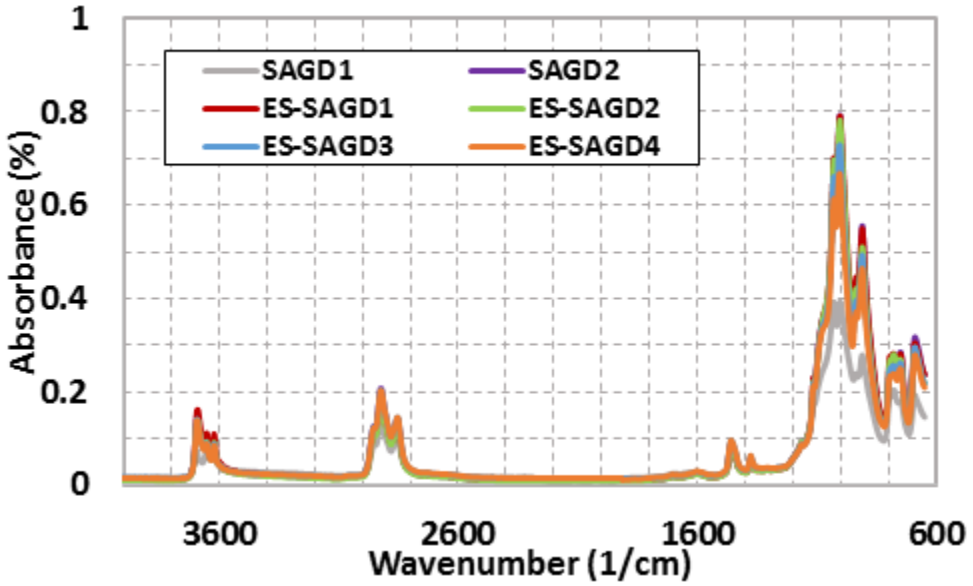

Figure 26: FTIR spectra of spent rock samples outside steam chamber from SAGD1, SAGD2, ES-SAGD1, ES-SAGD2, ES-SAGD3, and ES-SAGD4

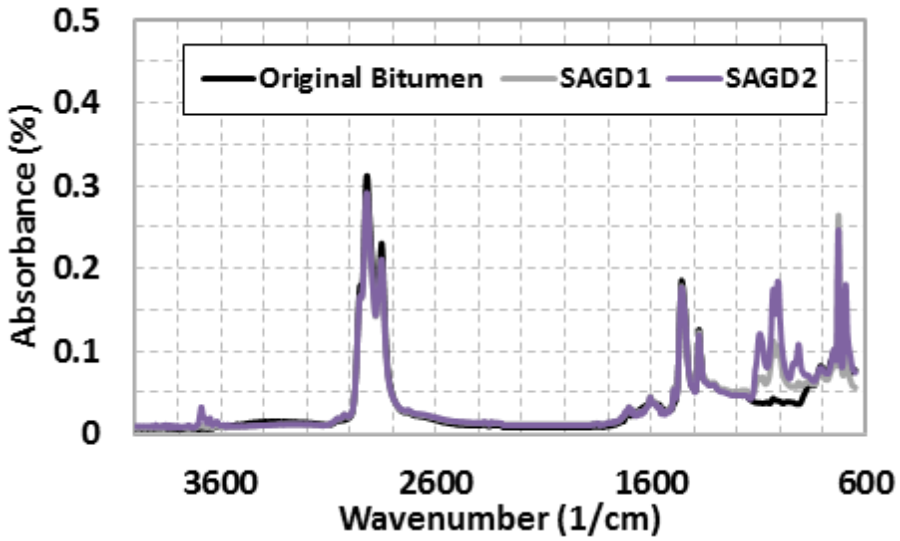

Figure 27: FTIR spectra of original bitumen and residual oil samples with clays inside steam chamber from SAGD1 and SAGD2

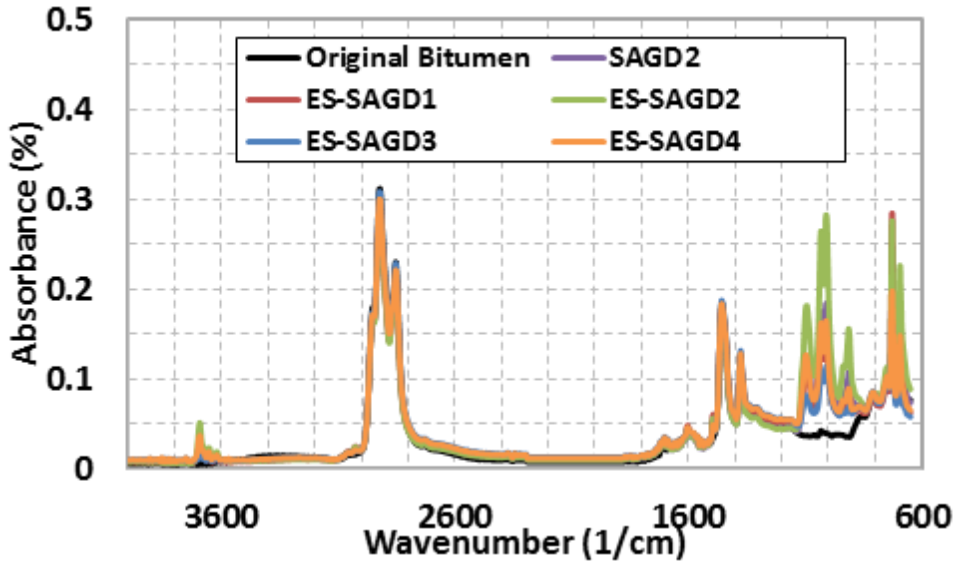

Figure 28: FTIR spectra of original bitumen and residual oil samples with clays inside steam chamber from SAGD2, ES-SAGD1, ES-SAGD2, ES-SAGD3, and ES-SAGD4

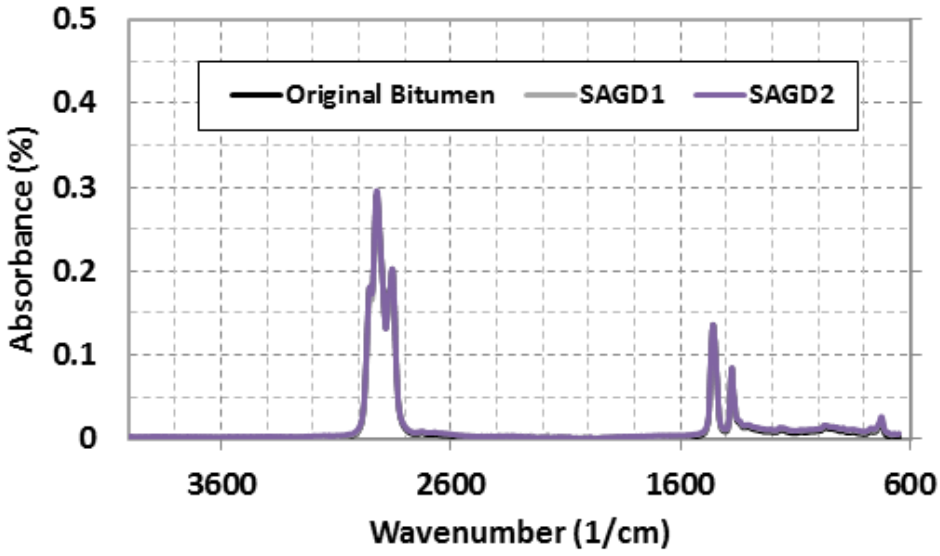

Figure 29: FTIR spectra of saturates in original bitumen and residual oil samples with clays inside steam chamber from SAGD1 and SAGD2

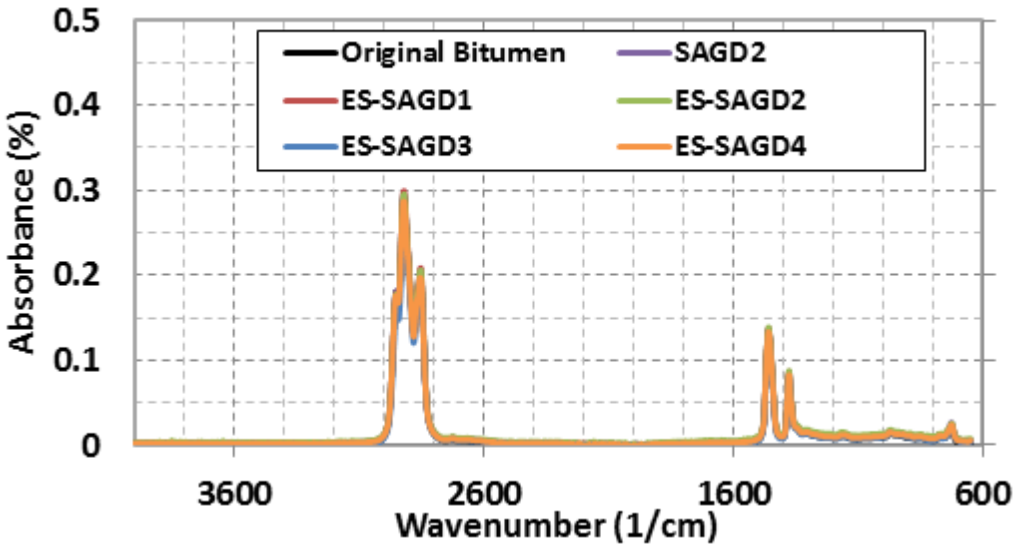

Figure 30: FTIR spectra of saturates in original bitumen and residual oil samples with clays inside steam chamber from SAGD2, ES-SAGD1, ES-SAGD2, ES-SAGD3, and ES-SAGD4

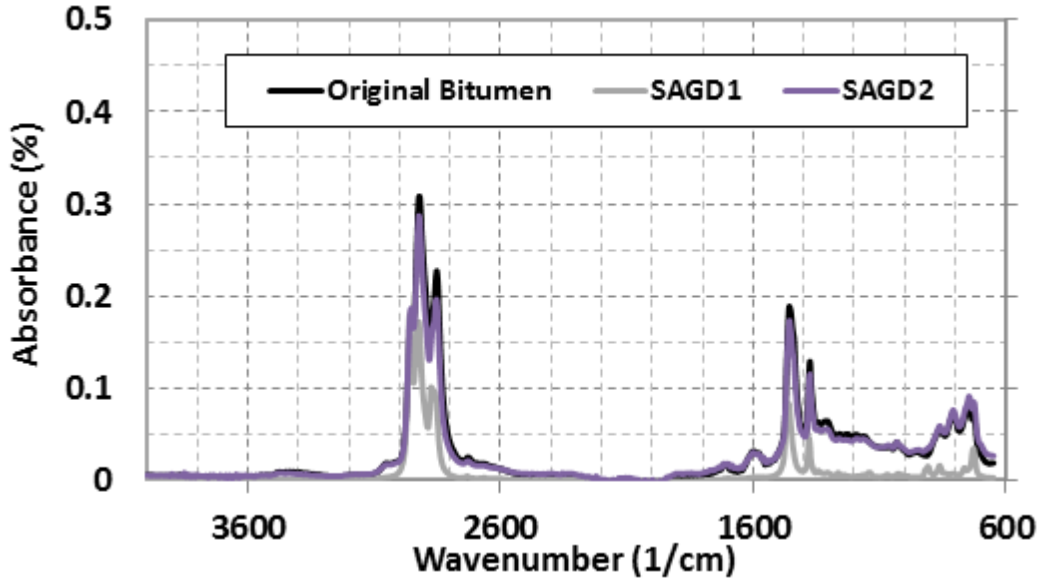

Figure 31: FTIR spectra of aromatics in original bitumen and residual oil samples with clays inside steam chamber from SAGD1 and SAGD2

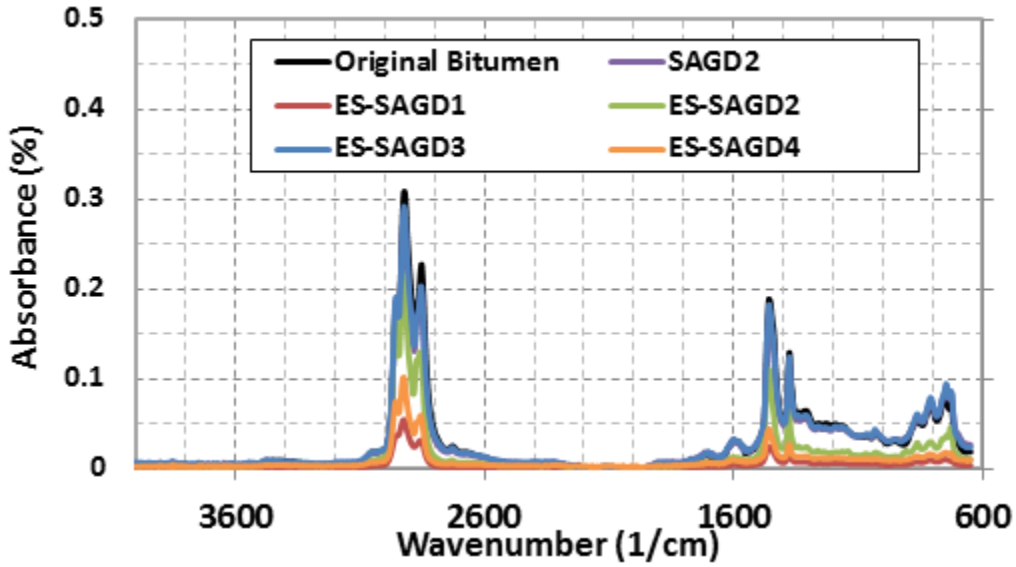

Figure 32: FTIR spectra of aromatics in original bitumen and residual oil samples with clays inside steam chamber from SAGD2, ES-SAGD1, ES-SAGD2, ES-SAGD3, and ES-SAGD4

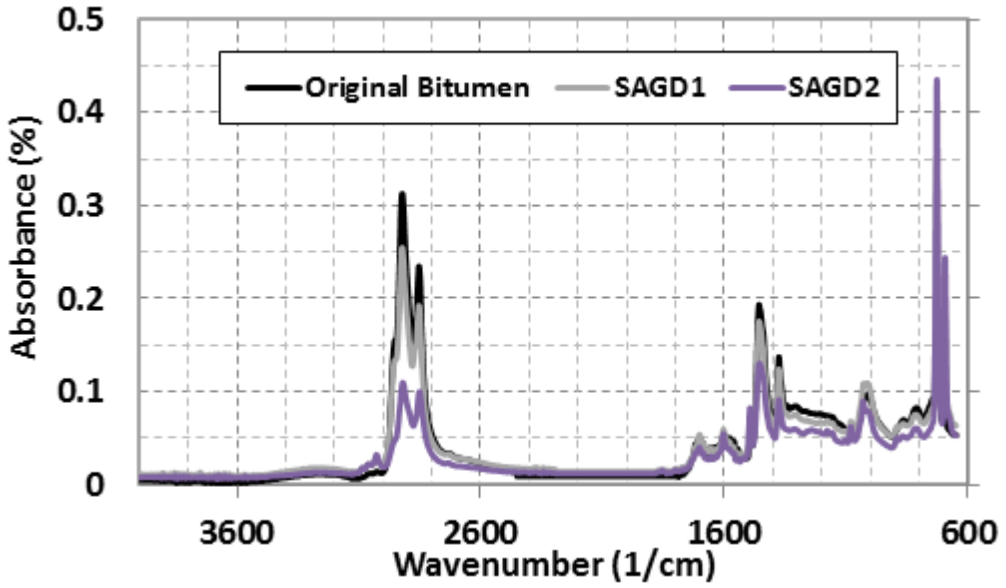

Figure 33: FTIR spectra of resins in original bitumen and residual oil samples with clays inside steam chamber from SAGD1 and SAGD2

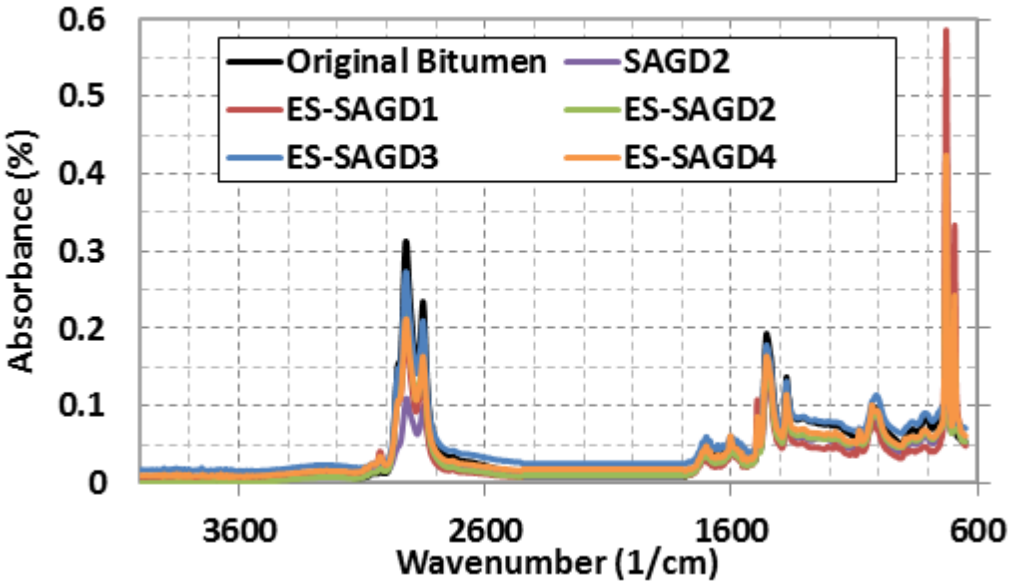

Figure 34: FTIR spectra of resins in original bitumen and residual oil samples with clays inside steam chamber from SAGD2, ES-SAGD1, ES-SAGD2, ES-SAGD3, and ES-SAGD4

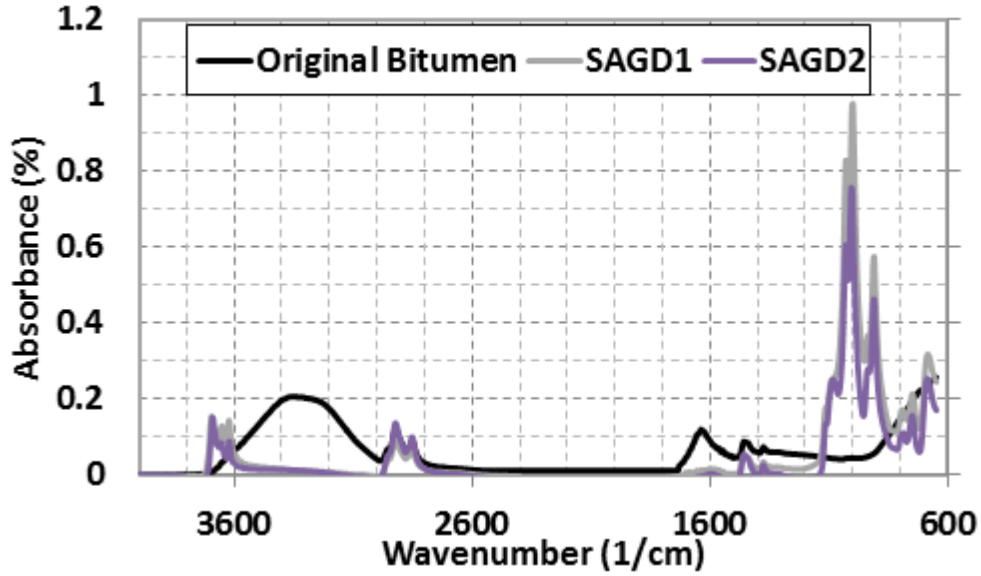

Figure 35: FTIR spectra of asphaltenes in original bitumen and residual oil samples with clays inside steam chamber from SAGD1 and SAGD2

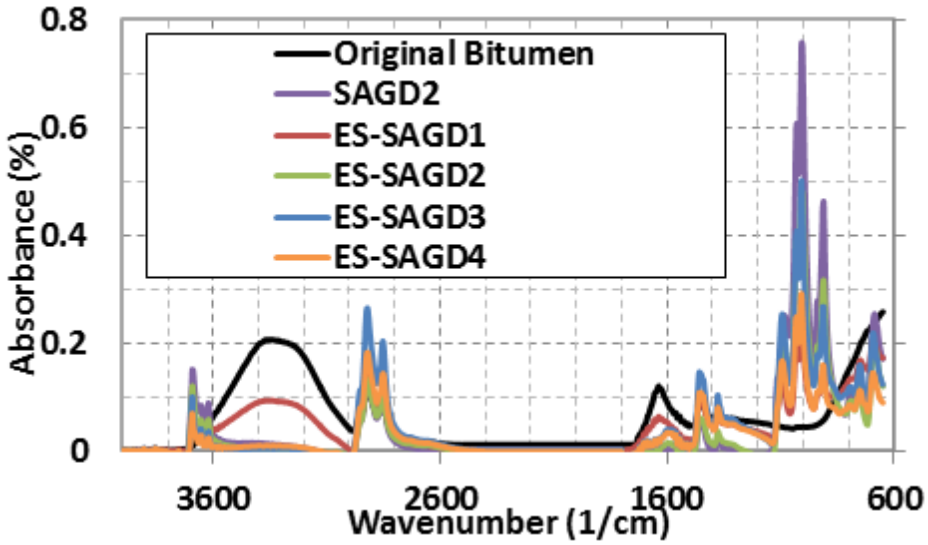

Figure 36: FTIR spectra of asphaltenes in original bitumen and residual oil samples with clays inside steam chamber from SAGD2, ES-SAGD1, ES-SAGD2, ES-SAGD3, and ES-SAGD4

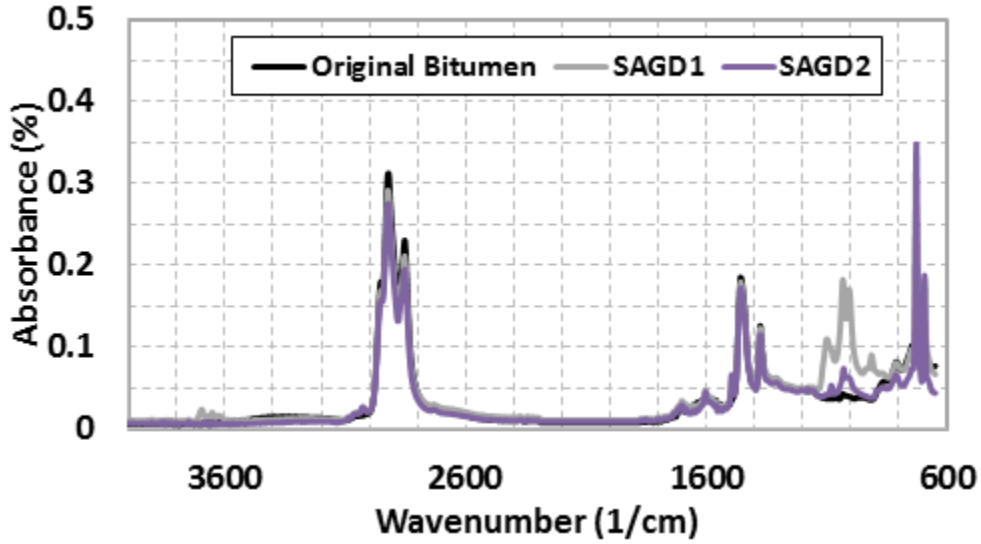

Figure 37: FTIR spectra of original bitumen and residual oil samples with clays outside steam chamber from SAGD1 and SAGD2

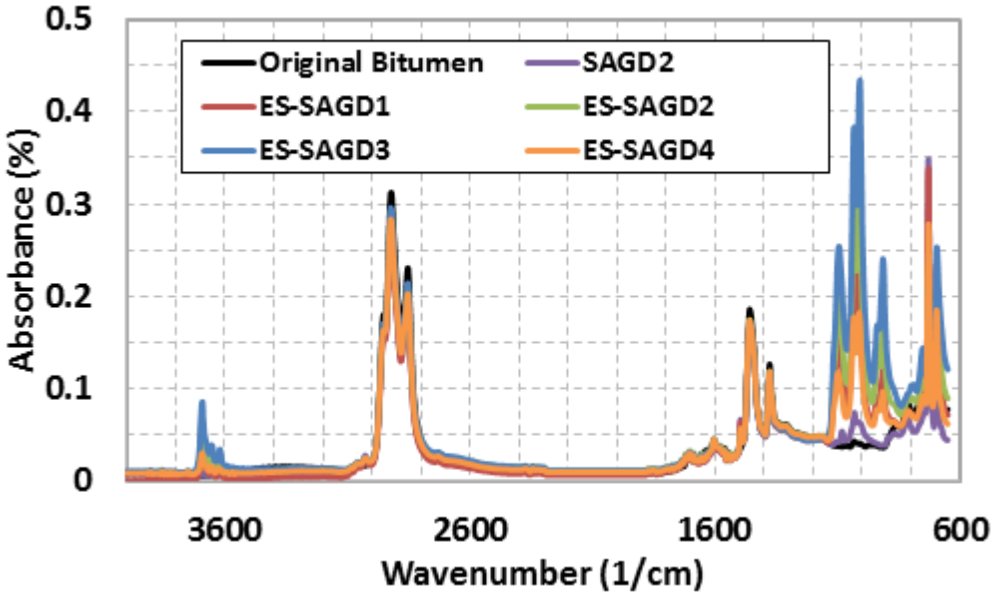

Figure 38: FTIR spectra of original bitumen and residual oil samples with clays outside steam chamber from SAGD2, ES-SAGD1, ES-SAGD2, ES-SAGD3, and ES-SAGD4

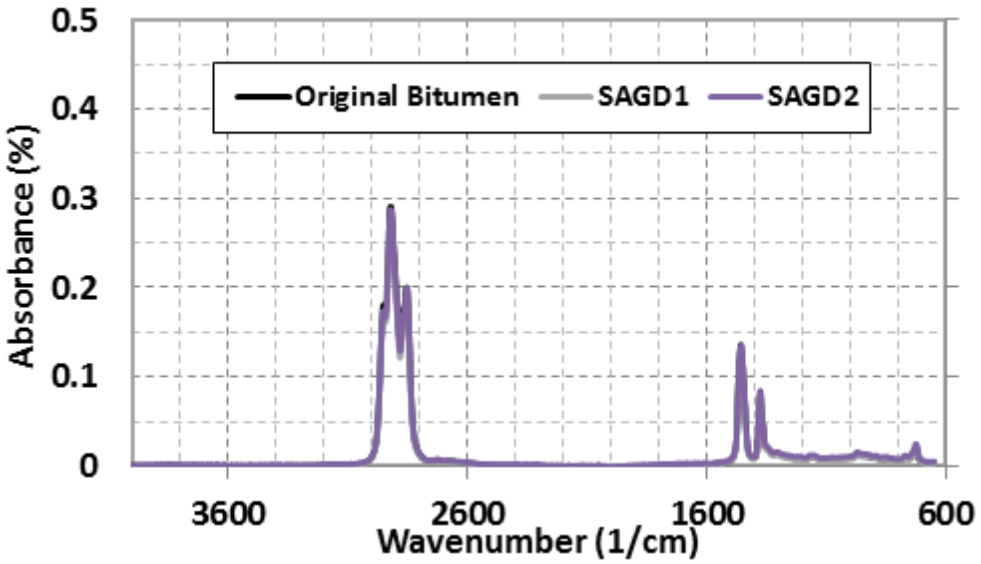

Figure 39: FTIR spectra of saturates in original bitumen and residual oil samples with clays outside steam chamber from SAGD1 and SAGD2

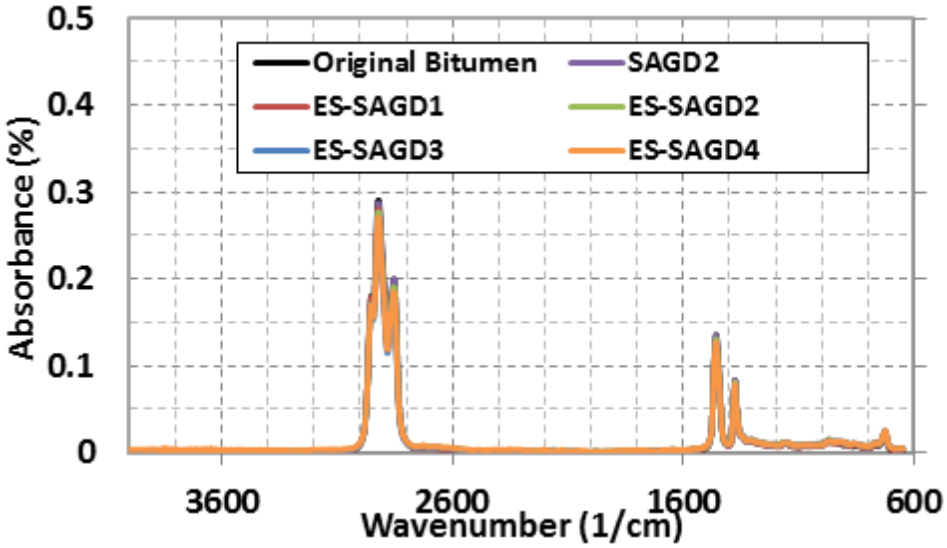

Figure 40: FTIR spectra of saturates in original bitumen and residual oil samples with clays outside steam chamber from SAGD2, ES-SAGD1, ES-SAGD2, ES-SAGD3, and ES-SAGD4

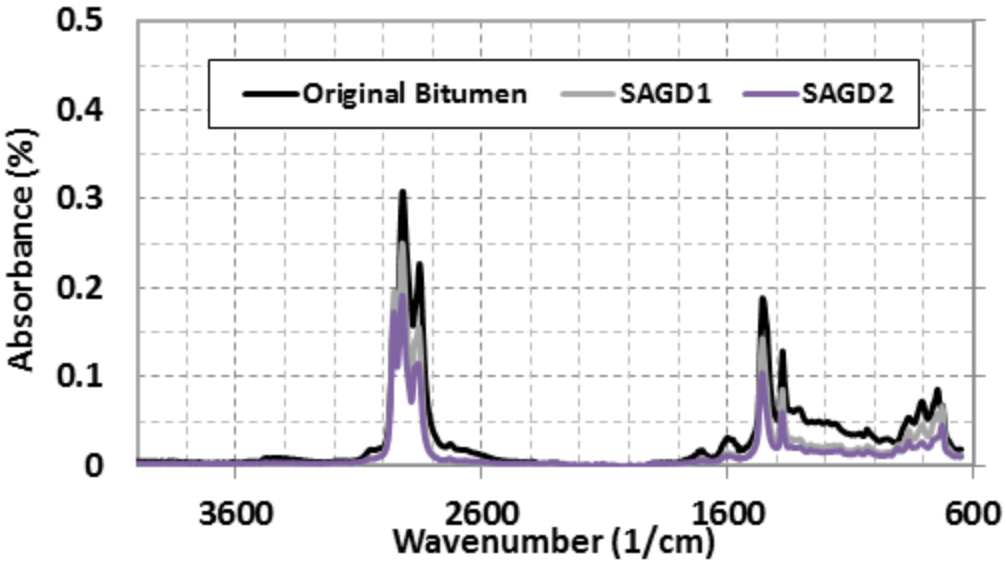

Figure 41: FTIR spectra of aromatics in original bitumen and residual oil samples with clays outside steam chamber from SAGD1 and SAGD2

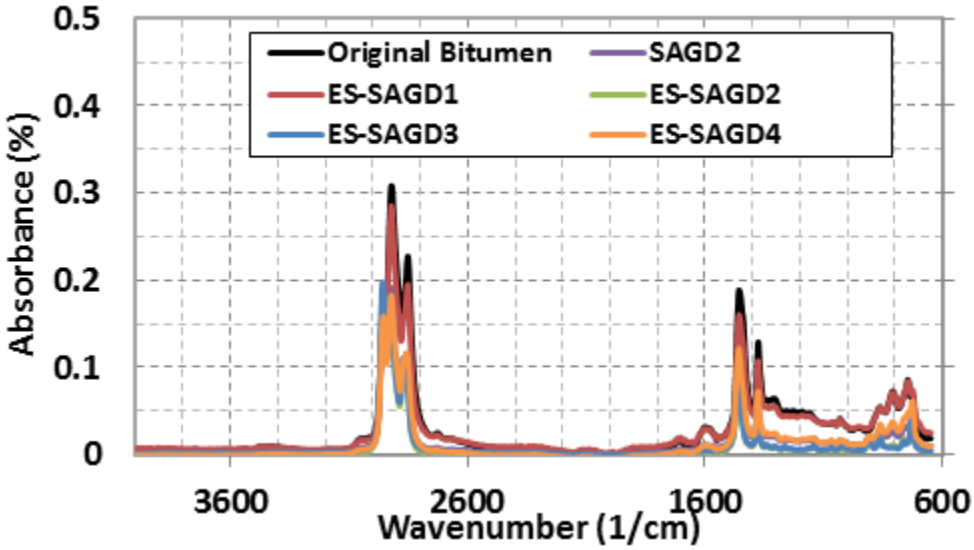

Figure 42: FTIR spectra of aromatics in original bitumen and residual oil samples with clays outside steam chamber from SAGD2, ES-SAGD1, ES-SAGD2, ES-SAGD3, and ES-SAGD4

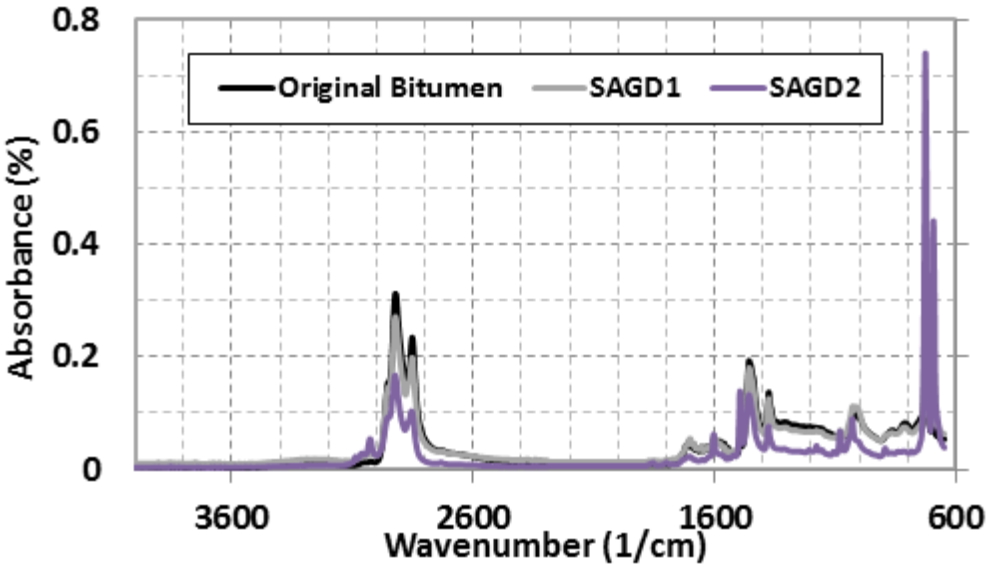

Figure 43: FTIR spectra of resins in original bitumen and residual oil samples with clays outside steam chamber from SAGD1 and SAGD2

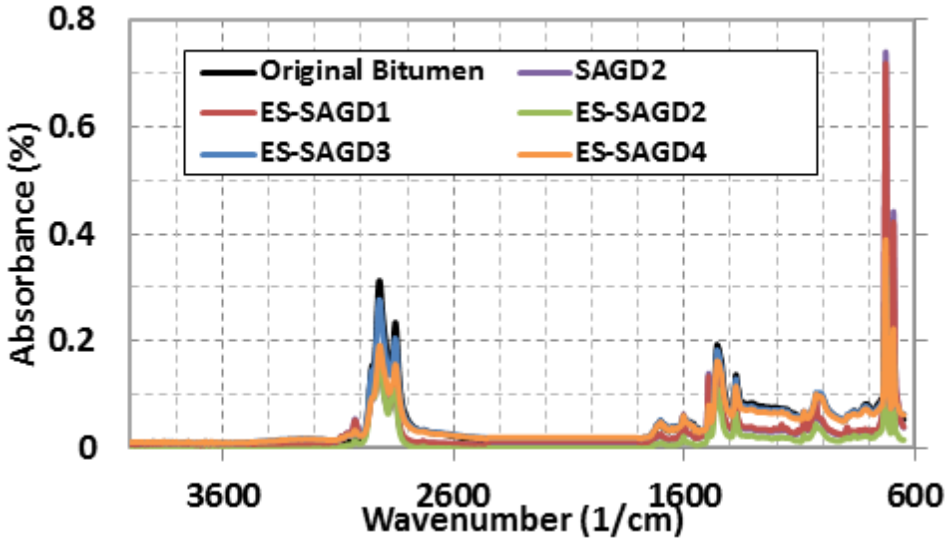

Figure 44: FTIR spectra of resins in original bitumen and residual oil samples with clays outside steam chamber from SAGD2, ES-SAGD1, ES-SAGD2, ES-SAGD3, and ES-SAGD4

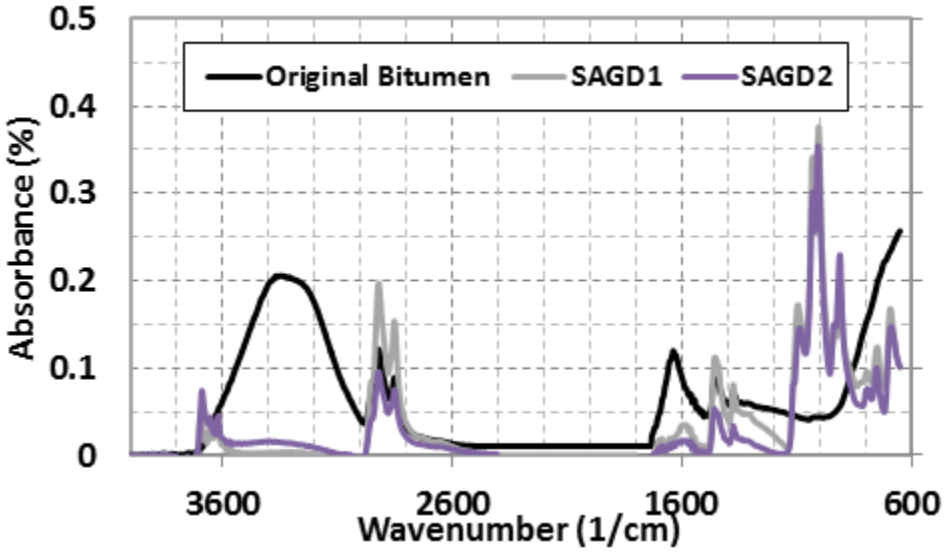

Figure 45: FTIR spectra of asphaltenes in original bitumen and residual oil samples with clays outside steam chamber from SAGD1, and SAGD2

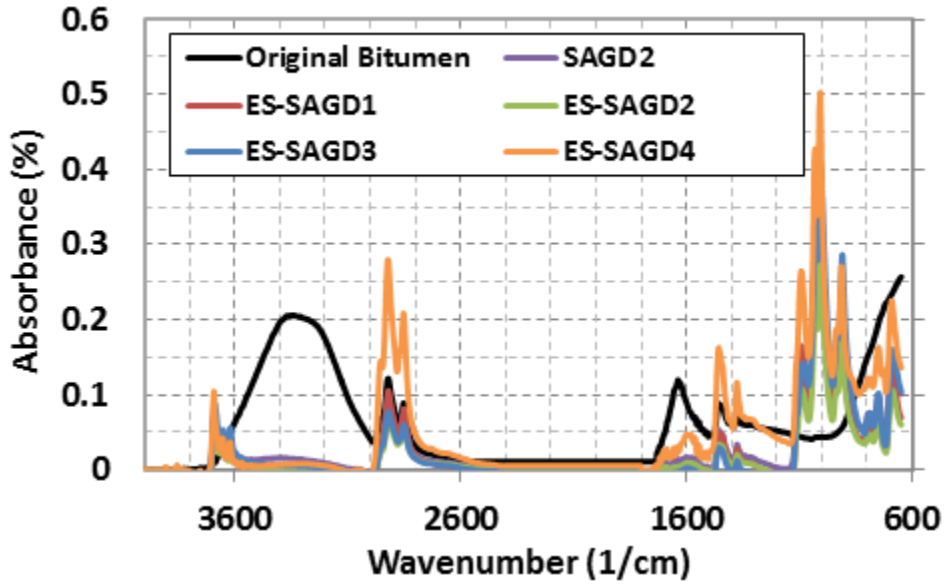

Figure 46: FTIR spectra of asphaltenes in original bitumen and residual oil samples with clays outside steam chamber from SAGD2, ES-SAGD1, ES-SAGD2, ES-SAGD3, and ES-SAGD4

APPENDIX II

THERMOGRAVIMETRIC ANALYSIS (TGA)/ DIFFERENTIAL SCANNING CALORIMETRY (DSC) RESULTS

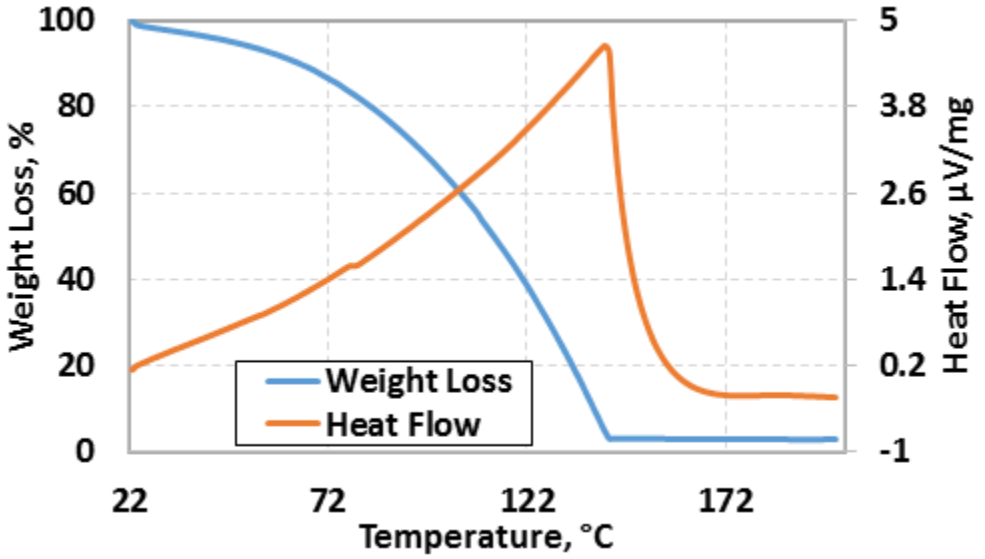

Figure 47: TGA/DSC curves for distilled water (Reference sample)

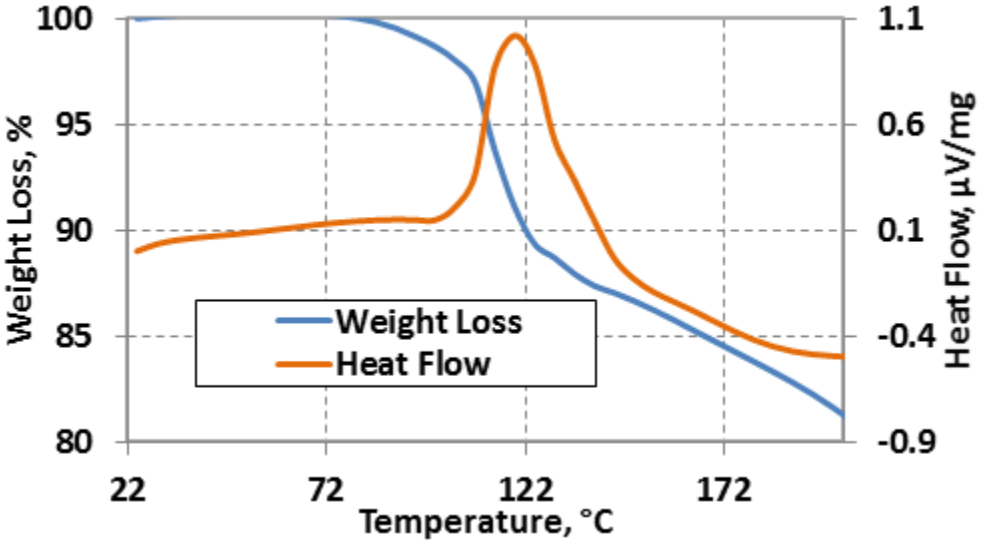

Figure 48: TGA/DSC curves for original bitumen

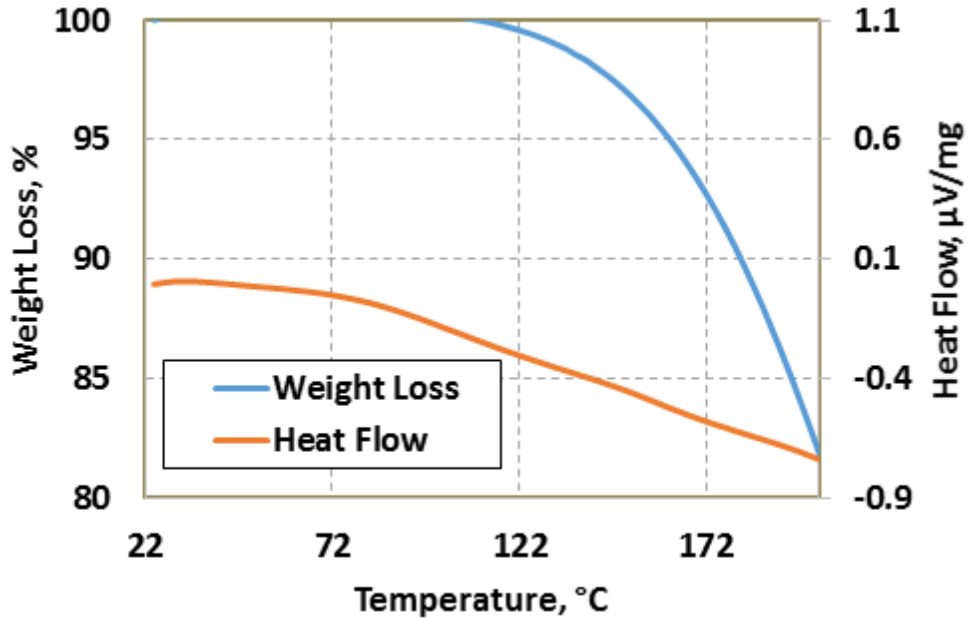

Figure 49: TGA/DSC curves for saturates in produced oil sample from SAGD1

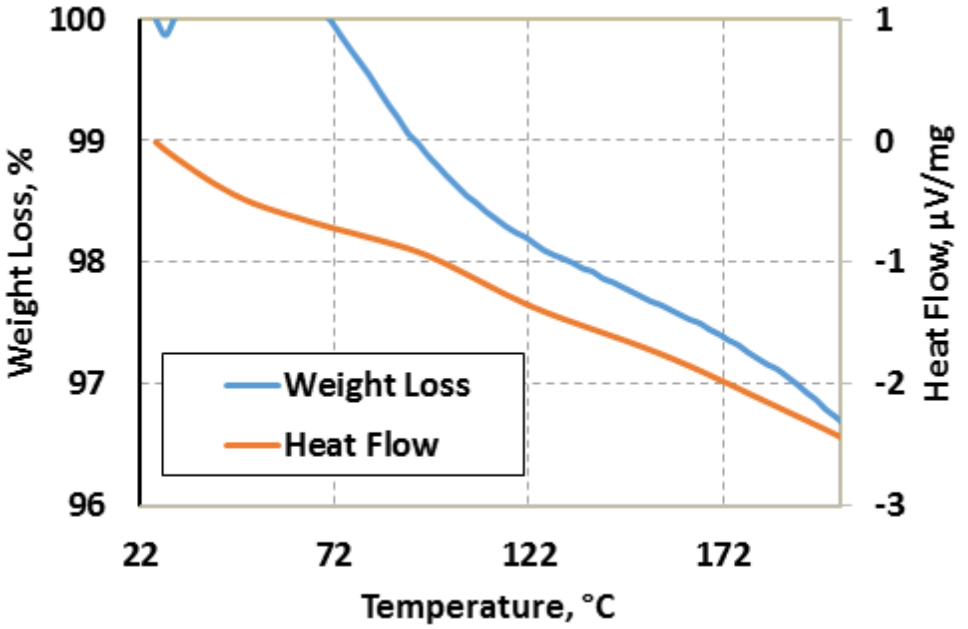

Figure 50: TGA/DSC curves for aromatics in produced oil sample from SAGD1

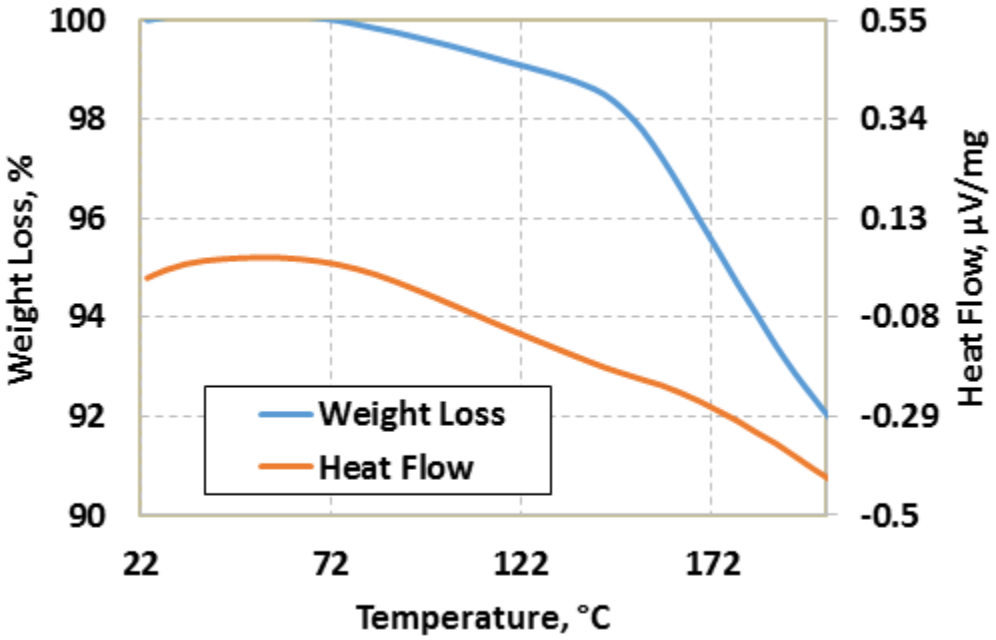

Figure 51: TGA/DSC curves for resins in produced oil sample from SAGD1

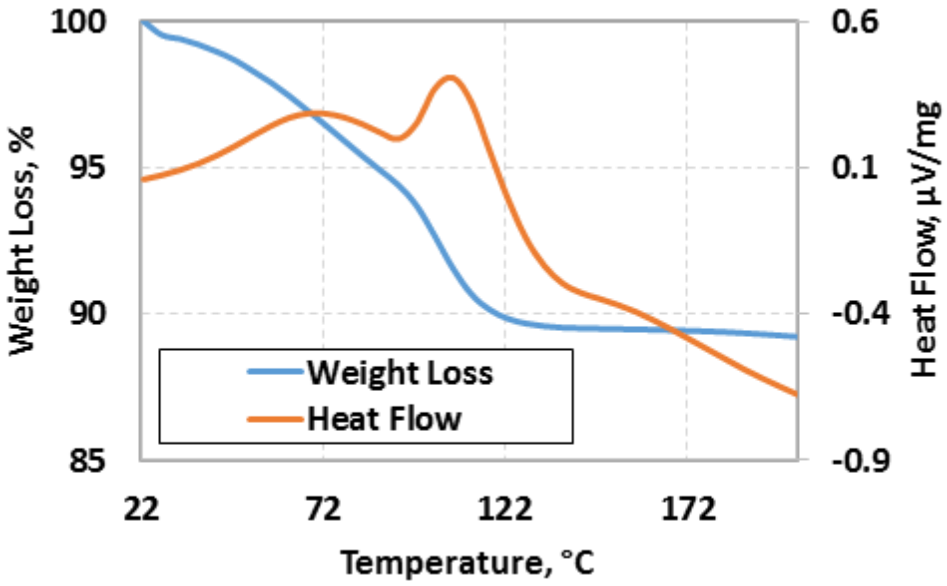

Figure 52: TGA/DSC curves for asphaltenes in original bitumen

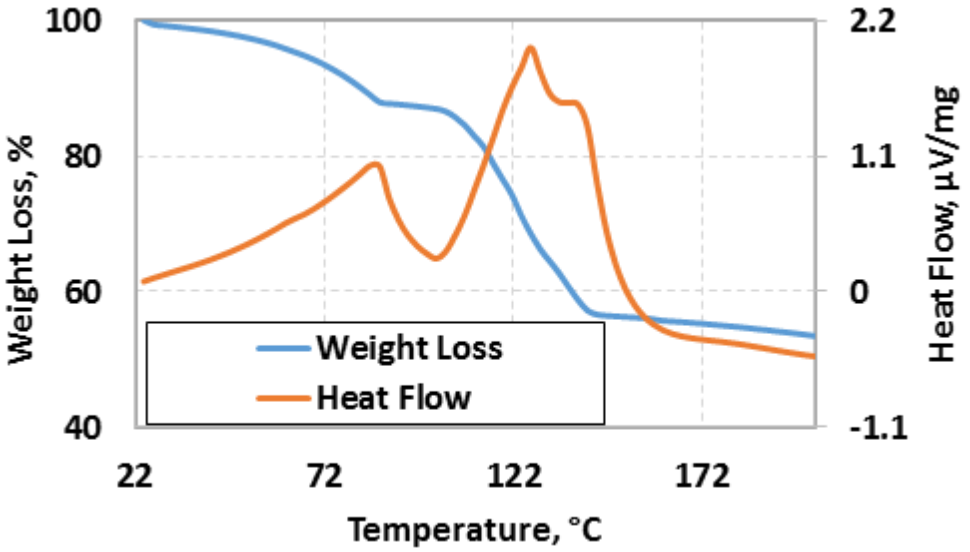

Figure 53: TGA/DSC curves for produced oil sample from SAGD1

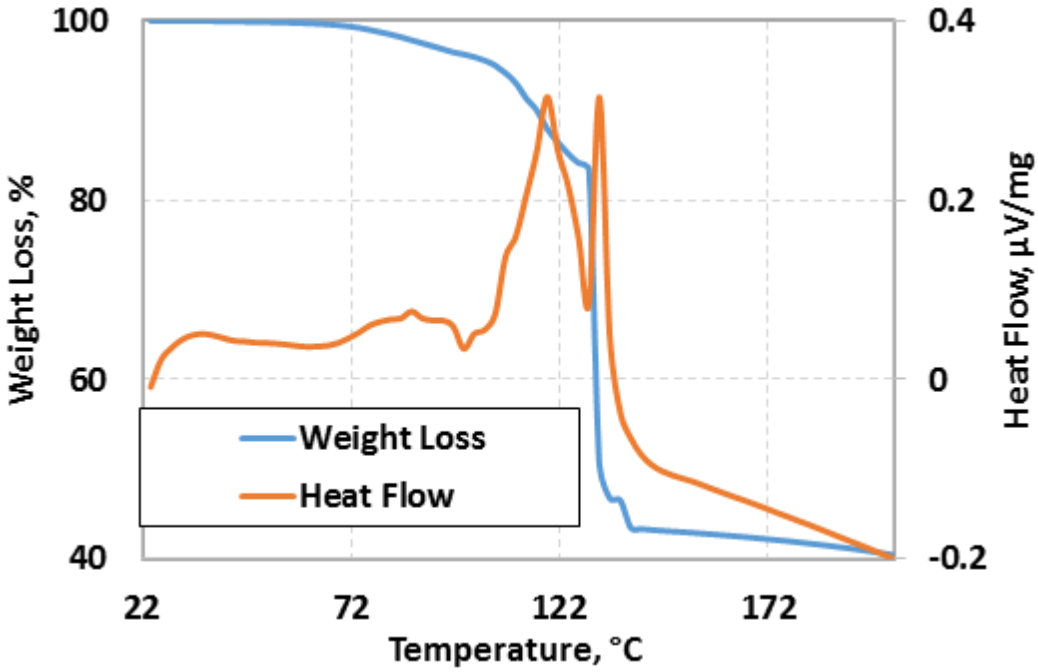

Figure 54: TGA/DSC curves for produced oil sample from SAGD2

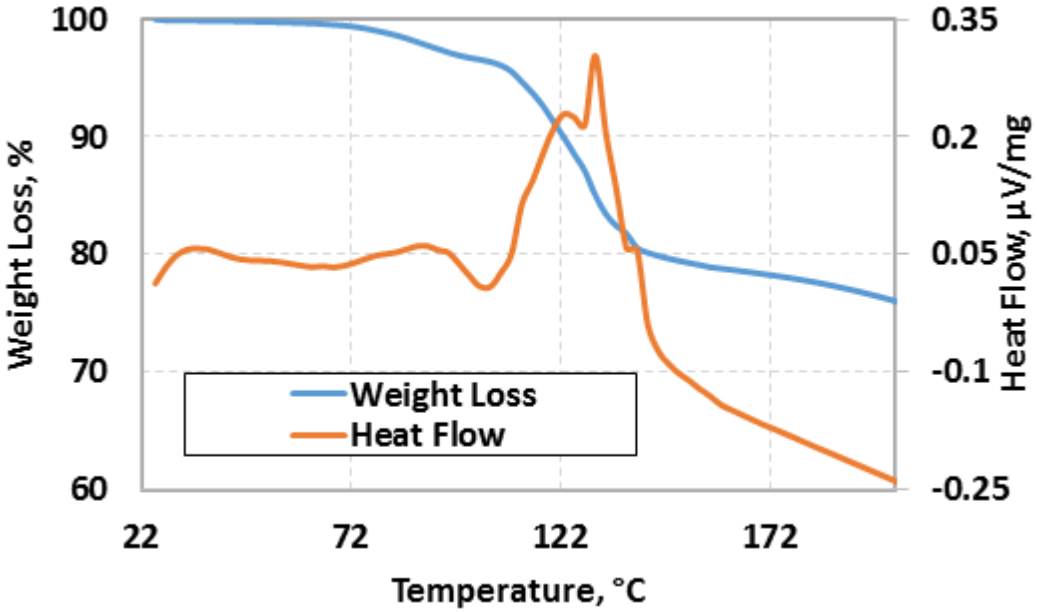

Figure 55: TGA/DSC curves for produced oil sample from ES-SAGD1

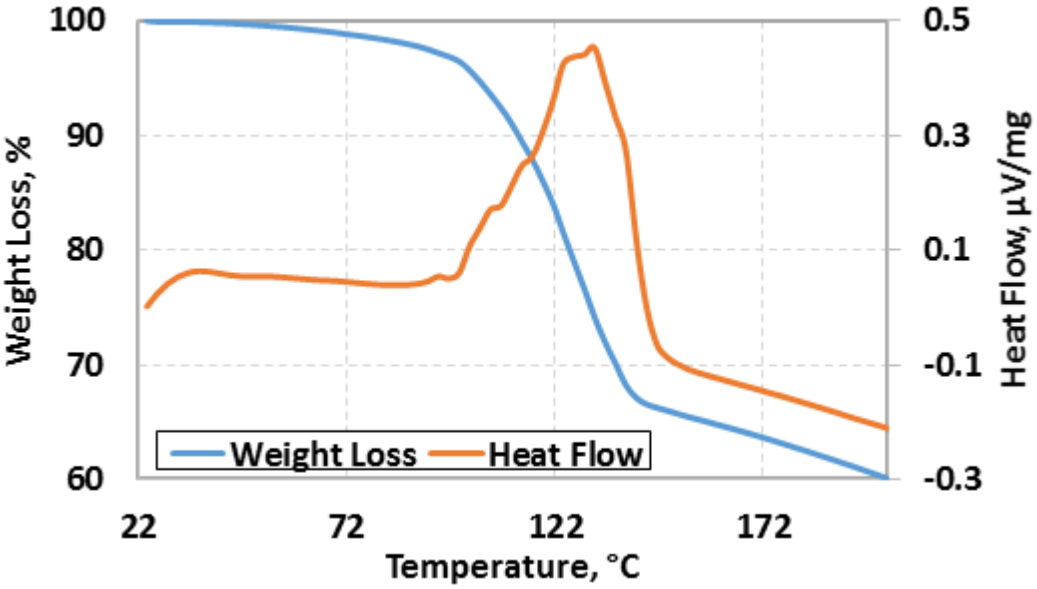

Figure 56: TGA/DSC curves for produced oil sample from ES-SAGD2

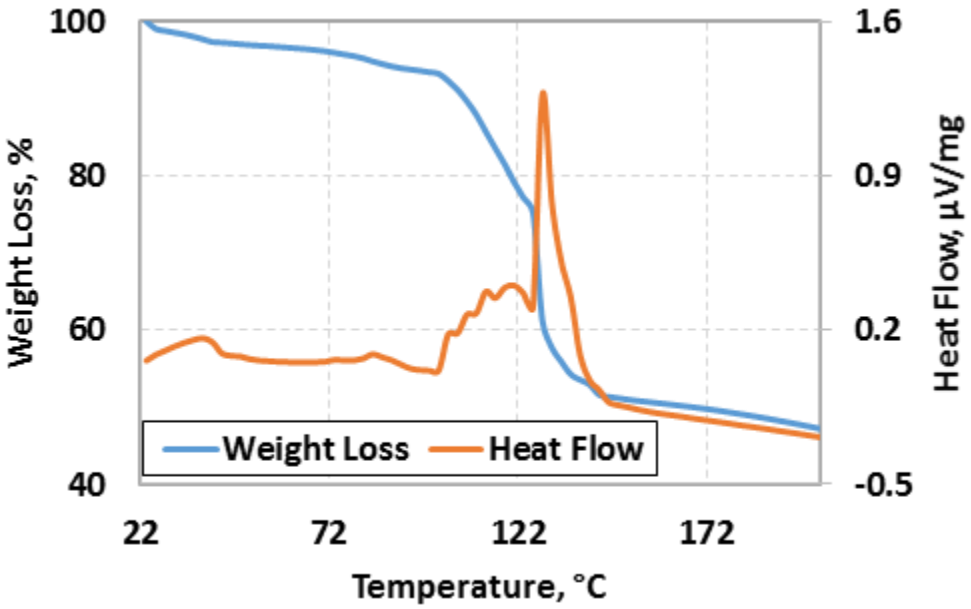

Figure 57: TGA/DSC curves for produced oil sample from ES-SAGD3

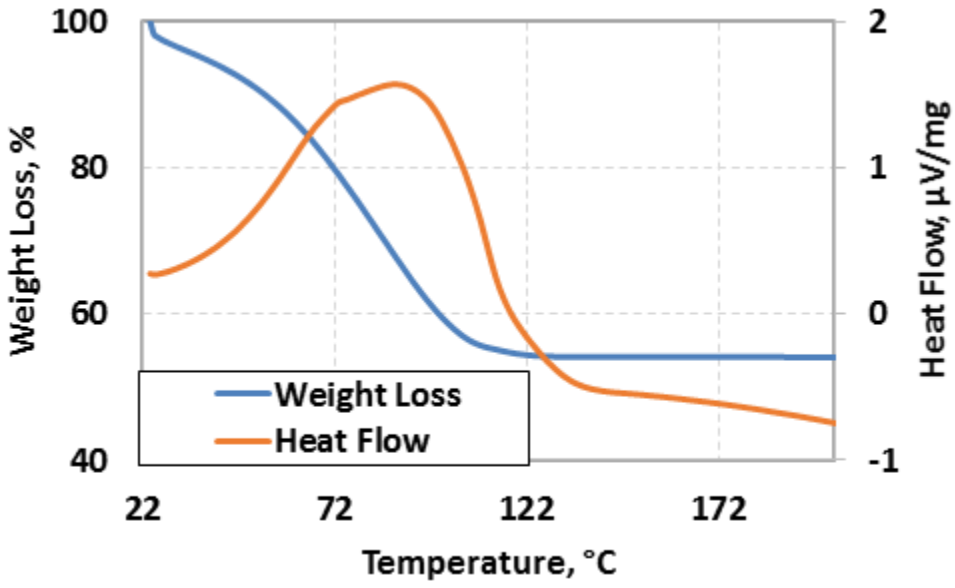

Figure 58: TGA/DSC curves for asphaltenes in produced oil sample from SAGD1

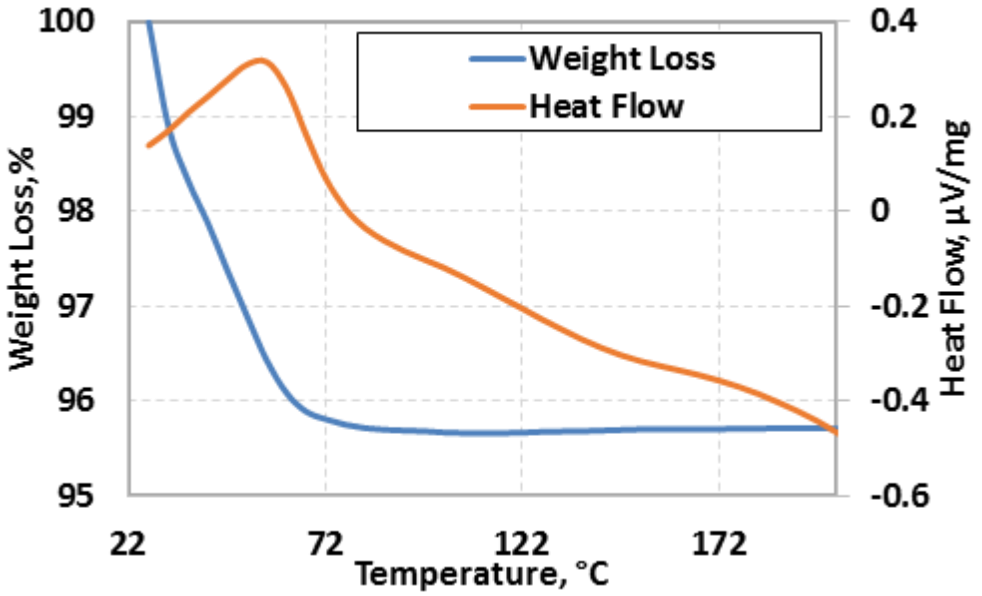

Figure 59: TGA/DSC curves for asphaltenes in produced oil sample from SAGD2

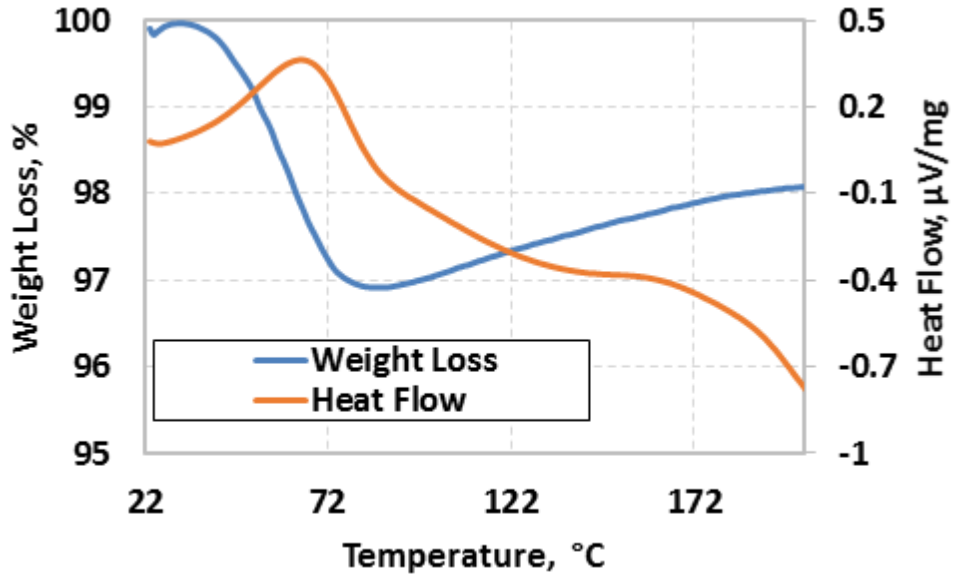

Figure 60: TGA/DSC curves for asphaltenes in produced oil sample from ES-SAGD1

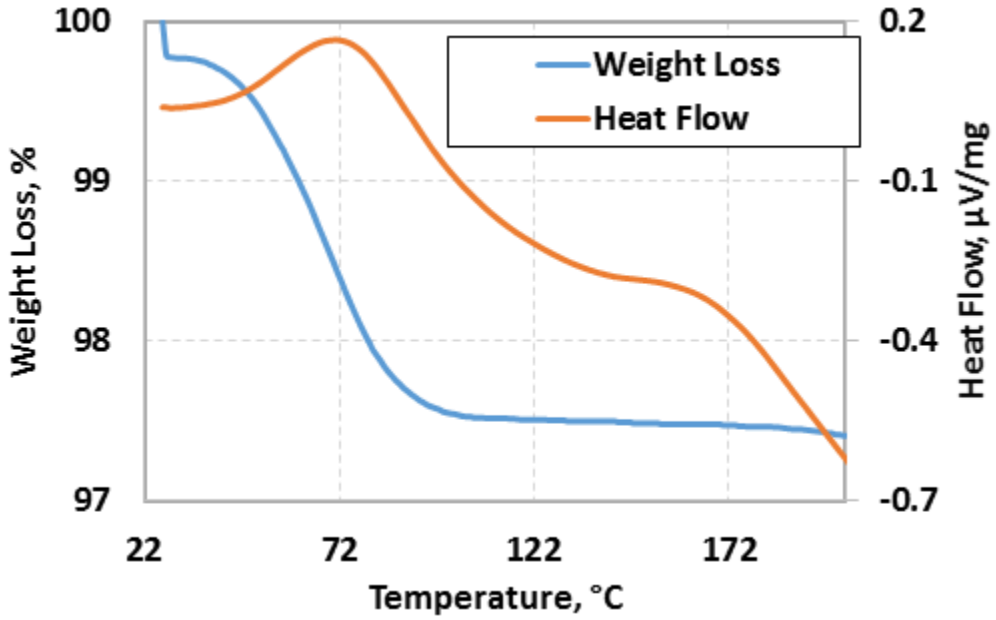

Figure 61: TGA/DSC curves for asphaltenes in produced oil sample from ES-SAGD2

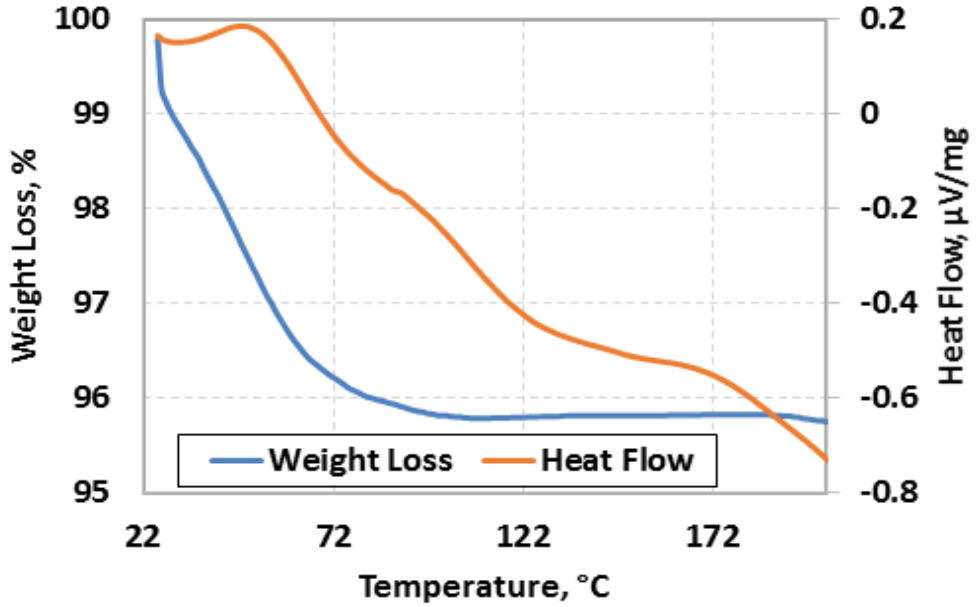

Figure 62: TGA/DSC curves for asphaltenes in produced oil sample from ES-SAGD3

APPENDIX III

VAPOR PRESSURE LINES FOR WATER, N-HEXANE, CYCLOHEXANE, AND TOLUENE

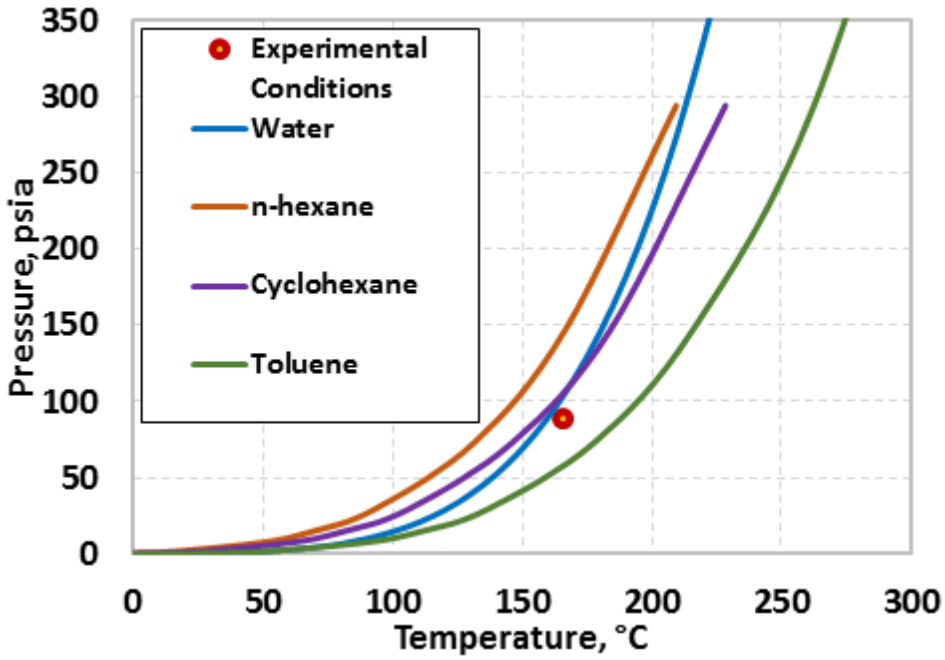

Figure 63: Phase diagrams of various solvents at experimental conditions (Dean, 1998; Hodgman, 1962)

APPENDIX IV

PROCEDURE FOR MATERIAL BALANCE CALCULATIONS

Table 16: Percentage distribution of precipitated and moved asphaltenes for inside and outside steam chamber zones based on 100 grams of asphaltenes in initial bitumen sample (same as Table 5)

Sample	**Inside steam chamber**		**Outside steam chamber**	
	Precipitated Asphaltenes (%)	**Moved Asphaltenes (%)**	**Precipitated Asphaltenes (%)**	**Moved Asphaltenes (%)**
SAGD1	79.80	20.20	67.80	32.20
SAGD2	85.22	14.77	79.62	20.38

For SAGD1 Inside steam chamber, in terms of 100 grams of spent rock:
Residual Oil (with clays) = 6.88 grams (calculated from Table 4)
Asphaltenes in residual oil = 23.51 wt% = 1.62 grams (from Fig. 4)
Residual Oil (without clays) = 5.86 grams (from Table 4)
Weight% of asphaltene in initial bitumen (excluding water contribution) = 34.59 wt% (calculated using Table 6 and Fig. 2)
Asphaltenes initially present = 34.59 wt% of 5.86 grams = 2.03 grams (from Table 4)
Precipitated asphaltenes = (1.62/2.03)*100 = 79.80 wt% (Table 16)
Moved asphaltenes = 100-79.80 = 20.20 wt% (Table 16)

Similar calculations are performed for the rest of the cases, both for inside and outside steam chamber.
The calculations of Table 12 are similar to those of Table 5, as explained in Table 16.

Table 17: Actual oil recovery vs cumulative oil recovery (* Mukhametshina, 2013) (same as Table 14)

Experiment	Actual Oil Recovery (wt%)	Cumulative Oil Recovery (wt%)*
SAGD1	27.03	47.41
SAGD2	10.20	32.12
ES-SAGD1	23.47	33.71
ES-SAGD2	24.52	45.15
ES-SAGD3	20.84	44.91

For SAGD1,
Initial oil in oil-sand packing before experiment = 3322.7 grams (from Mukhametshina, 2013)
Measured amount of oil recovered (including water and clays) = 1575.4 grams (from Mukhametshina, 2013)
Cumulative oil recovery = (1575.4/3322.7)*100 = 47.4 wt% (Table 17)
For 100 grams of produced oil, water = 43 grams, clay = 0 grams. (from Fig. 2)
Hence, for 100 grams of produced oil, actual oil weight = (100-43) = 57 grams.
Actual oil recovery = (57/100)*1575.4 = 897.98 grams = (897.98/3322.7) = 27.03 wt% (Table 17)

Similar calculations are performed for the rest of the cases.

Table 18: Normalized wt% of precipitated and produced asphaltenes (same as Table 8)

Sample	Precipitated Asphaltenes (wt%)	Produced Asphaltenes (wt%)
SAGD1	32.92	38.42
SAGD2	27.77	87.53
ES-SAGD1	36.39	29.53
ES-SAGD2	30.63	45.06
ES-SAGD3	20.56	80.72
ES-SAGD4	34.59	-

For SAGD1,
Initial oil in oil-sand packing before experiment = 3322.7 grams (from Mukhametshina, 2013)
Measured amount of oil recovered (including water and clays) = 1575.4 grams (from Mukhametshina, 2013)
Measured weight of asphaltenes in 100 grams of produced oil = 21.9 grams (from Fig. 2)
Actual weight of asphaltenes in produced oil = (21.9/100)*1575.4 = 345.01 grams
Actual oil recovery = 897.98 grams (from Table 17)
So, produced asphaltenes = (345.01/897.98)*100 = 38.42 wt% (Table 18)
Amount of asphaltenes in 100 grams of original bitumen sample = 30.92 grams (from Fig. 2)
So, amount of asphaltenes initially present in bulk oil = (30.92/100)*3322.7 = 1027.38 grams
Hence, remaining weight of asphaltenes in residual oil = 1027.38-345.01 = 682.37 grams
The remaining weight of saturates, aromatics, and resins is calculated in a similar way as asphaltenes and found to be 542.71 grams, 383.12 grams, and 464.32 grams respectively
Total weight of residual oil = weight of (saturates + aromatics + resins + asphaltenes) = 542.71+383.12+464.32+682.37 = 2072.52 grams
So, precipitated asphaltenes = (682.37/2072.52)*100 = 32.92 wt% (Table 18)

Similar calculations are performed for the rest of the cases.